University of Cincinnati

Date: 9/14/2021

I, Evan Lydon, hereby submit this original work as part of the requirements for the degree of Doctor of Philosophy in Chemistry.

It is entitled:

Synthesis and Reactivity of Cyclopentadienone Metal Complexes

Student's name: **Evan Lydon**

This work and its defense approved by:

Committee chair: Hairong Guan, Ph.D.

Committee member: Michael Baldwin, Ph.D.

Committee member: Allan Pinhas, Ph.D.

40538

Synthesis and Reactivity of Cyclopentadienone Metal Complexes

A dissertation submitted to the Graduate School of the University of Cincinnati in partial
fulfillment of the requirements for the degree of

Doctor of Philosophy (Ph.D.)

In the Department of Chemistry

of the College of Arts and Sciences by

Evan J. Lydon

Bachelor of Science (B.S.), Chemistry

University of Missouri, Columbia, MO 2016

Committee Chair: Hairong Guan, Ph.D.

Synthesis and Reactivity of Cyclopentadienone Metal Complexes

Abstract

Cyclopentadienone/hydroxycyclopentadienyl metal complexes have been of great interest to the homogenous catalysis community for their application as bifunctional hydrogenation/dehydrogenation catalysts. The stable pairing of a Lewis-acidic/basic site next to a reactive hydride or metal center creates a catalytic 'pocket' that can stabilize reaction transition states. Group 8 cyclopentadienone metal complexes have been extensively studied and applied to numerous organic and inorganic transformations; however, the reactivity of group 7 and 9 cyclopentadienone complexes remain comparatively less understood. Additionally, cyclopentadienone complexes have primarily been studied as standalone metal complexes, and only recently has interest in their application to bimetallic and tandem catalytic reactions emerged. Here, I will present research into newly synthesized cyclopentadienone metal complexes and their unique reactivities.

Cobalt cyclopentadienone complexes have been reported in the literature; however, their synthesis has been plagued by poor yields and unwanted side products and their applications remain sparse. Novel cobalt(I) cyclopentadienone complexes were synthesized and their unique reactivity was studied. These compounds showed fast hydride transfer reactivity with triphenyl carbenium tetrafluoroborate in acetonitrile, transferring the acidic OH proton and two electrons in an unusual umpolung type reaction. This reaction was shown to be highly sensitive to solvent conditions, ligand backbone and the presence of exogenous bases and electron donors, giving some insights to its mechanism. The hydride transfer reaction was optimized to yield a class of previously uncharacterized cationic cobalt(I) cyclopentadienone complexes which were shown to be highly diversifiable with three labile coordination sites. These newly synthesized cationic cobalt complexes were screened for their reactivity in organic transformations.

Manganese-based cyclopentadienone complexes are far less known; only one report was found in the literature for a manganese cyclopentadienone complex and no modern characterization data was present. A series of novel manganese(I) cyclopentadienone complexes were synthesized with increasing electron density on the metal and their reactivity with electrophiles was studied. In contrast to the cobalt system, pure manganese cyclopentadienone complexes were much less capable of umpolung hydride transfer to triphenyl carbenium tetrafluoroborates without greatly increasing the electron density on the manganese center. However, manganese cyclopentadienone complexes proved to be much more diversifiable than the cobalt analogs and a series of new ligands were installed on the manganese which allowed access to a unique manganese(III) hydride complex and an efficient manganese(I) hydride transfer reagent.

Iron-nickel bimetallic complexes have been studied extensively as model complexes for the FeNi-hydrogenases found in nature. However, increasingly in homogenous catalysis, bimetallic complexes are seeing increased attention for their application in organic transformations in which two metal centers can cooperate within a catalytic cycle. A novel series of iron-nickel bimetallic complexes were synthesized and characterized. They displayed varying stabilities and reactivities dependent on the steric and electronic properties of the coordinating ligands and represent an interesting starting point for new research.

Acknowledgements

I would like to express my appreciation for the University of Cincinnati for providing me the opportunity to conduct my doctoral chemistry studies with my advisor, Dr. Hairong Guan. I would like to sincerely thank Hairong for allowing me to join his group and mentoring me. Hairong has supported and guided me through my research and presented me with opportunities that I would not have had, otherwise. I am sincerely grateful for everything he has provided for me.

I would also like to thank the faculty members who have worked with me over the years. My current committee members Dr. Allan Pinhas and Dr. Michael Baldwin who have given me their time and attention and have provided invaluable feedback on my research. I would also like to thank and recognize my former committee member Dr. Bill Connick, who tragically passed away, for all his enthusiasm, insights and attention. Additionally, I would like to thank Dr. Jeanette Krause who has collected and solved numerous crystal structures which have been necessary to my research's progression. I would like to thank Dr. Larry Sallans and Dr. Stephen Macha for operating and maintaining the mass spectrometry facility, which has proved very useful over the course of my research. I would like to thank Dr. Alex Greenwald for his operation, maintenance and improvement of the NMR facility. Finally, I would like to thank all the staff who keep the chemistry department at the University of Cincinnati running behind the scenes such as Kim Carey, Sharon Stith and many others.

I would also like to thank all my current and former group members for their support and advice. Former group members Dr. Yingze Li, Dr. Huiguang Dai, Dr. Nathan Eberhardt, Dr. Rebecca Haley, Dr. Nadeesha Wellala, and Dr. Dewmi Ekanayake, have all helped me in my research and day to day lab activities, for which I am incredibly grateful. I would especially like to thank Dr. Ekanayake and Dr. Li for all their advices and assistance. I would like to thank my current group members Joel Collett, Bedraj Pandey, Dulmini Jayawardhena, and Rachna Bal for all their hard work maintaining the lab. I would especially like to express my gratitude to Joel, whose technical savvy with the mechanical and electrical equipment in our lab have proved crucial for its efficient operation. I would like to thank them for all their support and their insights into my research. I have truly enjoyed my time working with all the Guan group members.

Finally, I would like to thank my family. My parents Dr. Silvia Jurisson and Dr. John Lydon, and my sister Katy Lydon for all of their support.

Synthesis and Reactivity of Cyclopentadienone Metal Complexes

Table of Contents

Chapter 1: Introduction

Chapter 2: Tetracyclone Complexes of Cobalt and Manganese

Chapter 3: Silyl Group Protected Cyclopentadienones and Their Cobalt Complexes

Chapter 4: Iron Nickel Bimetallic Cyclopentadienone Complexes

Synthesis and Reactivity of Cyclopentadienone Metal Complexes

List of Figures

Chapter 2: Tetracyclone Complexes of Cobalt and Manganese

Chapter 3: Silyl Group Protected Cyclopentadienones and Their Cobalt Complexes

Chapter 4: Iron Nickel Bimetallic Cyclopentadienone Complexes

Synthesis and Reactivity of Cyclopentadienone Metal Complexes

List of Tables

Chapter 2 Tetracyclone Complexes of Cobalt and Manganese

Chapter 3 Silyl Group Protected Cyclopentadienones and Their Cobalt Complexes

Chapter 1 – Introduction

1.1 Catalysis with Earth Abundant Metals

The development of sustainable catalysts is a pressing challenge facing modern synthetic chemists. The reliance of industry on catalysts derived from scarce second and third row transition metals and stochiometric reagents leads to wasteful and expensive processes. Development of earth abundant metal-based catalysts are seen as one avenue to improve sustainability in the chemical industry.[1]

While heterogeneous transition metal catalysis predominates in the synthesis of most bulk chemicals, homogenous transition metal catalysts have found application in bulk chemical production[2] and are especially favored over heterogenous catalysis for more complex transformations.[3]

1.2 Cyclopentadienones

Cyclopentadienones (CPDs) are a class of antiaromatic dienes known for their unique electronic properties.[4] CPDs without sufficient steric protection act as efficient dienes and dienophiles in the Diels-Alder reaction,[5] making them useful synthetic intermediates for complex transformations (Scheme 1.1).[6]

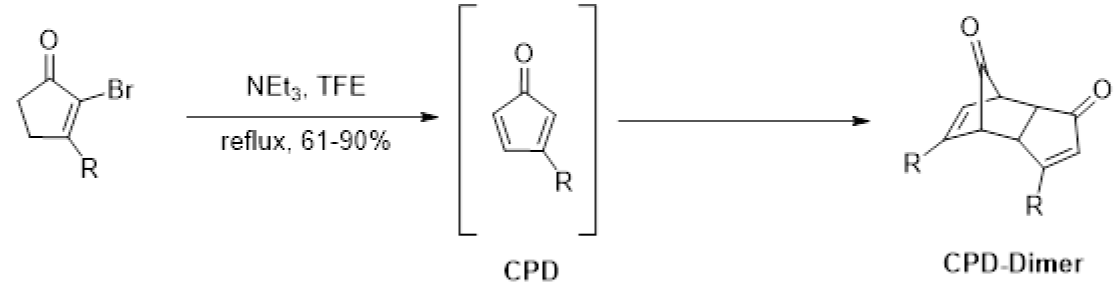

Scheme 1.1 Dimerization of CPDs.

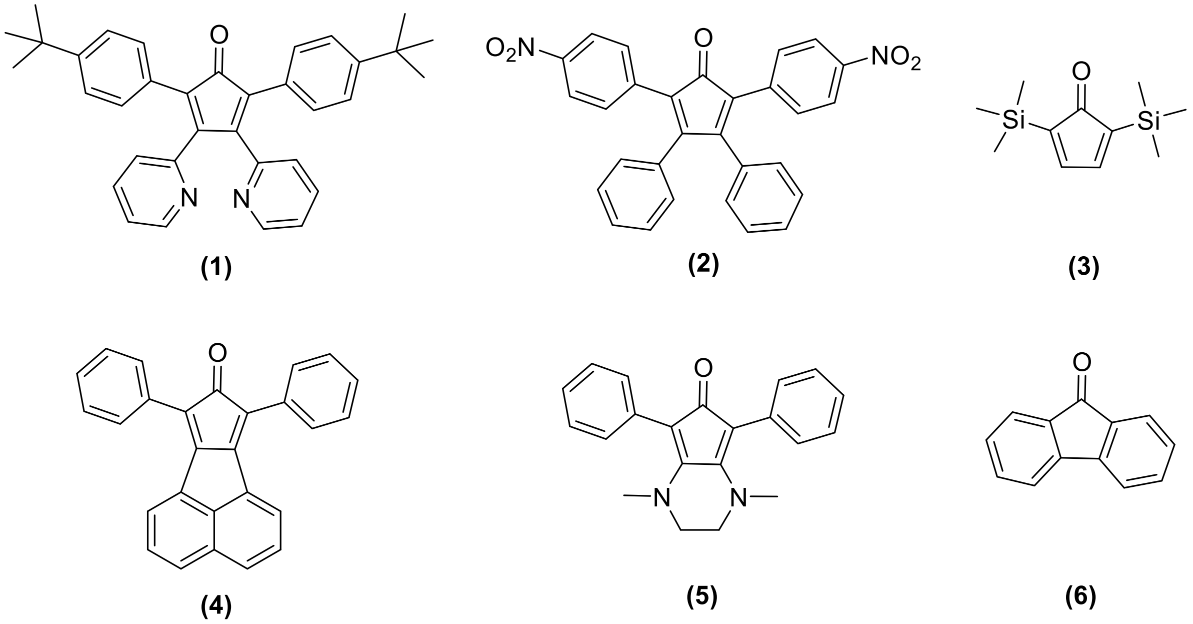

(1) (2) (3)

(4) (5) (6)

Scheme 1.2 Sterically stabilized CPDs.

CPDs can be isolated as stable products with the addition of sterically demanding groups to the four diene carbons (**1**-**3**) (Scheme 1.2) or incorporation into a ring system (**4-6**).[7] These stable CPDs have many interesting electronic properties due to their rigid and conjugate nature and have seen some application in fields of organic LEDs (e.g., **4**)[8] and dyes (e.g., **2**).[9] These molecules are still useful dienes in the Diels-Alder reaction, which can be activated by either increasing the temperature or, occasionally, cleaving the bulky groups (e.g., in **3**).[10]

CPDs are also a well-known class of redox-active ligands[11–14] for building organometallic compounds (Scheme 1.3). The polar carbonyl bond in a CPD can be reduced by a two-electron transfer from a low valent metal species **7**. This electron transfer produces a dianionic ligand with a negative charge delocalized in the cyclopentadienyl (Cp) ring and the other localized on the oxygen atom. The negatively charged Cp ring will bind the metal analogous to the parent Cp while the oxygen atom has no direct interaction with the metal. This is a useful binding mode because the anionic oxygen can be protonated (as in **8**) and act as an ancillary BrØnstead acid in catalytic reactions at the metal center.[15] Many catalytic reactions will involve a crucial step in which a nucleophilic and an electrophilic component react with a substrate or each other to form a product. With hydroxycyclopentadienyl metal complexes, these electrophilic and nucleophilic components can be held together, reducing their degrees of freedom and lowering the energy of the transition state.[16]

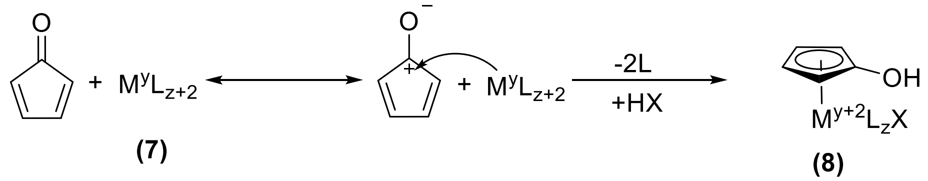

Scheme 1.3 *Electron transfer from metal to a CPD produces a hydroxycyclopentadienyl ligand.*

Well-known CPD metal complexes have been studied primarily as hydrogenation and dehydrogenation catalysts. Knölker's complex **9** (Scheme 1.4),[17] an iron(0) cyclopentadienone complex, which can be converted to the active iron(II) hydroxycyclopentadienyl hydride complex **10** using Me_3NO and H_2,[18] sodium hydroxide (reverse water gas shift),[19] alcohols,[20] or other drivers of the oxidation process,[21] was studied by Casey and Guan as an efficient hydrogenation catalyst for aldehydes and ketones. Shvo's complex **11** (Scheme 1.5),[22] the ruthenium analog of Knölker's complex, has very similar chemistry to Knölker's complex and has been extensively studied; however, ruthenium pincer complexes have become more favored for many applications.[23]

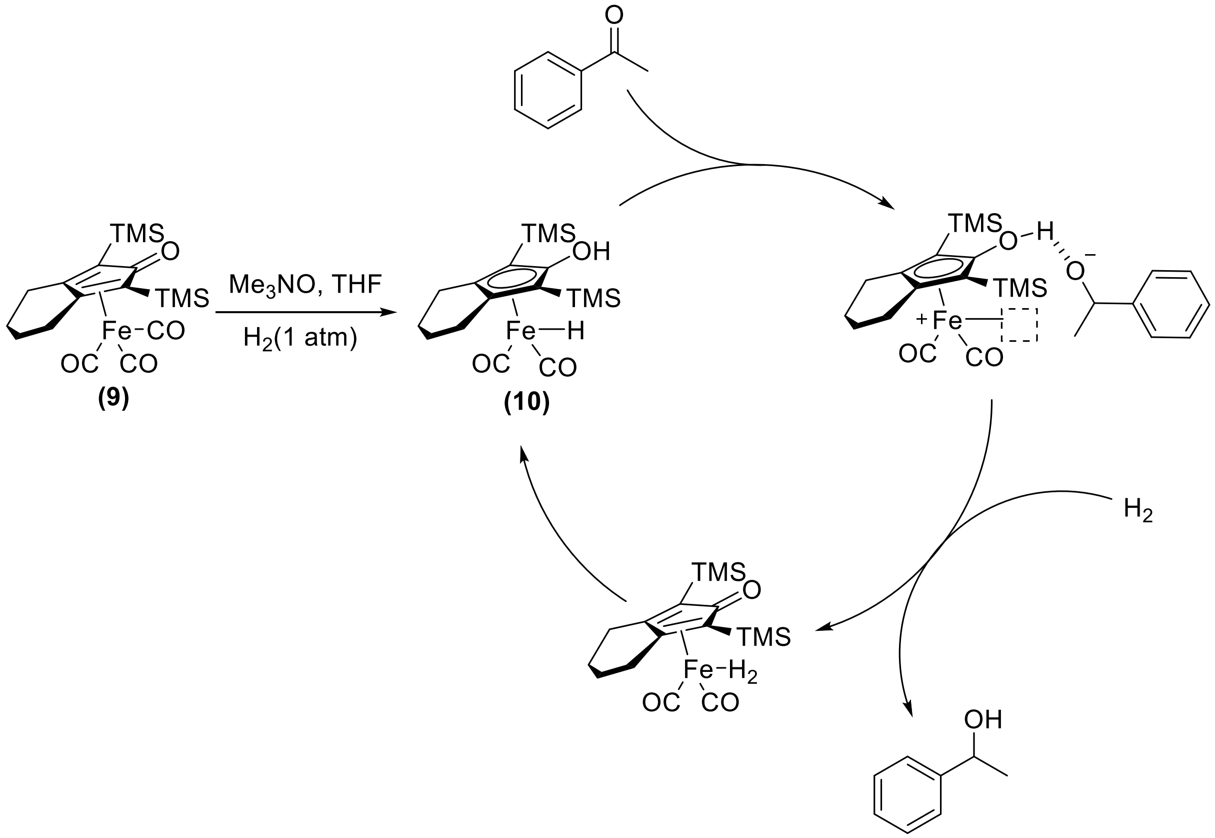

Scheme 1.4 Catalytic cycle for hydrogenation of acetophenone by Knölker's complex.

CPD complexes with metals other than iron or ruthenium are known and have catalytic applications. Examples include Mo (**12**),[24] Rh (**13**) [25] and Ir (**14**)[26] CPD complexes; however, they are comparatively less studied and show no significant advantages or reactivities over pincer complexes bearing the same metal or over group 8 CPD complexes.

CPD complexes of cobalt and manganese are known; however, they have proved to be difficult to synthesize partially because of their sensitivity to air and their tendency to participate in side-reactions. Because of this, these complexes remain poorly characterized and their reactivities remain poorly understood, especially when compared to the very well characterized

Cp and pentamethylcyclopentadienyl (Cp*) analogs. Some efforts recently have been made at improving the synthetic methods for accessing cobalt hydroxycyclopentadienyl complexes;[27] however, the scope of these methods remains narrow. Furthermore, manganese hydroxycyclopentadienyl complexes, while known, appear very sparsely in the organometallic literature and, to the best of our knowledge, their derivatives remain unexplored.

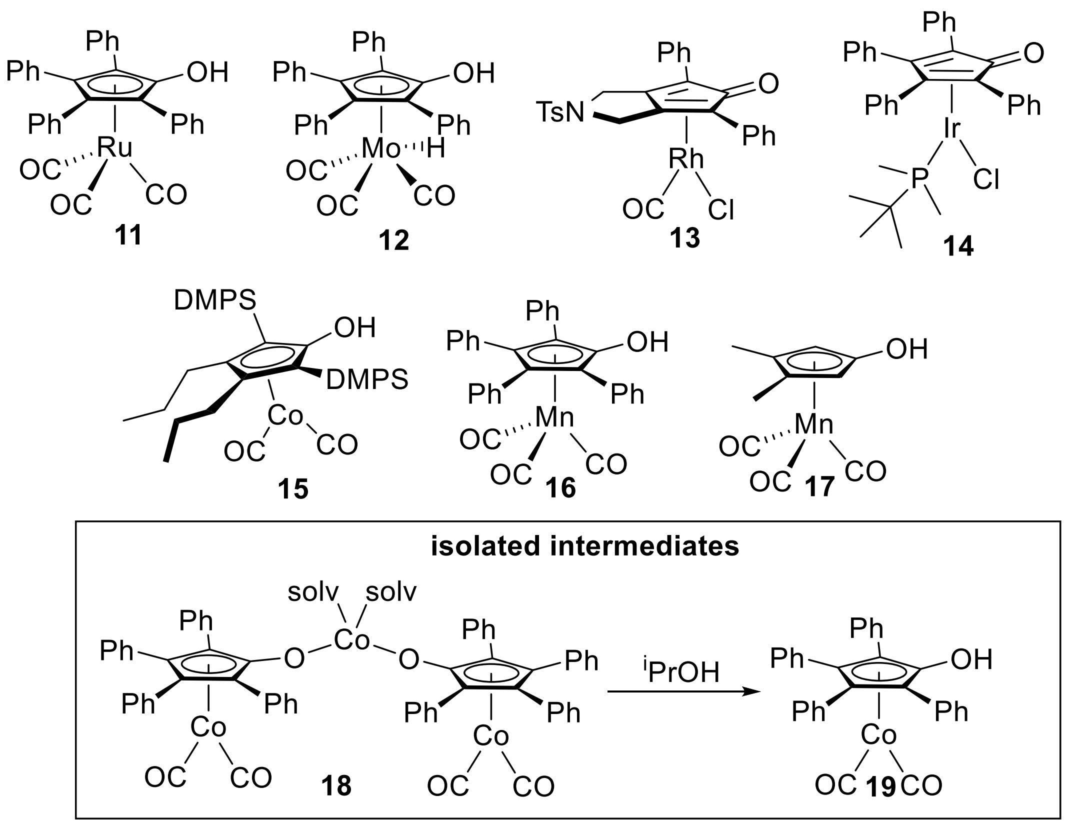

Scheme 1.6 Cyclopentadienone/hydroxycyclopentadienyl metal complexes.

Cobalt carbonyl CPD complexes were first characterized by Hübel in his investigation of reductive coupling of alkynes with $Co_2(CO)_8$ (Scheme 1.6).[28] His work showed that the reaction between excess alkyne and metal carbonyl complexes resulted in a wide range of species depending on the conditions, one of which was a CPD cobalt(0) dicarbonyl dimer. This product was observed along with other alkyne oligomerization products; none of these complexes catalyze the [2+2+1] cycloaddition of alkynes with CO due to the strong back-bonding from the metal to CPDs.

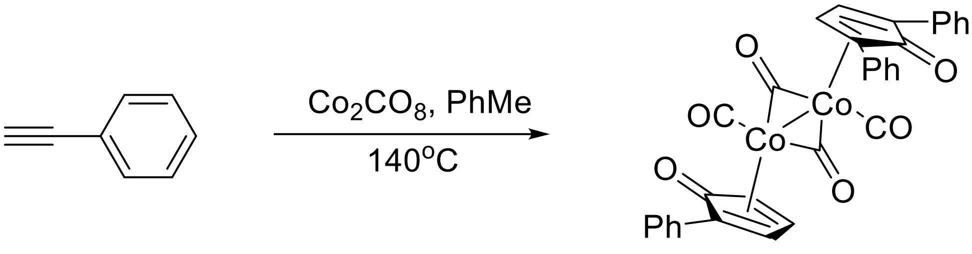

(20)

Scheme 1.7 *Cobalt mediated [2+2+1] cycloaddition of phenylacetylene with carbon monoxide.*

Further studies in 2014 by Roewer[29] showed that cobalt(I) hydroxycyclopentadienyl complex **15** could be made by cycloaddition of alkynes at high temperatures, albeit only at 21% yield. However, questions remained as to the source of the hydrogen atom in the reaction. This question was somewhat resolved by work of the Waymouth group,[27] which showed that the reaction between cobalt carbonyl and tetracyclone yielded a Co(II)-linked hydroxycyclopentadienyl Co(I) complex (**18**). This compound can be viewed as being formed by an initial disproportionation of three Co(0) fragments to two Co(-I) and one Co(II) and subsequent two electron reduction of two equivalents of cyclopentadienone by the Co(-I) fragments. However, because different cyclopentadienones were used by Roewer and Waymouth, questions remained about how the CPD substituents affected the outcome of the reaction.

Cobalt CPD complexes have also been studied in the context of cobaltocenium complexes with an objective to imitate the famous electron donor cobaltocene. These complexes are synthesized by the reaction of $CpCo(CO)_2$ with one equivalent of a cyclopentadienone.[30] The CO ligands are labile and a cobalt(I) sandwich complex is readily formed. These complexes react with electrophiles to from Co(III) sandwich complexes. A cobalt(II) sandwich complex bearing a CPD ligand have been reported in the literature;[31] however, it was not isolated.

Only two reports[28,32] of manganese CPD complexes were found in the literature, complexes **15** and **16**, and although these complexes have apparently been studied, characterization data is limited and no information on derivatives of these complexes exist. Evidently, the first report of the synthesis of these complexes comes from Hübel as well.

The potential application of these complexes is two-fold. First, these complexes, unlike traditional Cp complexes, are redox active, thus they can be thought of as reservoirs of electrons, with greater reducing power than typical metal complexes with the same oxidation state. This could be of interest, as stabilizing or *masking* low valent species could lead to novel reactivities and new applications. Second, and more obviously, hydroxycyclopentadienyl complexes may be protonated to form stable cationic hydrides if the ancillary ligands can support such a high valent state. These hydrides could potentially act as reduction catalysts in the same way that the group 8 hydroxycyclopentadienyl hydrides do and cationic hydrides may show unique solubilities and reactivities. The remainder of this chapter will briefly go into detail about precedence for these types of reactivities.

1.3 Masked Hydrides

Transition metal hydrides are important intermediates in many catalytic reactions and the rate of their formation or consumption is often the rate-determining step of a catalytic cycle. Thus, understanding these intermediates is essential to designing better catalysts.

The term ‘masked-hydride’ has traditionally meant a metal bound Si-H[33] or B-H[34] or a metal bound X type ligand with beta hydrogens.[35] In these cases, it is easy to see how a hydride could be formed in solution by β-hydrogen elimination or by nucleophilic attack on an electrophilic silicon or boron. However, recent research has shown that ‘masked-hydrides’ are not limited to these types of bonds and that X-H type bonds may act as hydride transfer reagents without the appearance of any observable hydride or direct interaction with the metal center.

This latter class of compounds is interesting for its umpolung type chemistry where an acidic hydrogen, still bearing all the features of an acid, could be transferred as though it were a hydride. This could be useful in deuteration reactions, ionic hydrogenation and electrochemical reactions where the complex could act as a redox mediator. This type of masked hydride chemistry may be common in nature in which reductases and dehydrogenases act without the formation of a metal hydride intermediate and instead rely on proton-coupled electron transfer (PCET) and cofactors such as $NADP^+$.[36]

A useful way to study hydride transfer in the lab is to use an outer sphere hydride acceptor such as trityl cation,[37] a pyridinium cation,[38] an iminium cation,[39] or a photo oxidant (e.g., $Ru(bpy)_2Cl_2$).[40] Trityl cation is by far the most common hydride acceptor for outer sphere hydride transfer studies in organometallic reactions. It is a strong oxidizing agent, readily studied spectroscopically (NMR, UV-Vis) and its products are readily separated from the cationic complexes it produces. The major drawback of using trityl cation is its tendency to dimerize after a one-electron transfer step. However, this can also give useful mechanistic information as metal complexes that readily undergo one-electron oxidation can be differentiated from those that only undergo hydride transfer.

One class of hydride transfer reagents that has been extensively studied are piano stool cobalt complexes. These complexes are composed of a CpCo(I/III) fragment and some bidentate ligand. The hydrides of these complexes have been isolated and studied in CO_2 reduction,[41] formate oxidation[42] and hydrogen evolution reactions. The formation of the CpCo(III) cationic hydride is dependent upon the ligand and a hydride will not form unless the coordinating ligand is electron donating enough to support it. For example, when 1,2-bis(diphenylphosphino)ethane (dppe) was used as the coordinating ligand, the Co(I) center could be easily protonated with HBF_4 to form the cationic Co(III) hydride.[43] When phenylazopyridine (azpy) was employed as the coordinating ligand and HBF_4 was added, the ligand was protonated at the non-coordinating nitrogen to generate complex **21** (Scheme 1.7). However, because the protonated nitrogen was conjugate to the Co(I) center, it displayed unusually facile hydride and hydrogen atom transfer reactivity to give complex **22**.[44] Similar reactivity was observed in Co(II) sandwich complexes which, instead of reducing an acid immediately to H_2, can stabilize it long enough to transfer a hydrogen atom to a ketone substrate via an efficient PCET pathway.[45]

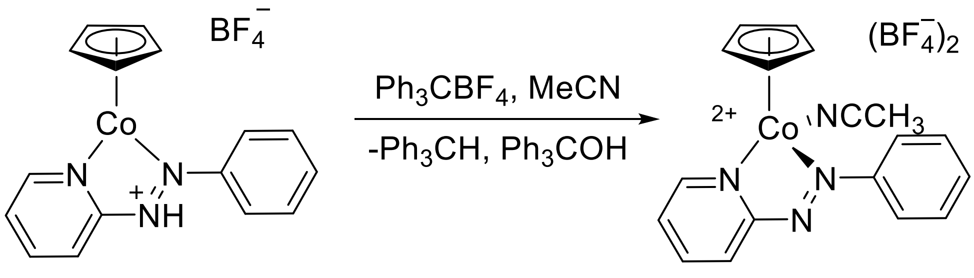

(21) **(22)**

Scheme 1.8 *Hydride and electron transfer from CpCo(azpyH$^+$) to [Ph$_3$C]BF$_4$.*

Geometrically constraint phosphorus (III) reagents have received a lot of attention recently for their interesting redox chemistry such as their ability to undergo oxidative addition of NH and RX bonds.[46] One of the driving forces for their reactivity is the transition from a strained T-shaped geometry to a more stable trigonal bipyramidal geometry. This has led to the development of an interesting ruthenium masked hydride complex **23** (Scheme 1.8) which accepts a hydride not at the metal center but instead at the coordinated phosphorus to yield complex **24**; however, it still acted as a hydride toward oxidants and was strangely inert to strong bases.[47] The driving force for this reactivity seems to be the shift from a T-shaped phosphorus molecule to a trigonal bipyramidal one.

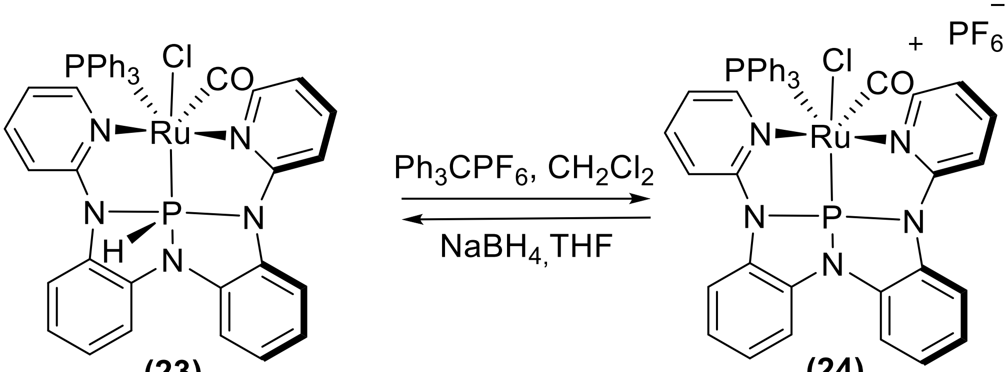

(23) **(24)**

Scheme 1.9 *Metallo-phosphorane as a reversible, masked hydride.*

Another interesting trend observed in masked hydride transfer chemistry is the ability of Cp* ligands to act as hydride transfer mediators while switching between X and L type ligands. Interestingly, these ligands seem to be quite strong hydride donors.[48] One interesting mechanistic investigation of an Cp*Ir(III) complex (**25**) (Scheme 1.9) showed that in the presence of trityl cation, the Cp* ligand would lose a hydride to become a tetramethyl fulvene complex (**26**). This is unusual because it results in a loss of aromaticity for the ligand which is the opposite trend observed for most hydride transfer cofactors in nature.[49]

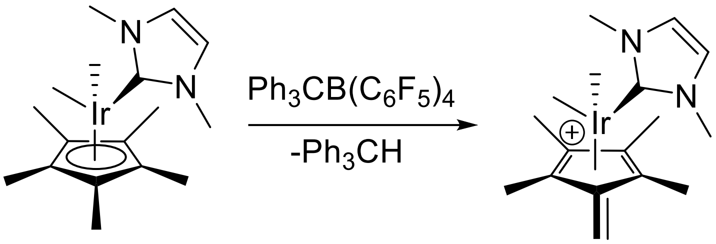

(25) **(26)**

Scheme 1.10 *Cp*IrMe$_2$(NHC) complex as an unusual hydride rather than methyl donor.*

1.4 Bimetallic Hydrides

Bimetallic complexes have attracted much attention from the inorganic and catalysis research communities. Metal-metal cooperativity, metal-metal bonds, and bridging ligands are attractive features to build into new metal complexes to study the effects on reactivity and spectroscopic properties. Furthermore, multimetallic clusters and bimetallic active sites are present in some of the most important and catalytically interesting proteins in nature and chemists are still trying to fully understand these systems.

The iron-nickel bimetallic pair has attracted considerable attention because of its appearance in the active sites of the [FeNi]-hydrogenase and the CO dehydrogenase enzymes. These enzymes catalyze the reversible oxidation of hydrogen and the water-gas shift reaction, respectively, making them attractive targets for small molecule models. Complex **27** (Scheme 1.10) synthesized by the Lee group modeled the CO-dehydrogenase active site with an unusual nickel-carboxylate and a terminal iron PNP pincer ligand.[50] This represents the first example of a bimetallic, bridging CO_2 ligand. [NiFe]-hydrogenase structural mimics **28** and **29** are some of the closest representations to date of the [NiFe]-hydrogenase active site and are capable of activating H_2 reversibly.[51] Complex **30**, a functional hydrogenase mimic which substitutes Ru for Fe, showed efficient catalytic activity with high turnover frequency for electrocatalytic H_2 evolution.[52]

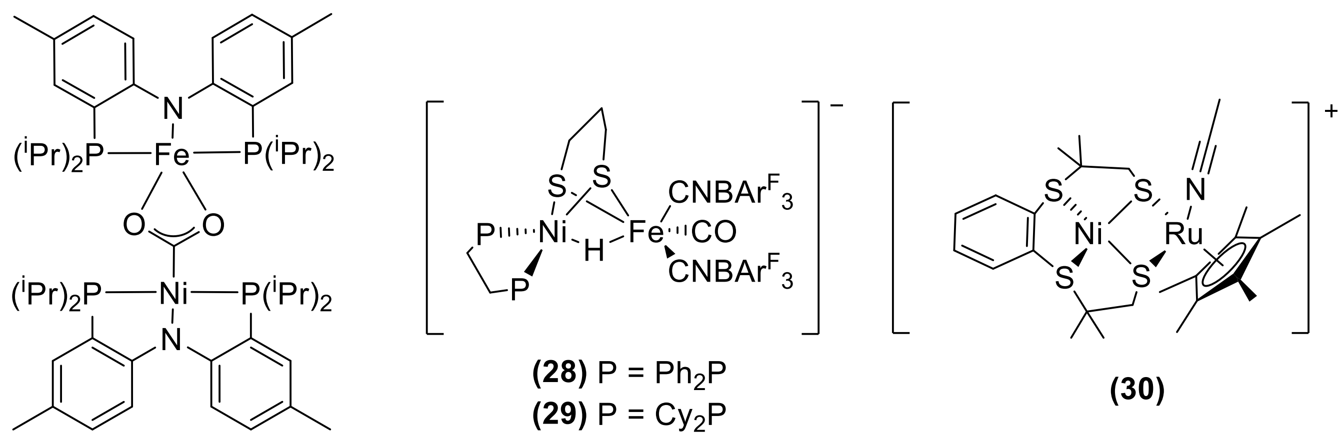

(27)

(28) P = Ph_2P
(29) P = Cy_2P

(30)

Scheme 1.11 *Models of [FeNi]-hydrogenases and CO-dehydrogenase.*

Understanding heterobimetallic metal-metal and metal-ligand-metal bonding is still an important challenge in modern inorganic and organometallic chemistry and considerable efforts have been made towards stabilizing these unique structures. One prominent type of heterobimetallic complex is the polarized-metal-metal bond motif. In these structures, a coordination sphere holds a low valent late transition metal such as nickel, as in complex **31**[53] (Scheme 1.11), or cobalt, as in complex **33**,[54] in close contact with a more electropositive metal. These complexes have several interesting features, such as the strong trans effect of electropositive metal on the electronegative one, and the efficient stabilization of charge. Nickel complex **31** was one of the first nickel complexes shown to hydrogenate CO_2 and cobalt complex **33** could allow substrates to be added oxidatively across the two metals, opening the possibility for useful transformations. Another interesting class of heterobimetallic complexes involve the non-polarized metal-metal bonds, such as that in complex **32**.[55] These are interesting because they can act similarly to homobimetallic metal-metal bonds in that they can undergo oxidative addition across the metal-metal bond; however, each fragment has a different and sometimes complimentary reactivity. This latter class of compound is really at the forefront of bimetallic catalysis.

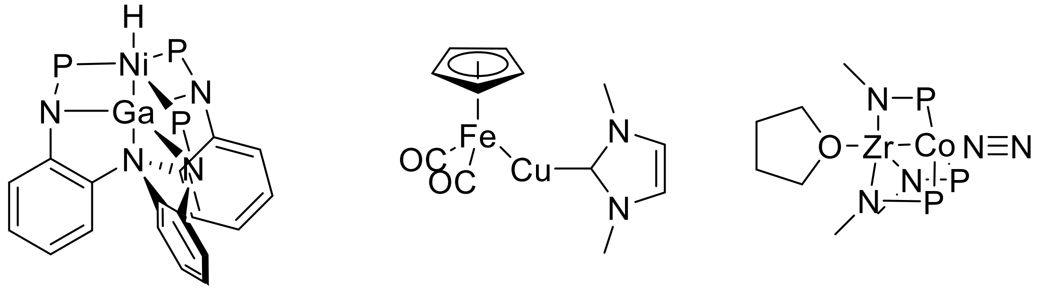

(31) P = $^{i}Pr_2P$ **(32)** **(33)** P = $^{i}Pr_2P$

Scheme 1.12 *Heterobimetallic Catalysts*

1.5 Research Objectives

Cyclopentadienone/hydroxycyclopentadienyl metal complexes have been of great interest to the homogenous catalysis community for their application as bifunctional hydrogenation/dehydrogenation catalysts. The stable pairing of a BrØnstead-acidic/basic site next to a reactive hydride or metal center creates a catalytic ‘pocket’ that can stabilize reaction transition states. Group 8 cyclopentadienone metal complexes have been extensively studied and applied to numerous organic and inorganic transformations; however, the reactivity of group 7 and 9 cyclopentadienone complexes remain comparatively less understood. Additionally, cyclopentadienone complexes have primarily been studied as standalone metal complexes, and only recently has interest in their application to bimetallic and tandem catalytic reactions emerged. Here, I will present research into newly synthesized cyclopentadienone metal complexes and their unique reactivities.

Chapter 2 – Tetracyclone Complexes of Cobalt and Manganese

2.1 Introduction

Tetraphenylcyclopentadienone (or tetracyclone for short) and its para substituted derivatives are a well-known class of cyclopentadienones which can be readily synthesized from cheap building blocks via a double aldol condensation[56] or metal catalyzed[57] or mediated [2+2+1] cycloaddition reactions with carbon monoxide. These molecules show strong absorptions in the UV-vis spectra[9] and have synthetic utility as precursors to extended aromatic frameworks.[58] Because of the ease of synthesis and tunable para positions, these ligands represent a simple and powerful place to start the investigations of cyclopentadienone complexes.

Tetracyclone, like other CPDs, can coordinate to a metal as a neutral L_2-type ligand or as an anionic, η^5-Cp or L_2X-type ligand. Many examples of tetracyclone complexes exist in the literature and have been applied to various catalytic reactions,[22] acting as bifunctional, proton-hydride donors. Typical syntheses of these complexes involve CO ligand displacement by the tetracyclone ligand,[27] or a [2+2+1] cycloaddition of an alkyne[29] on the metal to yield the desired complex.

The related $CpMnL_2$[59] and $CpCoL_2$[60] complexes are well known, and many derivatives of these complexes exist and have been applied to various reactions.

2.2 Synthesis and Characterization

Synthesis of tetracyclone metal complexes can be achieved through several methods; however, in the case of group 7 and 9 metals, the most convenient synthetic method is the direct mixing of tetracyclone with 0.75 equiv of either $Mn_2(CO)_{10}$ or $Co_2(CO)_8$. In practice, due to unwanted side reactions, it is often necessary to add more than one equivalent of the metal carbonyl in order to fully convert the tetracyclone ligand. Synthesis of 1,2,3,4-tetraphenylhydroxycyclopentadienyl cobalt dicarbonyl complex **1** was first reported by the Waymouth group (Scheme 2.1) (and was shown to be formed through intermediate **3**)[27] and their methods are used here with a few minor alterations described in the experimental section. Synthesis of 1,2,3,4-tetraphenylhydroxycyclopentadienyl manganese tricarbonyl complex **2** was first reported by Hübel;[28] however, the synthesis used here was modified substantially to obtain higher yields and purity. These modifications are described in the experimental section. To our knowledge, this represents the first report of modern characterization data of **2** in the literature (Figure 2.1).

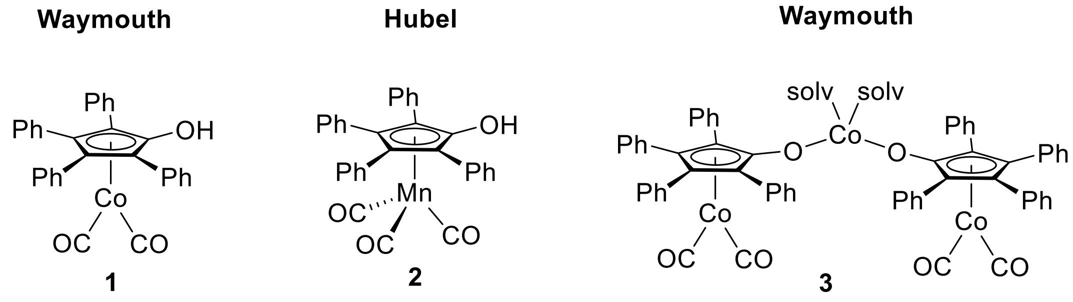

***Scheme 2.1** Manganese and cobalt carbonyl complexes bearing 1,2,3,4-tetraphenyl hydroxycyclopentadienyl.*

Both synthetic methods proceed by displacement of two carbonyl ligands from each metal by tetracyclone, and a two-electron transfer from the metal clusters to the ligand to form one equivalent of the deprotonated hydroxycyclopentadienyl ligand and 0.5 equiv of M(II) salt (M = Co, Mn). The exact mechanism of this reaction is up for debate and may include an initial step in which the metal clusters disproportionate to form anionic-cationic pairs which then react with the tetracyclone. These steps are likely dependent on the solvent conditions.

The rate of this transformation is very dependent on the identity of the metal and may be related to the CO binding strength in the cluster as well as the thermodynamics of the reactions. Kinetically, the binding energy of CO on manganese(I) is greater than the binding energy of CO on cobalt(I),[61] suggesting that it will take more energy to displace the two CO ligands on manganese. Additionally, the greater binding energy of CO to manganese likely slows down the oxidation of manganese compared to cobalt. Thermodynamically, $Mn(OH)_2$ is more stable than $Co(OH)_2$ relative to the zero oxidation state of the metal.[62] This means that the redox reaction in which Mn(II) is formed should be more favorable than the redox reaction in which Co(II) is formed.

These trends may help explain the significant differences seen in the synthesis and reactivity of the two metal complexes. For the reaction between $Co_2(CO)_8$ and tetracyclone, an immediate evolution of carbon monoxide gas is observed at room temperature as the cobalt carbonyl decomposes and reacts with the tetracyclone. In contrast, the CO ligands on manganese carbonyl are relatively stable even at slightly elevated temperatures and the reaction between tetracyclone and manganese carbonyl requires forcing conditions of 160 ^{o}C to reach completion.

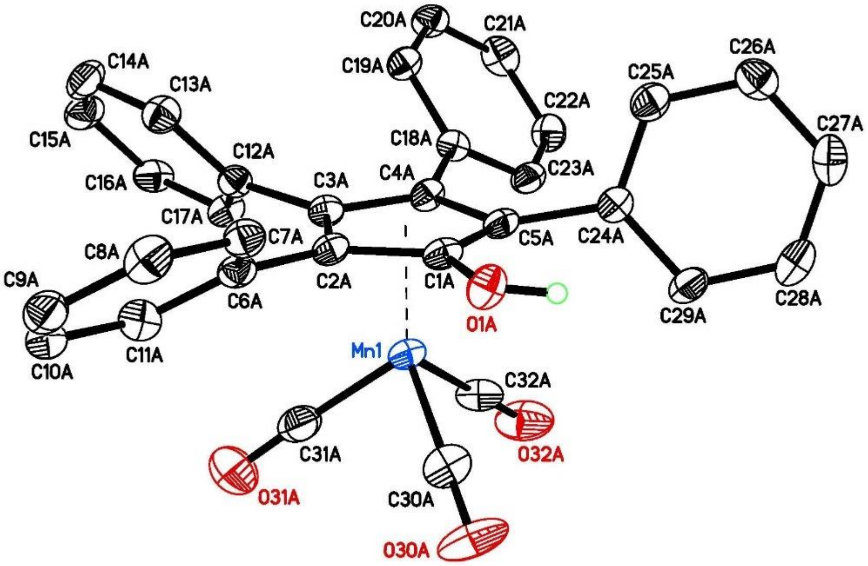

Figure 2.1 *ORTEP drawing of* ***2*** *at the 50 % probability level. One of two independent molecules in the crystal lattice is shown. Selected bond lengths (Å) and angles (°): O(1A)-C(1A) 1.353(5), O(30A)-C(30A) 1.143(6), C(5A)-C(24A)1.485(5), Mn(1)-C(1A) 2.183(4), C(30B)-Mn(2)-C(32B) 93.5(2).*

Cobalt complex **1** was shown by Waymouth to be prone to ligand substitution, and $CpCo(CO)_2$ could be readily modified by mono and bidentate ligands. In contrast to this finding, manganese complex **2** proved to be more stable to derivatization with phosphine ligands.

Irradiation of **2** with 365 nm light in the presence of one equivalent of a monodentate or bidentate phosphine resulted in a ligand substitution reaction replacing one or two of the carbonyl ligands, respectively (Scheme 2.2). Yields for this reaction after recrystallization ranged from 50% to 83% depending on the ligand. Ph_3P (Figure 2.2) and Cy_3P (Figure 2.3) substituted manganese complexes showed good stabilities and could be easily isolated. However, upon their addition, the metal complexes became much less soluble in acetonitrile compared to the starting complex **2**.

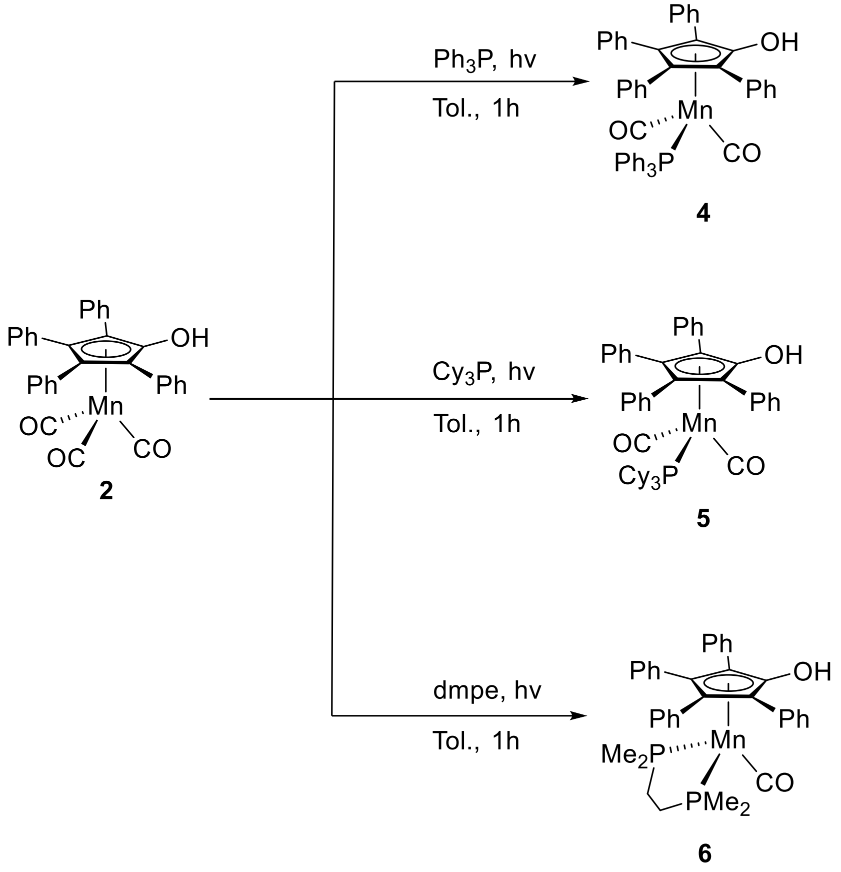

__Scheme 2.2__ Synthesis of phosphine-substituted manganese complexes.

Substitution of two CO ligands by a 1,2-bis(dimethylphosphino)ethane (dmpe) produced the desired product in 80% NMR yield along with an intractable mixture of by-products. Further complicating its isolation, the product composition was unusually sensitive to changes in solvent conditions. Dissolution in acetonitrile initially appeared to produce a stable mixture; however, over 15 min, an orange solid precipitated out of solution, likely due to a ligand substitution reaction with acetonitrile. The complex is stable indefinitely in benzene and methylene chloride;

however, adding pentane to these solutions results in the precipitation of a paramagnetic yellow solid. Unfortunately, this did not result in the removal of unwanted by-products. Luckily, there was enough of the desired product in the crude material to grow crystals (Figure 2.4) and obtain NMR and IR spectra. An interesting feature of the crystal structure of **6** compared to **2** was the noticeably tight bite angle of the phosphine ligands at 85° (the angle between CO ligands was between 90°-93°). This difference is possibly enforced by the dmpe linker carbons which attain a nearly perfect tetrahedral geometry as well as differences in π-backbonding ability of the ligands (CO vs dmpe).

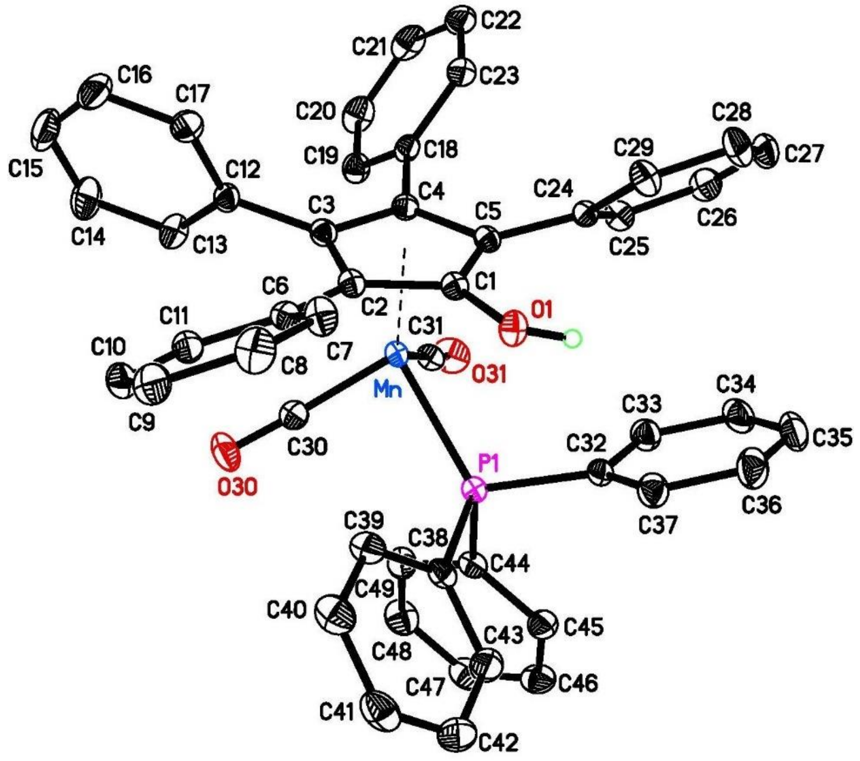

Figure 2.2 ORTEP drawing of **4** at the 50% probability level. Selected bond lengths (Å) and angles (˚): O(30)-C(30) 1.159(2), O(1)-C(1) 1.363(2), Mn-C(1)2.2119(18), C(5)-C(24) 1.477(3).

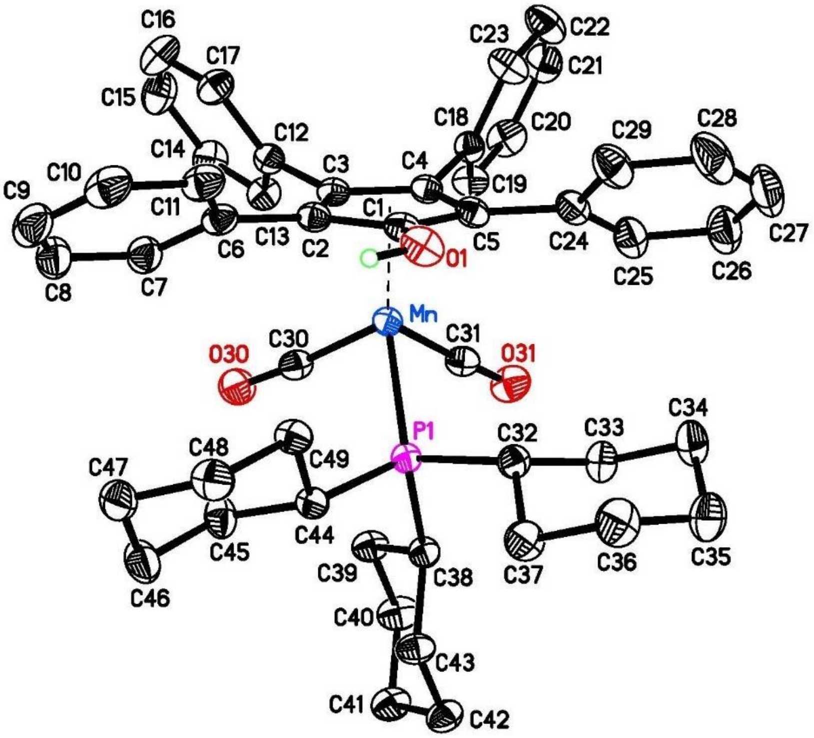

Figure 2.3 ORTEP drawing of **5** at the 50% probability level. Selected bond lengths (Å) and angles (˚): O(30)-C(30) *1.157(3)*, O(1)-C(1) *1.358(2)*, Mn-C(1) *2.2580(18)*, C(5)-C(24) *1.480(3)*.

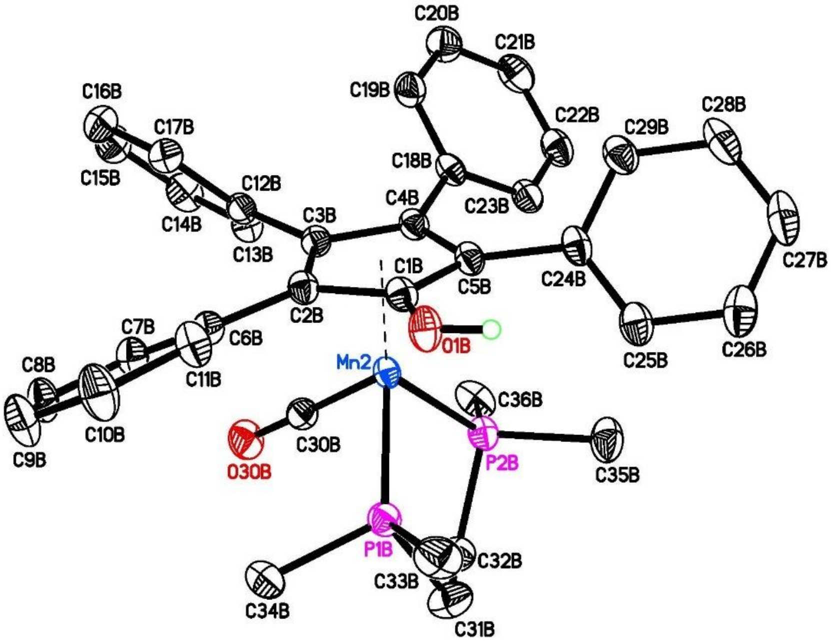

Figure 2.4 *ORTEP drawing of* ***6*** *at the 50 % probability level. One of two independent molecules in the crystal lattice is shown. Selected bond lengths (Å) and angles (˚): O(30B)-C(30B) 1.179(2), O(1B)-C(1B) 1.366(2), Mn(2)-C(1B) 2.2045(17), C(5B)-C(24B) 1.491(2), P(2B)-Mn(2)-P(1B) 85.01(2), C(31B)-C(32B)-P(2B) 108.13(14).*

Attempts to substitute two CO ligands with other bidentate ligands were less successful. Addition of 1,2-bis(diphenylphosphino)ethane (dppe), 1,2-bis(diphenylphosphino)methane (dppm) or 1,2-bis(dimethylphosphino)methane (dmpm) to manganese complex **2** followed by irradiation by 365 nm light produced bright red solutions. However, upon evaporation and redissolution of the residue in C_6D_6 or CD_2Cl_2, brown solutions were produced, and the resulting spectra were broad and indicative of a mixture of products. The bite angle and steric bulk of the bidentate phosphine ligands are likely important in stabilizing the resulting compounds.

While carbonyl ligands on cobalt complex **1** could not be substituted to yield a stable complex, another avenue to diversify the system was to oxidize the cobalt complex by two electrons to produce a cationic complex with an η^4-tetracyclone, rather than a 1,2,3,4-tetraphenyl-hydroxycyclopentadienyl ligand. This cationic complex would likely be immune to the reductive decomposition pathway seen with **1**. To achieve this oxidation, triphenylcarbenium tetrafluoroborate ($[Ph_3C]BF_4$), a bifunctional hydride acceptor/1e$^-$ acceptor, was mixed with the complex in a 1:1 molar ratio in acetonitrile. $[Ph_3C]BF_4$ can accept two electrons and a proton from cobalt complex **1**, producing a cationic tetracyclone cobalt tris(acetonitrile) complex and triphenylmethane (Scheme 2.3). However, one-electron transfer reaction also unavoidably occurs, producing the so called Gomberg dimer, the product of combining two triphenyl methyl radicals. When the latter process occurs, **1** consumes two equivalents of $[Ph_3C]BF_4$. This affects the stoichiometry of the reaction and produces unwanted HBF_4; however, control of reaction conditions and recrystallizations seem to remove most of the unwanted by-products.

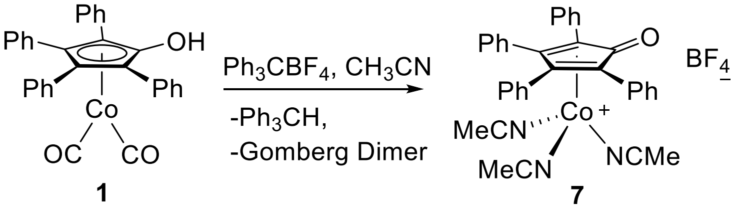

Scheme 2.3 *Synthesis of cationic cobalt complex 7.*

Complex **7** was isolated as a red solid in 60% yield by precipitating the complex out of acetonitrile through the addition of diethyl ether and cooling to –20 °C (Figure 2.5). The complex could be redissolved in acetonitrile but was insoluble in benzene and diethyl ether. It could be dissolved into methylene chloride; however, it gradually decomposed to paramagnetic products. Addition of bidentate ligands to an acetonitrile solution of **7** resulted in a color change from purple to red. Substitution reactions followed a similar trend as the substitution reactions with the manganese complex **2**, where the steric bulk of the coordinating ligand affected its ability to form stable complexes.

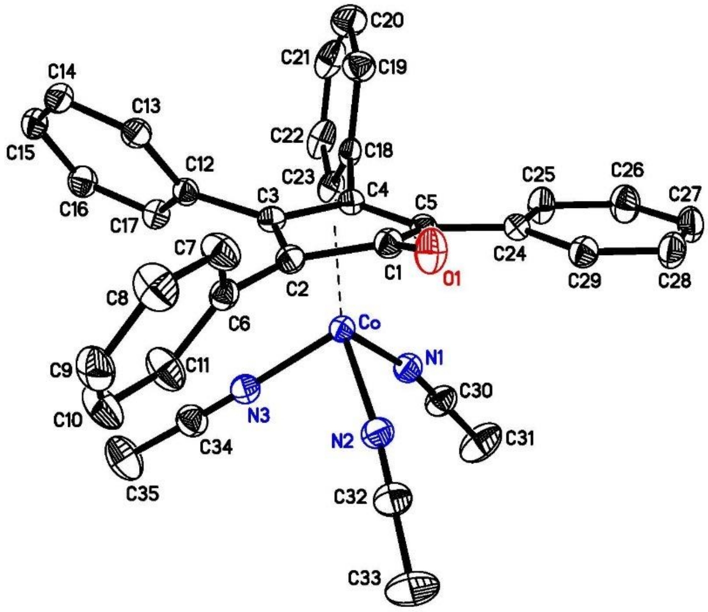

***Figure 2.5** ORTEP drawing of 7 at the 50 % probability level. Selected bond lengths (Å) and angles (˚): Co-N(1) 1.9471(14), O(1)-C(1), C(5)-C(24) 1.479(2), C(1)-C(2) 1.490(2), C(2)-C(3) 1.426(2), 1.2216(19), N(1)-Co-N(2) 90.53(6),*

Mixing **7** with one equivalent of 2,2’-bipyridine resulted in a color change from dark purple to dark red (Scheme 2.4). The proton NMR spectrum of the resulting solution is indicative of coordination of 2,2’-bipyridine to the cobalt center by displacing two acetonitrile ligands. Over several hours, a brown solid precipitated out of solution and could not be redissolved in acetonitrile. Additionally, new peaks appeared downfield in the 14-20 ppm region of the proton

NMR spectrum, indicating the presence of paramagnetic species, possibly produced by charge transfer from the cobalt to the 2,2'-bipyridine ligand.

Mixing **7** with one equivalent of dmpe in acetonitrile produced a dark red solution after stirring for 30 min at room temperature. The solution was stable over days in a sealed NMR tube. Addition of diethyl ether to the solution and cooling to –20 °C resulted in the formation of a light orange precipitate. Dissolution of this precipitate in methylene chloride and filtration through Celite yielded a clear red solution. Phosphorus NMR spectrum showed a sharp singlet; however, proton NMR spectrum showed the formation of side products in the aliphatic region, which were likely cobalt acetonitrile clusters reported by Waymouth.[27]

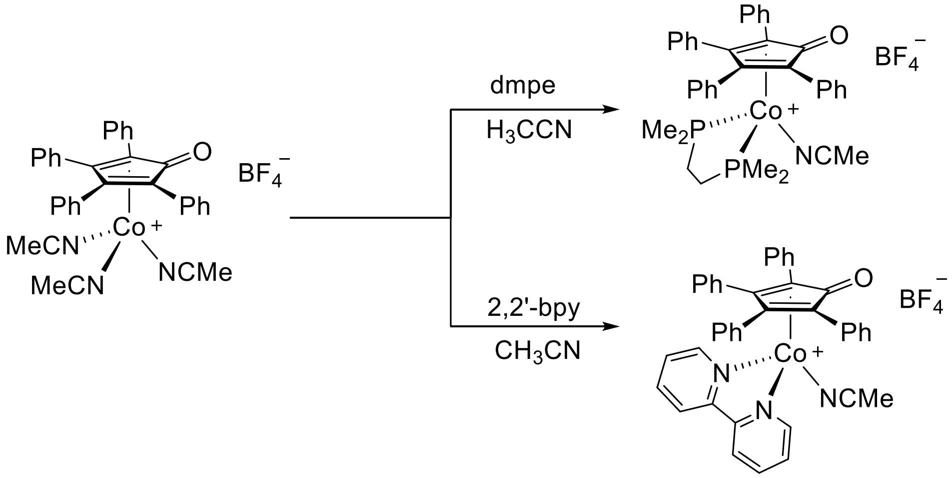

Scheme 2.4 *Synthesis of substituted cationic cobalt complexes **8** and **9**.*

2.3 Electronic Properties of the Complexes

2.3.1 Acidities

The acidities of the cobalt complex **1** and manganese complex **2** were investigated via proton and carbon NMR techniques commonly used to determine the pK_a values of nitrogen-containing bases. The theory behind the method is that in an equilibrium mixture of acid and conjugate base, the NMR spectrum will show only one set of resonances. This is because any individual molecule of acid or conjugate base is rapidly shifting between these two states and cannot be resolved on the NMR timescale. However, the acid and conjugate base are two distinct molecules with distinct chemical shifts, and thus the resonance that their mixture produces in the NMR spectrum is the mole fraction weighted average of the two species. Thus, if the resonances for the pure acid and pure conjugate base are known, an estimation of the mole fraction of each in a mixture can be obtained. From there, it is relatively straightforward to determine the pK_a of the acid.

This determination requires that a reference base of known basicity be used to deprotonate the acid. The choice of reference base here is important because the conjugate base must still be completely soluble in acetonitrile and must have an NMR spectrum different enough from the acid so that the error in measurement of peak position has as little impact as possible. I the case of **1** and **2**, the ideal reference bases found were triethylamine and Hünig's base. Both bases are reasonably well characterized in terms of basicity and appeared to be capable of fully deprotonating both metal complexes. Using these bases and the reported method, the pK_a for both complexes were determined (Figure 2.6).

The pK_a for cobalt complex **1** in acetonitrile was determined to be 18.7 ± 0.2 using triethylamine and 18.7 ± 0.2 using Hünig's base. For manganese complex **2** in acetonitrile, the pK_a was determined to be 18.9 ± 0.5 using triethyl amine and 18.7 ± 0.2 using Hünig's base. The pK_a values of these complexes are too close to definitively say one is more acidic than the other; however, large error bars on the measurement may contribute to this ambiguity. For reference, these acidity values are in the range of polyfluorinated alcohols and polyfluorinated carboxylic acids.[63] It should be noted, however, that transition metal carbonyl hydrides have been known to be significantly acidic.[64]

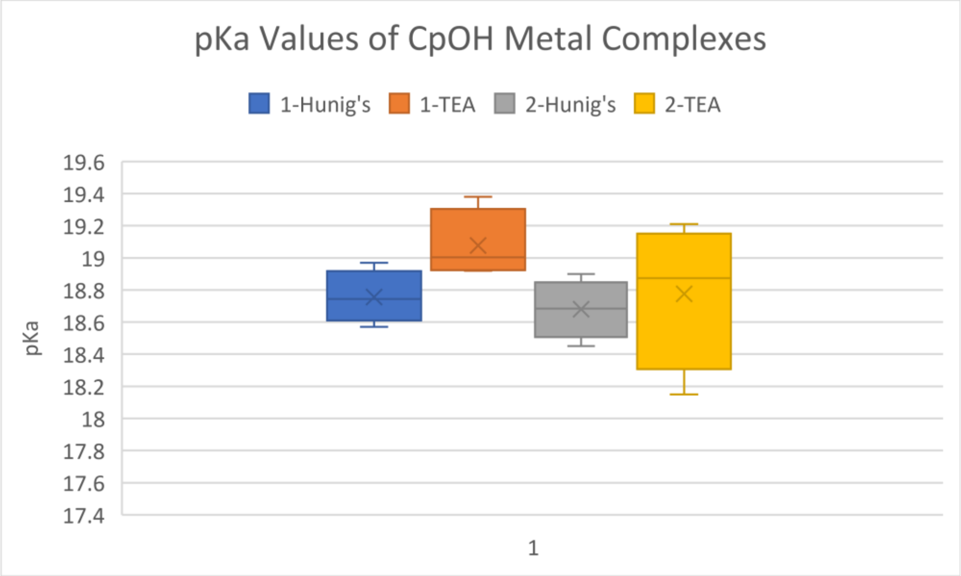

Figure 2.6 *pK_a values determined by NMR spectroscopy.*

2.3.2 Carbonyl Stretch

The carbonyl stretching bands for the series of complexes were much more informative and followed a trend seen in manganese and cobalt cyclopentadienyl carbonyl complexes (Table 2.1). Despite having more CO ligands, manganese complex **2** has a lower CO stretching frequency than cobalt complex **1**, indicating that there is more back donation from manganese to the CO ligands and thus a stronger bond. From this perspective, manganese-bound cyclopentadienone ligands have less localized electron density on the ligand when compared to cobalt complex **1**. Without highly localized charge, hydride transfer from hydroxycyclopentadienyl may not be possible. It is interesting to note that these differences in CO stretches do not correlate well with the acidities.

***Table 2.1** Carbonyl stretches for a series of Co(I) and Mn(I) complexes*

Complex	CO Stretch (cm^{-1})
$(Ph_4C_5OH)Co(CO)_2$ (**1**)	2010, 1954
$(Ph_4C_5OH)Mn(CO)_3$ (**2**)	2005, 1919
$(Ph_4C_5OH)Mn(CO)_2(PPh_3)$ (**4**)	1918, 1854
$(Ph_4C_5OH)Mn(CO)_2(PCy_3)$ (**5**)	1905, 1834
$(Ph_4C_5OH)Mn(dmpe)(CO)$ (**6**)	1808
$Cp^*Mn(CO)_3$[65]	2010, 1927
$Cp^*Co(CO)_2$[27]	2011, 1949

2.4 Hydride Transfer Reactivity of $(Ph_4C_5OH)Co(CO)_2$

To gain insight into the mechanism by which $[Ph_3C]BF_4$ reacts with these group 7 and 9 metal carbonyl complexes bearing a 1,2,3,4-hydroxocyclopentyl ligand, a series of experiments were performed to evaluate different reaction conditions effects.

The observation of Gomberg's dimer seemed to indicate that hydride transfer was taking place in two steps. First, a one-electron transfer from **1** to $[Ph_3C]BF_4$ to make [**1**']BF_4 and Ph_3C radical, then a hydrogen atom transfer from [**1**']BF_4 to Ph_3C radical to make Ph_3CH and **7**. The formation of the Gomberg dimer is then explained by diffusion of two Ph_3C radicals together before they can react with [**1**']BF_4. The inverse concentration dependence on the formation of Gomberg dimer also supports this mechanism; however, it could be more complicated than shown (Scheme 2.5).

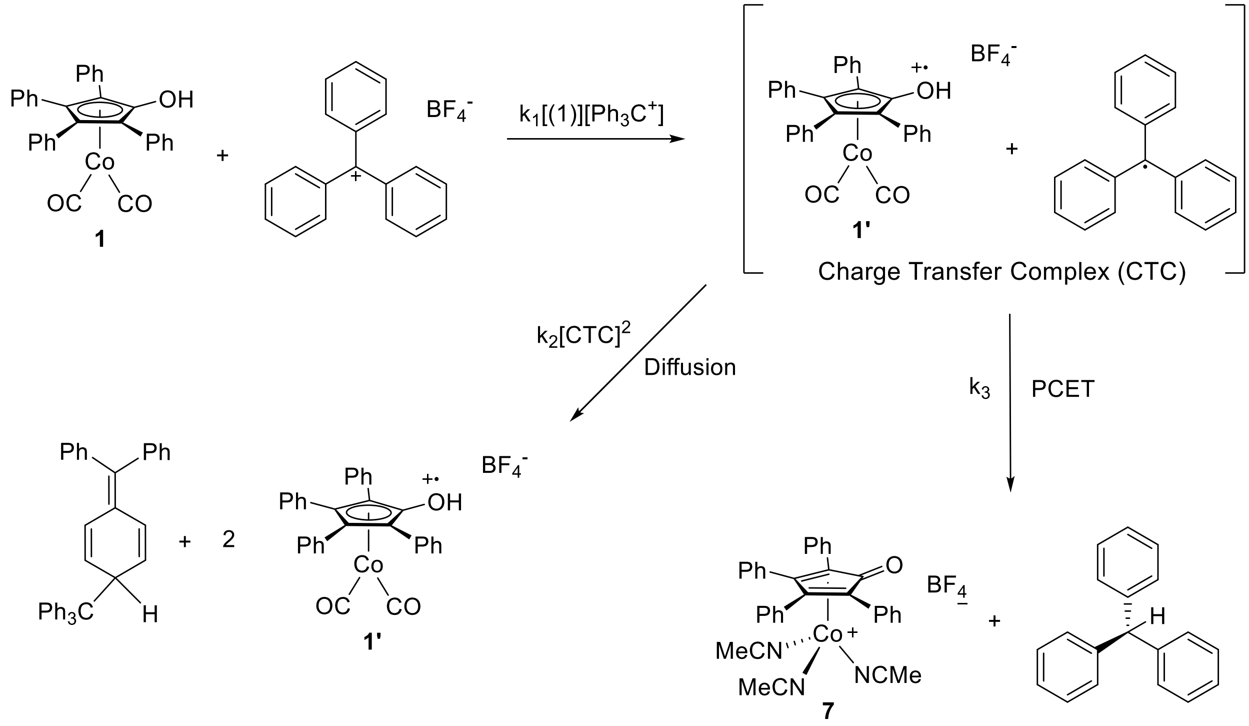

__Scheme 2.5__ Possible mechanism for hydride/1e- transfer from __1__ to [Ph_3C]BF_4

Another interesting mechanistic feature of the reaction is the observed evolution of carbon monoxide gas (no hydrogen gas evolution was observed). This indicates that, in order to form a stable cobalt complex, a coordinating ligand must be present in solution to take the place of the CO ligands. Acetonitrile obviously assumed this role given the crystal structures obtained; however, it has been shown in previous work[66] that the BF_4 anion can serve as a weakly coordinating ligand which can stabilize metal species after hydride transfer. To test if coordinating ligands were necessary, cobalt complex **1** and [Ph_3C]BF_4 were combined in methylene chloride. Minimal reaction was observed over several hours (Figure 2.7). However, when three equivalents of acetonitrile were added, the solution quickly evolved CO gas and the yellow and red solution quickly turned dark purple, indicating the consumption of the [Ph_3C]BF_4 and formation of the cobalt complex **7**. This suggests that a ligand substitution is necessary to drive the loss of CO and make the electron transfer irreversible. It should be noted that when [Ph_3C]BF_4 was replaced by Ph_3CCl, no acetonitrile was necessary, and the reaction would proceed in noncoordinating solvents. This can be explained by the greater donor strength of Cl anion.

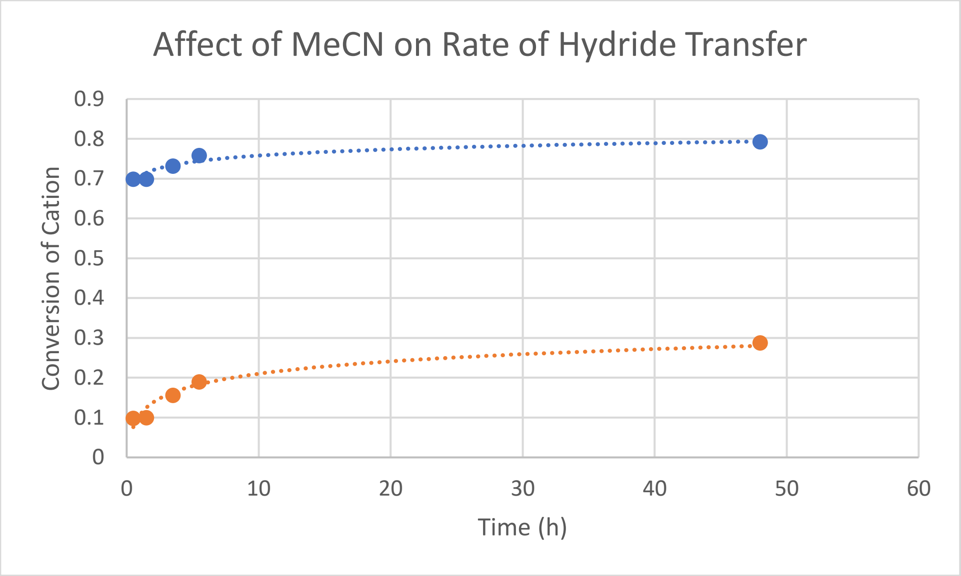

Figure 2.7 *Effect of coordinating ligand (blue dots, with MeCN; orange dots, without MeCN) on the extent of complex oxidation.*

It is well known that the presence of external bases affects PCET reactions, and in some cases, accelerates them. Here, cobalt complex **1** and an amine-type base (triethylamine or pyridine) were premixed in acetonitrile and then a solution of [Ph_3C]BF_4 was added. The [Ph_3C]BF_4 was rapidly consumed with concomitant loss of CO; however, the formation of Ph_3CH was almost entirely suppressed and the formation of Gmberg's dimer was heavily favored. A possible mechanism explaining this observation is that the added base deprotonates the radical cation intermediate, and the resulting cobalt complex is too slow in transferring the hydrogen atom for the Ph_3CH to form. This may also suggest that it is necessary for the proton to be bound to the metal complex for it to transfer as a hydride.

Lastly, the idea of a polarity reversal catalyst was briefly investigated. The rate of a hydrogen atom transfer reaction is often kinetically controlled and the polarity theory of hydrogen atom transfer states that the rate of the reaction is determined by the charge matching in the transition state. It has been shown[67] that for many hydrogen atom transfer reactions, the addition of an easily polarizable additive can drastically accelerate the process. Common additives are thiols, boranes and metal carbonyls. Here, the ability of $Mn_2(CO)_{10}$ to act as a hydrogen atom transfer reagent for the hydride transfer from cobalt complex **1** to $[Ph_3C]BF_4$ was investigated. 10 mol% of $Mn_2(CO)_{10}$ was premixed with cobalt complex **1** and then a solution of $[Ph_3C]BF_4$ in acetonitrile was added dropwise. Again, the reaction proceeded quickly with loss of CO observed immediately upon addition. The effects were not dramatic; however, it seems that addition of $Mn_2(CO)_{10}$ increased the amount of Ph_3CH relative to Gomberg dimer by ~50%. This suggests that $Mn_2(CO)_{10}$ may act as a hydrogen atom transfer reagent during the multistep of the hydride transfer reaction.

2.5 Reactivities of the Manganese Complexes

After the manganese and cobalt complexes were characterized, it became clear that the electronic properties between the two groups of compounds were quite different. While manganese complex **2** and cobalt complex **1** were similar in their measured acidities, the carbonyl stretching bands in the IR spectra suggested that the extent of backbonding was very different. Given the result, it seemed that manganese system would less likely to donate two electrons to a substrate when compared to the cobalt system and that increased electron density on the manganese might be necessary to alter its reactivity in this way.

Manganese complex **2** showed no reactivity towards [Ph_3C]BF_4 over days in acetonitrile (Figure 2.8); heating to 80 ºC for 2 h did not affect conversion of the cation either. Manganese complex **4** showed some conversion of the cation in hours (in methylene chloride), and over 2 days, about 20% of the manganese complex had reacted with the cation. Manganese complex **5** appeared to react faster than **4**, which could be explained by the greater donor ability of alkyl phosphines compared to aryl phosphines; however, the rate increase was no more than a factor of 2-3. Manganese complex **6** reacted very rapidly with [Ph_3C]BF_4 in acetonitrile, producing a mixture of Gomberg dimer and triphenyl methane (Table 2.2) and reaching full conversion in 10 min. Like cobalt complex **1**, upon addition of [Ph_3C]BF_4 to manganese complex **6**, an immediate gas evolution was observed while no hydrogen was observed in the proton NMR, suggesting that CO gas was being released from the complex. This trend in reactivity supports the idea that increased electron density in the form of phosphines was necessary for this class of manganese complexes to undergo net hydride transfer to [Ph_3C]BF_4.

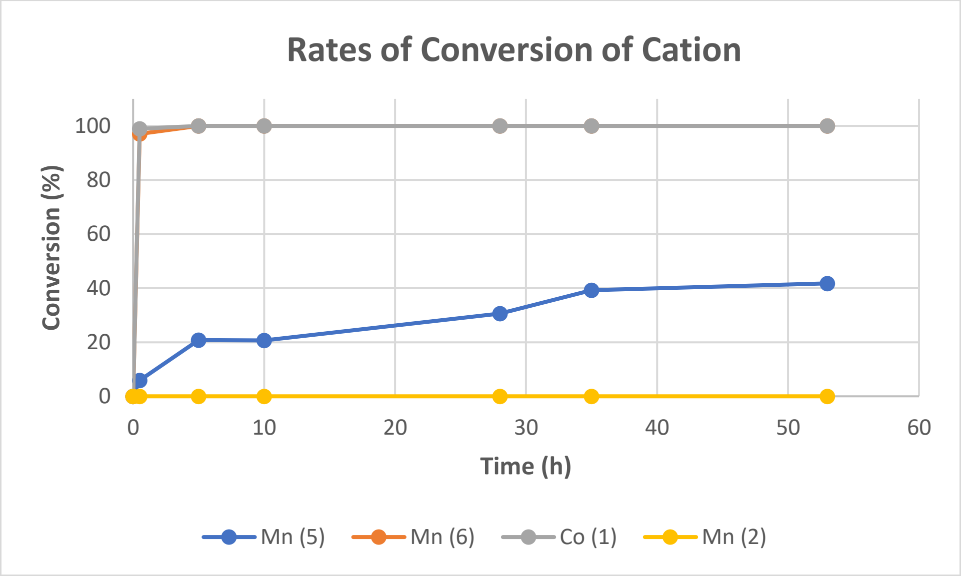

__Figure 2.8__ Conversions of [Ph_3C]BF_4 by manganese and cobalt metal complexes over time.

***Table 2.2** Percent of converted trityl cation that was converted to triphenyl methane.*

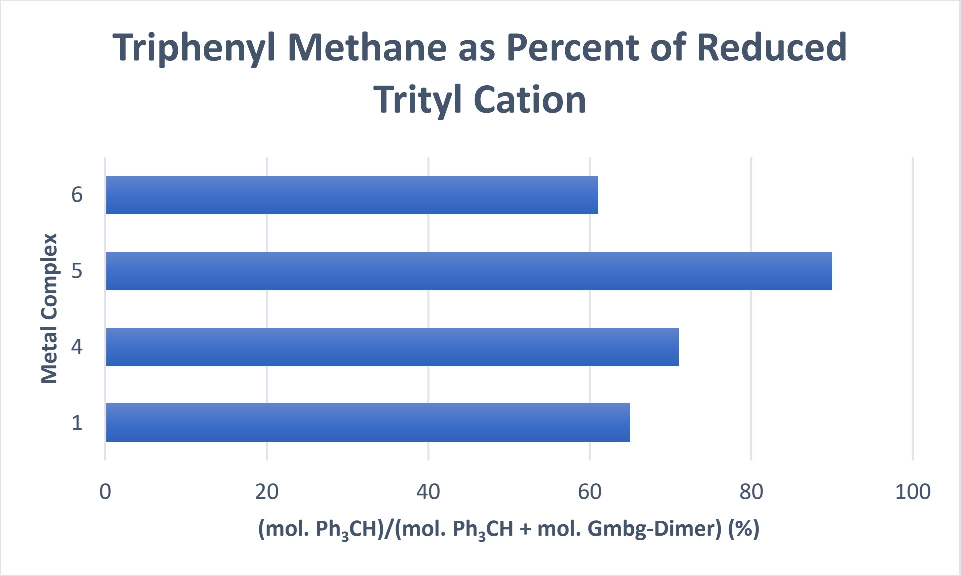

Given that the electron rich manganese complexes could be isolated, it seemed that interesting reactivity might be observed when these complexes were mixed with a strong acid. Cobalt complex **1** was shown by Waymouth[27] to decompose in the presence of strong acids, with the tetracyclone ligand being reduced.[27] In contrast, manganese complex **2** was stable to triflic acid in acetonitrile even at elevated temperatures. Reaction of manganese complex **4** showed minimal reactivity towards triflic acid and manganese complex **5** reacted to form trace amounts of a hydride and other unidentified products. Manganese complex **6** reacted very rapidly with triflic acid in acetonitrile, evolving hydrogen and carbon monoxide gas and forming manganese hydride complex **10** (Scheme 2.6) which slowly decomposed in 24 h. This decomposition could be slowed down if the hydride were formed in methylene chloride; however, no crystals could be isolated from the solution. NMR data indicate that the reaction generates two manganese products, one bearing the hydride and the other possibly interacting with the first in an agostic fashion.

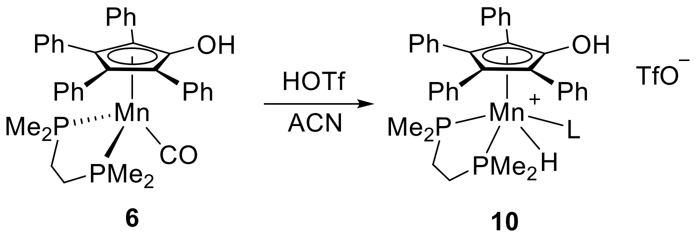

*Scheme 2.6 Formation of a manganese hydride via protonation of **6** with HOTf*

2.6 Catalytic Screening

Given the success of cationic cobalt[42] and manganese hydrides[68] in various organic and inorganic transformations, we were interested to see if the cationic metal complexes we isolated had any catalytic applications. We chose the cobalt dmpe complex **8** and manganese hydride complex **10** for screening of hydrogenation reactivity. We also investigated cobalt complex **7** for C–H bond activation activity with 2-phenyl-pyridine.

In the case of manganese complex **10**, the hydride was formed in situ by addition of the acid and followed by addition of the substrate. If the substrate and acid were premixed, and then added to manganese complex **10**, no hydride would form and instead, a single electron transfer process predominated which yielded an uncharacterized mixture of products. In the case of cobalt complex **8**, no confirmation of hydride formation could be obtained, so the cationic complex was added as a precatalyst with the hope that it would form a hydride in situ.

Table 2.3 *Attempted hydrogenation reactions catalyzed by* ***9*** *and* ***10****.*

$$H_2\text{ (80psig) + substrate} \xrightarrow[\text{24h}]{\textbf{9}\text{ or }\textbf{10}\text{ (10 mol \%)}}$$

Complex	*Substrate*	*Solvent*	*Temp. (°C)*	*Conversion (%)*
9	PhCHO	THF	RT	0
9	PhCH=CH$_2$	THF	RT	0
10	PhCHO	THF	RT	0
10	PhCHO	THF	60	0
10	PhCH=CH$_2$	THF	RT	0
10	PhCHO	Toluene	RT	0

Hydrogenation of benzaldehyde and styrene using manganese hydride complex **10** or cobalt complex **9** were unsuccessful (Table 2.3). Heating these mixtures resulted in decomposition to yield the free tetracyclone ligand as evidenced by the change in color of the solution.

Cationic CpCo(III) complexes have been successfully used to activate C–H bonds[69] through the chelate effect. This methodology has been applied to numerous organic transformations using both nucleophilic and electrophilic coupling partners. Because cobalt complex **7** closely resembles some of these cationic complexes used in C–H bond activation, it seemed plausible that it would be competent in this reaction. However, the reaction would likely require that the cobalt complex be able to oxidatively add a C–H bond, which could be difficult given the back-bonding taking place to the bound tetracyclone ligand.

***Table 2.4** Attempted C–H bond activation of 2-phenylpyridine catalyzed by cobalt complex 7.*

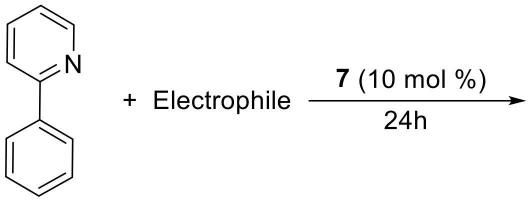

Electrophile	*Solvent*	*Temp. (°C)*	*Conversion*
PhC≡CH	THF	80	0
Cinnamaldehyde	THF	80	0
PhC≡CH	THF	60	0
PhC≡CH	CH_2Cl_2	55	0

No C–H bond activation was observed in these reactions (Table 2.4) and stochiometric reactions between cobalt complex **7** and 2-phenyl pyridine resulted in the formation of Co(II) species, suggesting that the complex may decompose under the reaction conditions.

2.7 Experimental

All compounds described in this chapter were prepared under an argon atmosphere using standard glovebox and Schlenk techniques. Benzene-d_6, acetonitrile-d_3 and methylene chloride-d_2 were purchased from Cambridge Isotope Laboratories, Inc. Benzene-d_6 was dried over sodium-benzophenone and distilled under an argon atmosphere. Acetonitrile-d_3 and acetonitrile were dried over CaH_2 and distilled under an argon atmosphere. Methylene chloride-d_2 was dried over 4 Å molecular sieves and degassed by three freeze-pump-thaw cycles. Acetic acid was dried over 4 Å molecular sieves and then deoxygenated by bubbling argon for 0.5 h. All other dry and oxygen-free solvents used for synthesis and workup (THF, diethyl ether, toluene, and pentane) were collected from an Innovative Technology solvent purification system. Benzaldehyde was freshly distilled prior to use. ^{1}H, ^{13}C{^{1}H}, and ^{31}P{^{1}H} NMR spectra were recorded on a Bruker Avance 400 MHz NMR spectrometer. Chemical shift values in ^{1}H and ^{13}C{^{1}H} NMR spectra were referenced internally to the residual solvent resonances. ^{31}P{^{1}H} NMR spectra were referenced externally to 85% H_3PO_4 (0 ppm). Infrared spectra were recorded on a PerkinElmer Spectrum Two FT-IR spectrometer equipped with a smart orbit diamond attenuated total reflectance (ATR) accessory.

Synthesis of (Ph_4C_5OH)Co$(CO)_2$

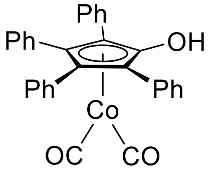

1

Procedure used is based on the originally reported synthesis of the compound with some modification.[27] To an oven-dried Schlenk flask equipped with stir bar were placed $Co_2(CO)_8$ (1.00 g, 2.92 mmol) and 50 mL of acetonitrile. The brown mixture evolved a considerable amount of CO gas. The solution was stirred at room temperature for 30 min over which time the color changed to hazy pink. To this solution, tetracyclone (1.19 g, 3.10 mmol) was added and an additional 5 mL of acetonitrile was used to wash the residual solids into solution. The opaque purple mixture, still containing significant amounts of undissolved tetracyclone, was stirred under argon for 24 h, over which time the color became dark red. The acetonitrile was evaporated, and the black tar residue was redissolved in 20 mL of toluene. This brown solution was passed through a pad of celite and then washed out with an additional 10-15 mL of toluene. The filtrate was added dropwise to 100 mL of pentane in which a tan precipitate formed. The brown filtrate was removed by filtration and the precipitate was washed with 15 mL of pentane. Drying under a flow of argon gave a light tan solid as the crude product. This product was redissolved in 20 mL of acetonitrile and acetic acid was added dropwise. The solution was stirred for 3 h and then filtered through celite to remove purple Co(II) solid. Solvent was removed from the filtrate under vacuum yielding a red oil which fractionally crystallized to yield red crystals as the product mixed with more purple Co(II) salts. Methylene chloride (5 mL) was used to selectively dissolve the red crystals and was passed through celite to remove the remaining Co(II) salts. To the methylene chloride was added 15 mL of pentane and the solution was placed in a freezer at –20 °C for 24 h, over which time the product formed as dark red crystals in 55% yield. NMR data are consistent with those reported in the literature.[6]

Synthesis of [$(Ph_4C_5O)Co(NCCH_3)_3](BF_4)$

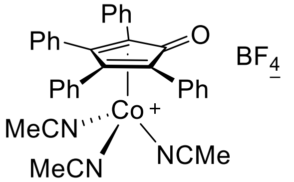

7

To an oven-dried Schlenk flask equipped with stir bar were added cobalt complex **1** (0.50 g) and 10 mL of acetonitrile. To the stirring, orange/red cobalt solution was added a solution of triphenyl carbenium tetrafluoroborate in 5 mL of acetonitrile dropwise over several minutes. The addition of the $[Ph_3C]BF_4$ resulted in a fast color change to deep purple and the evolution of CO gas. After the $[Ph_3C]BF_4$ solution had been completely added, the combined mixtures were allowed to stir for an additional 5 min before 10 mL of pentane was added and the mixture was cooled to –20 °C for 24 h after which time red blocky crystals of the product had formed in 46% yield. ^1H NMR (400 MHz, CD_3CN) δ 7.78 (d, *J* = 8.2 Hz, 4H), 7.52 (d, *J* = 7.5 Hz, 4H), 7.46 (d, *J* = 7.5 Hz, 2H), 7.40 (t, *J* = 7.5 Hz, 2H), 7.33 – 7.16 (m, 8H). $^{13}C\{^1H\}$ NMR (101 MHz, CD_3CN) δ 167.75, 132.76, 130.94, 130.73, 129.18, 128.82, 128.39, 128.09, 127.58, 100.79, 63.55. Selected ATR-IR data (solid, cm^{-1}): 3051 (ν_{Ph-H}), 2098 ($\nu_{C\equiv N}$), 2032 ($\nu_{C\equiv N}$), 1651

($\nu_{C=O}$). ESI-MS m/z Calcd 566.18, found 525.14 (this discrepancy is explained by the loss of CH_3CN under the MS conditions). Anal. Calcd for $C_{35}H_{29}N_3MnOBF_4$: C, 64.34; H, 4.47; N, 6.43; Found: C, 60.42; H, 4.63; N, 7.78.

Synthesis of $(Ph_4C_5OH)Mn(CO)_3$

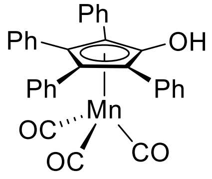

2

Procedure used is based on the originally reported synthesis of the compound with some modification.[28] To an oven-dried Fisher-Porter bottle (FPB) equipped with a stir bar were placed $Mn_2(CO)_{10}$ (0.50 g, 1.46 mmol), tetracyclone (0.56 g, 1.46 mmol) and toluene (15 mL). The FPB apparatus was sealed, placed into an oil bath and heated at 160 °C for 24 h over which time the solution changed from an opaque purple to a slightly cloudy yellow and the pressure in the bottle rose to 60 psig. The solution was cooled, and the pressure was slowly vented. The yellow solution was filtered through celite yielding a clear yellow solution. **Method A:** The yellow solution was added dropwise to 50 mL of pentane, resulting in the formation of a tan precipitate. The precipitate was collected by filtration and washed with 15 mL of pentane. The precipitate was dried under a steady argon stream to yield the crude product, which was redissolved in 15 mL of toluene and 1 mL of water was added. The solution was stirred for 3 h and then filtered through celite to remove Mn(II) salts. The filtrate was evaporated under vacuum and redissolved in 5 mL of Et_2O. 15 mL of pentane was added and the solution was cooled to – 20 °C for 24 h to produce the product as fine yellow crystals in 65% yield. **Method B:** This method is the same as method A, except that the crude product is not isolated by precipitation and instead the filtered mother liquor from the original FPB reaction was combined with 1 mL of water and stirred for 3 h giving the product in 70% yield. ^{1}H NMR (400 MHz, CD_2Cl_2) δ 7.48 – 7.42 (m, 5H), 7.38 – 7.33 (m, 5H), 7.21 – 7.05 (m, 10H), 4.75 (s, 1H). $^{13}C\{^1H\}$ NMR (101 MHz, CD_2Cl_2) δ 225.50, 132.65, 132.51, 131.92, 131.58, 130.48, 128.97, 128.63, 128.04, 127.97, 98.73, 86.71. Selected ATR-IR data (solid, cm^{-1}): 3524 ($\nu_{O–H}$), 3064 (ν_{Ph-H}), 2005 ($\nu_{C≡O}$), 1919 ($\nu_{C≡O}$). Anal. Calcd for $C_{32}H_{21}O_4Mn$: C, 73.29; H, 4.00; Found: C, 73.14; H, 4.02.

Synthesis of (Ph_4C_5OH)Mn(CO)$_2$(PPh_3)

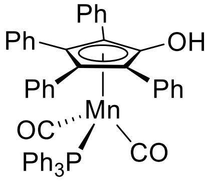

4

To an oven-dried Schlenk flask equipped with a stir bar were placed manganese complex **2** (0.50 g, mmol), Ph_3P (0.25g, 0.95 mmol) and 20 mL of toluene. The solution was irradiated under a flow of argon with a 365 nm blue LED array for 1 h, over which time the solution changed from pale yellow do dark yellow/light orange. The solvent was removed under vacuum and the yellow residue was dissolved in 5 mL of methylene chloride and filtered through a pad of celite. 15 mL of pentane was added to the filtrate and the mixture cooled to –20 °C for 24 h after which time boxy yellow crystals of the product had formed in 83% yield. ^{1}H NMR (400 MHz, CD_2Cl_2) δ 7.31 (dd, *J* = 14.5, 6.5 Hz, 8H), 7.25 – 7.03 (m, 21H), 6.96 (d, *J* = 7.7 Hz, 6H), 3.23 (s, 1H). $^{31}P\{^1H\}$ NMR (162 MHz, CD_2Cl_2) δ 82.91$^{13}C\{^1H\}$ NMR (101 MHz, CD_2Cl_2) δ 234.57 (d, *J* = 22.9 Hz), 135.68, 133.56, 133.45, 133.37, 133.28, 133.08, 130.59, 129.75, 129.73, 128.67, 128.26, 128.16, 127.42, 127.26, 127.07, 97.97, 84.00. Selected ATR-IR data (solid, cm^{-1}): 3490 ($\nu_{O–H}$), 3055 (ν_{Ph-H}), 1918 ($\nu_{C≡O}$), 1854 ($\nu_{C≡O}$). HRMS (ESI) calcd (found) for $[C_{49}H_{35}O_3PMn]^+$ 758.17433 (758.17404). Anal. Calcd for $C_{49}H_{35}O_3MnP$: C, 77.57; H, 4.783; Found: C, 70.92; H, 4.62.

Synthesis of $(Ph_4C_5OH)Mn(CO)_2(PCy_3)$

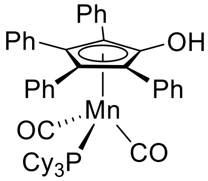

5

To an oven-dried Schlenk flask equipped with a stir bar were placed manganese complex **2** (0.50 g, mmol), Cy_3P (0.267g, 0.95 mmol) and 20 mL of toluene. The solution was irradiated under a flow of argon with a 365 nm blue LED array for 1 h, over which time the solution changed from pale yellow do dark yellow/light orange. The solvent was removed under vacuum and the yellow residue was dissolved in 10 mL of methylene chloride and filtered through a pad of celite. 10 mL of acetonitrile was added to the filtrate and the mixture cooled to –20 °C for 24 h after which time long yellow crystals of the product had formed in 78% yield. ^1H NMR (400 MHz, CD_2Cl_2) δ 7.67 – 6.98 (m, 20H), 4.60 (s, 1H), 1.93 (q, 3H), 1.76 (d, 6H), 1.51 (m, 9H), 1.27 – 1.04 (m, 6H), 0.87 (m, 9H). $^{31}P\{^1H\}$ NMR (162 MHz, CD_2Cl_2) δ 76.66. $^{13}C\{^1H\}$ NMR (101 MHz, CD_2Cl_2) δ 237.23, 236.99, 134.11, 133.59, 133.45, 131.40, 130.43, 129.35, 128.72, 128.55, 127.18, 127.08, 126.97, 96.71, 82.21, 37.42, 37.26, 30.12, 27.84, 27.75, 26.45. Selected ATR-IR data (solid, cm^{-1}): 3542 ($\nu_{O–H}$), 2925 (ν_{Csp3-H}), 1905 ($\nu_{C≡O}$), 1834 ($\nu_{C≡O}$). HRMS (ESI) calcd (found) for $[C_{49}H_{53}O_3PMn]^+$ 776.31518 (776.31536). Anal. Calcd for $C_{49}H_{53}O_3MnP$: C, 75.76; H, 7.01; Found: C, 75.56; H, 7.46.

Synthesis of $(Ph_4C_5OH)Mn(dmpe)(CO)$

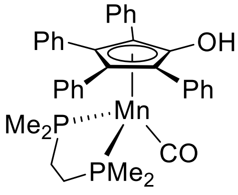

6

To an oven-dried Schlenk flask equipped with a stir bar were placed manganese complex **2** (0.50 g, mmol), dmpe (0.14g, 128.4 μL, 0.95 mmol) and 20 mL of toluene. The solution was irradiated under a flow of argon with a 365 nm blue LED array for 1 h, over which time the solution changed from pale yellow do bright red. The solvent was removed under vacuum and the red residue was dissolved in 10 mL of methylene chloride and filtered through a pad of celite. Solvent was evaporated and the red oil was allowed to slowly crystallize giving a 50% yield. ^{1}H NMR (400 MHz, C_6D_6) δ 7.72 (d, *J* = 7.7 Hz, 4H), 7.61 – 7.55 (m, 4H), 7.19 – 7.08 (m, 6H), 7.02 (d, *J* = 7.2 Hz, 6H), 3.67 (s, 1H), 1.51 (d, *J* = 5.3 Hz, 4H), 1.29 – 1.09 (m, 4H), 1.07 – 0.99 (m, 4H). ^{31}P NMR (162 MHz, C_6D_6) δ 79.74. $^{13}C\{^1H\}$ NMR (101 MHz, C_6D_6) δ 216.89 (t, J = 24.4 Hz), 137.65, 133.01, 132.98, 131.55, 129.09, 128.33, 127.20, 126.2, 126.18, 125.46, 98.08, 92.70, 17.28, 16.28 (d, *J* = 26.7 Hz). Selected ATR-IR data (solid, cm^{-1}): 3517 ($\nu_{O\text{–}H}$), 2899 ($\nu_{csp3\text{-}H}$), 1808 ($\nu_{C\equiv O}$).

Synthesis of [(Ph_4C_5O)Co(dmpe)(MeCN)]BF_4

To an oven-dried Schlenk flask equipped with stir bar were placed cobalt complex **7** (0.50 g, mmol), dmpe (0.115g, 103μL, 0.76 mmol) and 10 mL of acetonitrile. The solution was stirred under a flow of argon for 0.5 h, over which time the solution changed from dark purple to dark red. 10 mL of diethyl ether was added and the solution was cooled to –20 °C for 24 h, over which time orange precipitate formed. The precipitate was filtered off, redissolved in methylene chloride, filtered through celite and precipitated with diethyl ether to collect the final product in

55% yield. ^{1}H NMR (400 MHz, CD_2Cl_2) δ 7.51 – 6.79 (m, 20H), 1.87 (d, *J* = 71.5 Hz, 4H), 1.22 (d, *J* = 8.9 Hz, 6H), 1.08 (d, *J* = 8.9 Hz, 6H). ^{31}P NMR (162 MHz, CD_2Cl_2) δ 43.2

Synthesis of [(Ph_4C_5O)Co(2,2'-bpy)(MeCN)]BF_4

To an oven-dried Schlenk flask equipped with stir bar were placed cobalt complex **7** (0.50 g, mmol), 2,2'-bpy (??) and 10 mL of acetonitrile. The solution was stirred under a flow of argon for 0.5 h, over which time the solution changed from dark purple to dark red. The solution was allowed to sit for 24 h hours at room temperature over which time, brown precipitate formed. The brown precipitate was insoluble in acetonitrile and methylene chloride. Yield not determined. ^{1}H NMR (400 MHz, CD_3CN) δ 18.18 (s, 3H), 14.50 (s, 2H), 9.27 (d, *J* = 5.5 Hz, 2H), 8.26 (d, *J* = 8.0 Hz, 2H), 8.17 (t, *J* = 7.6 Hz, 2H), 7.70 (t, *J* = 6.6 Hz, 2H), 7.45 (t, *J* = 7.2 Hz, 5H), 7.37 – 7.18 (m, 10H), 7.16 (m, 5H)

Chapter 3 – Silyl Group Protected Cyclopentadienones and Their Cobalt Complexes

3.1 Introduction

Small changes in the steric environment around a metal center can have profound impacts on its reactivity. In the case of cyclopentadienone-iron tricarbonyl complexes, it has been shown that the substituent groups at the 2-5 positions of the cyclopentadienone ligand impacts the catalytic activity of the metal complex.[56,70] Given this, we wanted to explore the effect of the bound cyclopentadienone ligand on the reactivity of the cobalt hydroxocyclopentadienyl dicarbonyl complex it formed. The cobalt complexes synthesized bearing these unique ligands will be referred to as Co-Knölker complexes in this chapter in reference to the bifunctional iron hydrogenation catalyst named after Knölker and applied to catalysis by Casey and Guan.[71]

3.2 Synthesis of Cyclopentadienones

Work by the Roewer group has shown that Co-Knölker type complexes can be synthesized via a [2+2+1] cycloaddition reaction of an alkyne with CO mediated by $Co_2(CO)_8$.[29] However, Roewer reported that this reaction is low yielding for the desired product, and the work by other groups has shown that cyclopentadienone synthesis via the cycloaddition approach can be highly sensitive to the structure of the alkyne.[57,72] The work in the Roewer group also showed marked differences from the later work by the Waymouth group discussed in Chapter 2 (Scheme 3.1).[27] Specifically, the Roewer group observed an entirely different intermediate when synthesizing hydroxocyclopentadienyl cobalt complex **1**, namely the dicobalt(0) cyclopentadienone carbonyl complex **2**. Additionally, the products found in Roewer's study were more resistant to heat than those from Waymouth's, and the origin of the proton in Roewer's Co-Knölker complex was ambiguous because of the dry conditions used in the synthesis. For these reasons, further investigation into the properties of these molecules seemed warranted.

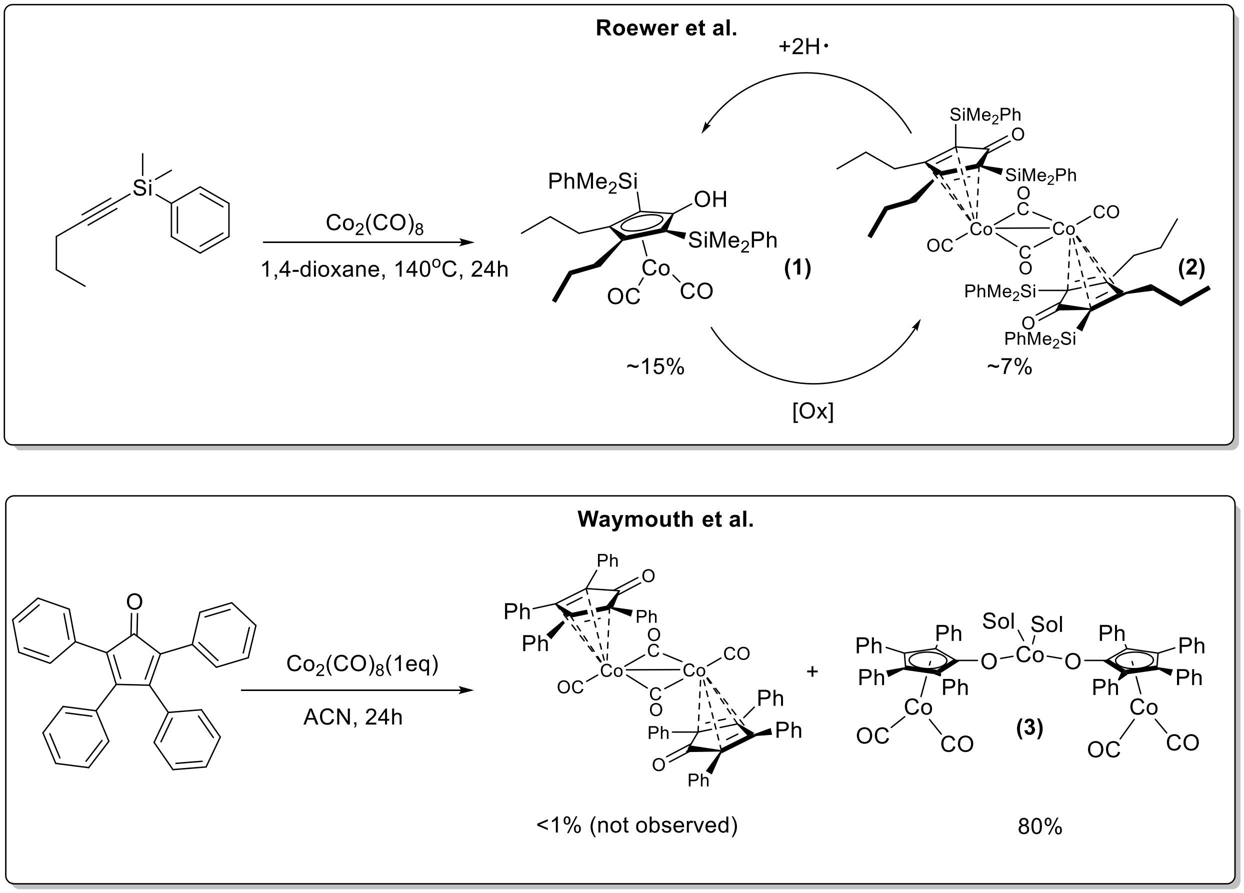

Scheme 3.1 Differences in ligands affects stability of Co(0) cluster.

Replicating Roewer's synthesis of complex **1** seemed to be a natural place to start an investigation into these Co-Knölker complexes. In our hands, the reported procedure produced the desired hydroxocyclopentadienyl cobalt carbonyl complex **1** in 20% yield. Unfortunately, expanding the scope of the synthesis to other alkynes proved unsuccessful. Heating one equivalent of bis-1,8-trimethylsilyl-1,7-octadiyne with one equivalent of $Co_2(CO)_8$ in 1,4-dioxane in a sealed Fisher-Porter bottle did not yield the desired product, but instead produced a cobalt carbonyl alkyne cluster (Figure 3.1). $NaCo(CO)_4$ was briefly investigated as a possible [2+2+1] mediator. The low oxidation state of Co(-I) should make 2e$^-$ oxidative addition more efficient;[73] however, production of the Co(-I) reagent was difficult and its reaction with alkynes produced an intractable mixture of paramagnetic products.

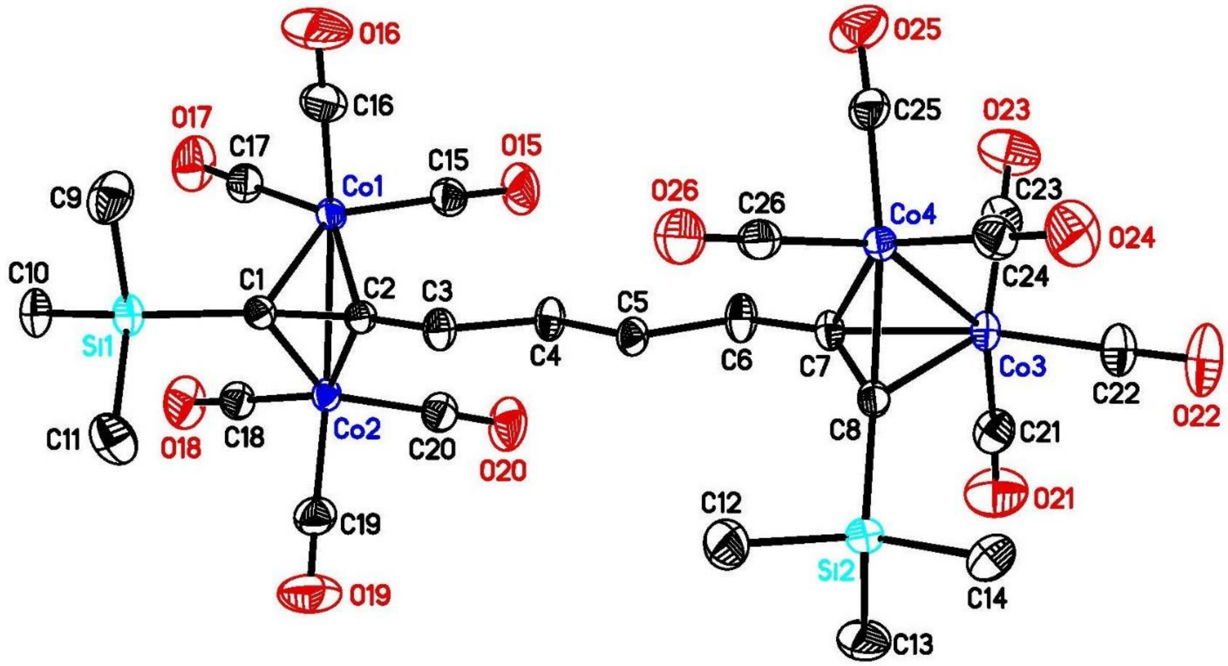

***Figure 3.1** ORTEP drawing of cobalt alkyne cluster at the 50 % probability level. Selected bond lengths (Å) and angles (°): Co(1)-Co(2) 2.4789(3), Co(3)-Co(4) 2.4815(3), Co(3)-C(8) 1.9914(13), C(7)-C(8) 1.3358(19).*

Given the success found by the Waymouth group in adding free tetracyclone to a solution of $Co_2(CO)_8$ to produce hydroxycyclopentadienyl cobalt carbonyl complex **3**, we decided to investigate this reaction with other cyclopentadienones. We started this investigation by synthesizing Knölker's complex (Scheme 3.2), which could be accomplished by the reported methods[74] in 50-80% yields, followed by demetallation to give the free cyclopentadienone ligand as an orange oil that slowly crystallized in ~30% yield. Three bicyclic cyclopentadienones were isolated this way bearing $SiMe_3$, $SiMe_2Ph$, and $SiMe_2{}^tBu$ groups at the 2 and 5 positions. Three demetallation methods were investigated with the objective to optimize the yield for the ligand

(Scheme 3.3). All demetallation procedures follow a two-step approach: the iron center is first destabilized by the removal of a CO ligand; the resulting intermediate is then oxidized and the dissociated ligand is collected. This two-step process is characteristic of many demetallation procedures; however, in this case, care must be taken in the choice of methods as the silyl groups can be easily cleaved.

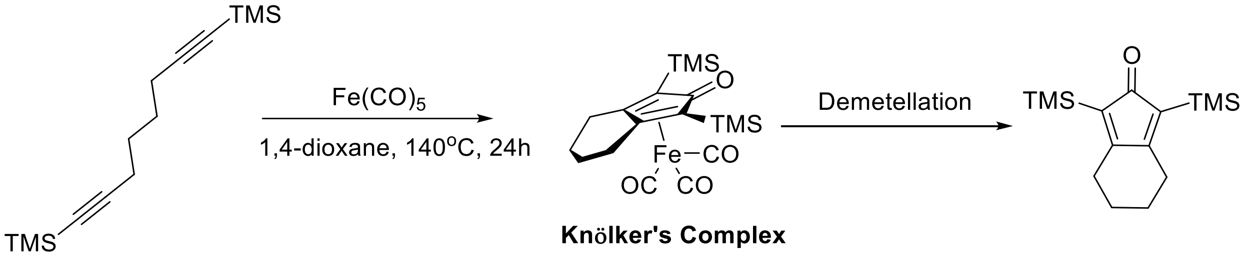

Scheme 3.2 *Synthesis of Knölker's complex and demetallation to release the cyclopentadienone ligand.*

The first method investigated for cyclopentadienone demetallation was the reported iron-hydride oxidation method.[19] In this method, the Knölker complex was converted to the iron hydride by the reverse-water-gas shift reaction, after which the hydride was exposed to air for decomposition, resulting in the release of the cyclopentadienone ligand. This method could produce the free ligand in ~35-40% yield.

The second method investigated was a photo-assisted demetallation, in which Knölker's complex was irradiated with UV light in acetonitrile to produce a tris-acetonitrile iron cyclopentadienone complex.[75] Without the CO ligands, the complex becomes much less resistant to oxidation and is efficiently decomposed in air. This method yielded the free ligand in 25-35% yield.

The third method investigated was a trimethylamine-*N*-oxide (TMANO) assisted demetallation, in which Knölker's complex was heated in the presence of 5 equivalents of TMANO to remove CO ligands, followed by air oxidation to release the free cyclopentadienone ligand.[76] This method yielded the desired cyclopentadienone ligand in 30-40% yield.

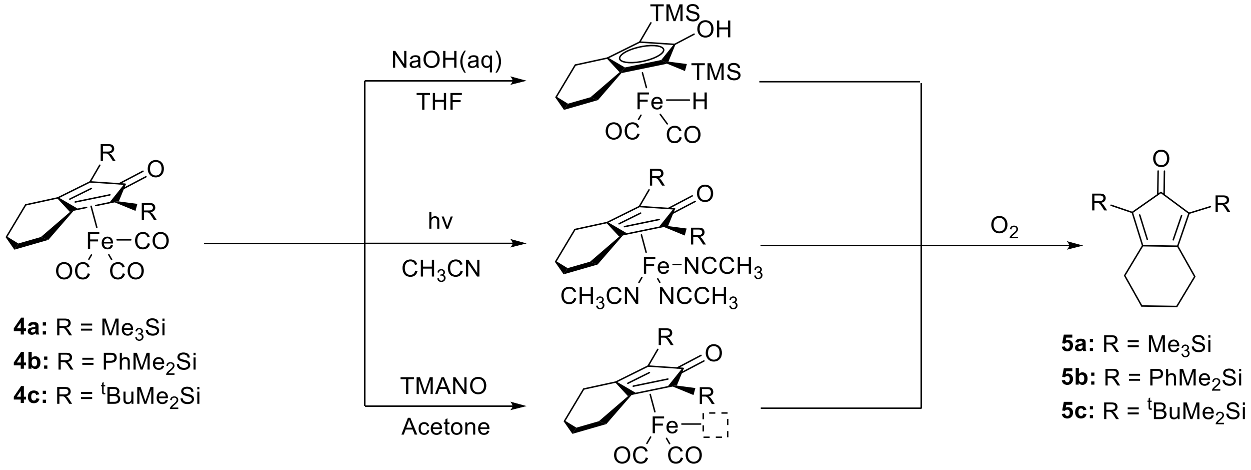

Scheme 3.3 *Three methods for demetallation of Fe(0) cyclopentadienone complexes.*

The low yields for these reactions relative to reported yields is difficult to explain. Several considerations for ligand decomposition pathways were taken, such as generation of reactive iron oxide species which might damage silyl groups and protodesilylation by moisture present in the solvent. Iron oxide generation should be inhibited by addition of sodium thiosulfate and protodesilylation should be minimized by dry conditions. However, consistently attaining high yields for the free ligand from the Knölker complexes proved challenging.

Two other methods for the synthesis of free cyclopentadienones were investigated. First, titanium and zirconium mediated reductive coupling of alkynes were investigated, following reports by the groups of Tamao[77] and Negishi[78], respectively. Using zirconocene dichloride, alkynes could be converted to 1,4-dihalobutadienes in decent yields. Unfortunately, subsequent steps by which the 1,4-dihalobutadienes were lithiated and reacted with carbon dioxide did not form the desired cyclopentadienone complexes. This may be attributed to the presence of sensitive silyl groups in our 1,4-dihalobutadienes. The reported 1,4-dihalobutadienes that successfully underwent the transformation to form the cyclopentadienones do not contain silyl groups.[79]

The possibility of using palladium-catalyzed cyclization of alkynes was briefly investigated following reports of successful Pd(II)/Cu(II) mediated [2+2+1] cyclization reactions with aryl alkynes.[57] Unfortunately, attempts to modify this system for purely alkyl and silyl substituted alkynes proved unsuccessful.

3.3 Synthesis of Cobalt Complexes

Guided by the work of Waymouth and co-workers,[27] directly mixing $Co_2(CO)_8$ with free cyclopentadienones seemed like a promising route to hydroxylcyclopentadienyl cobalt carbonyl complexes. Indeed, $Co_2(CO)_8$ reacted with any of the Knölker-complex derived cyclopentadienones **5a/b/c** to give a mixture of products, one of which was the desired hydroxycyclopentadienyl cobalt complex which was isolable by recrystallization. The other by-products were cobalt complexes bearing cyclopentadienone and carbonyl ligands; however, they lacked the OH resonance as judged by the IR and ^{1}H NMR spectra. This indicated that they were likely Co(0) complexes observed by Roewer[29] and Hübel,[28] with either one or two cyclopentadienone ligands coordinated, as illustrated in Scheme 3.4 (**7a/b/c** and **8a/b/c**). Attempts to convert these Co(0) complexes to Co(I) complexes with dihydrogen showed some promise, but purification was difficult. Addition of one equivalent of a stable free radical such as galvinoxyl to a benzene solution of **6a** resulted in disappearance of the hydroxide resonance and appearance of a new complex proposed to be **7a**. Complex **8a** could be made by reacting the free ligand **5a** with dicobalt octacarbonyl in toluene in a closed Fisher-Porter bottle under a CO atmosphere, although it was contaminated with a trace amount of **8a** (Figure 3.2). Crystal structures for these complexes have not yet been solved, so these structures are educated guesses made on proton and carbon NMR spectra.

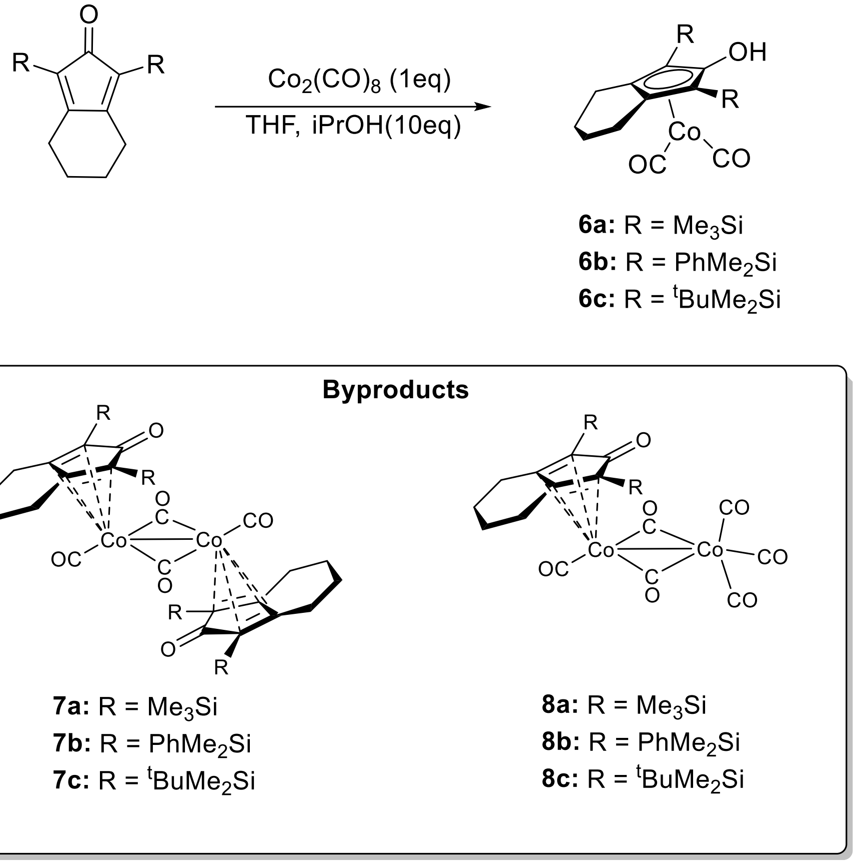

6a: R = Me_3Si
6b: R = $PhMe_2Si$
6c: R = $^tBuMe_2Si$

7a: R = Me_3Si
7b: R = $PhMe_2Si$
7c: R = $^tBuMe_2Si$

8a: R = Me_3Si
8b: R = $PhMe_2Si$
8c: R = $^tBuMe_2Si$

Scheme 3.4 *Synthesis of cobalt cyclopentadienyl complexes* ***6a/b/c*** *and the observed by-products.*

Addition of ten equivalents of a protic compound such as isopropyl alcohol and longer reaction times between **5a** and dicobalt octacarbonyl favored the formation of the hydroxycyclopentadienyl cobalt complex, as did the increase of the steric bulk on the ligand. This latter point supports the idea that the by-products of this reaction are dinuclear because sterically more demanding cyclopentadienone ligands should promote the separation of the two cobalt atoms due to steric clash between the R-groups of the cyclopentadienone ligand and the CO groups. As mentioned previously, drier solvents and a CO atmosphere favored the formation of the by- products over the hydroxycyclopentadienyl product, suggesting that the disproportionation of the two cobalt centers is inhibited by CO and the lack of acidic hydrogens.

The three new Knölker-cobalt complexes **6a/b/c** (Figures 3.3, 3.4, 3.5) were successfully synthesized and fully characterized. The yields of the complexes were lowered by the need to repeatedly purify the mixture to remove unwanted by-products. Aside from the cyclopentadienone-containing by-products, additional by-products could be observed by the marked darkening of solution samples. These by-products were invisible in ^{13}C NMR, but crystallographic evidence suggests cobalt carbonyl clusters lacking cyclopentadienone ligands.

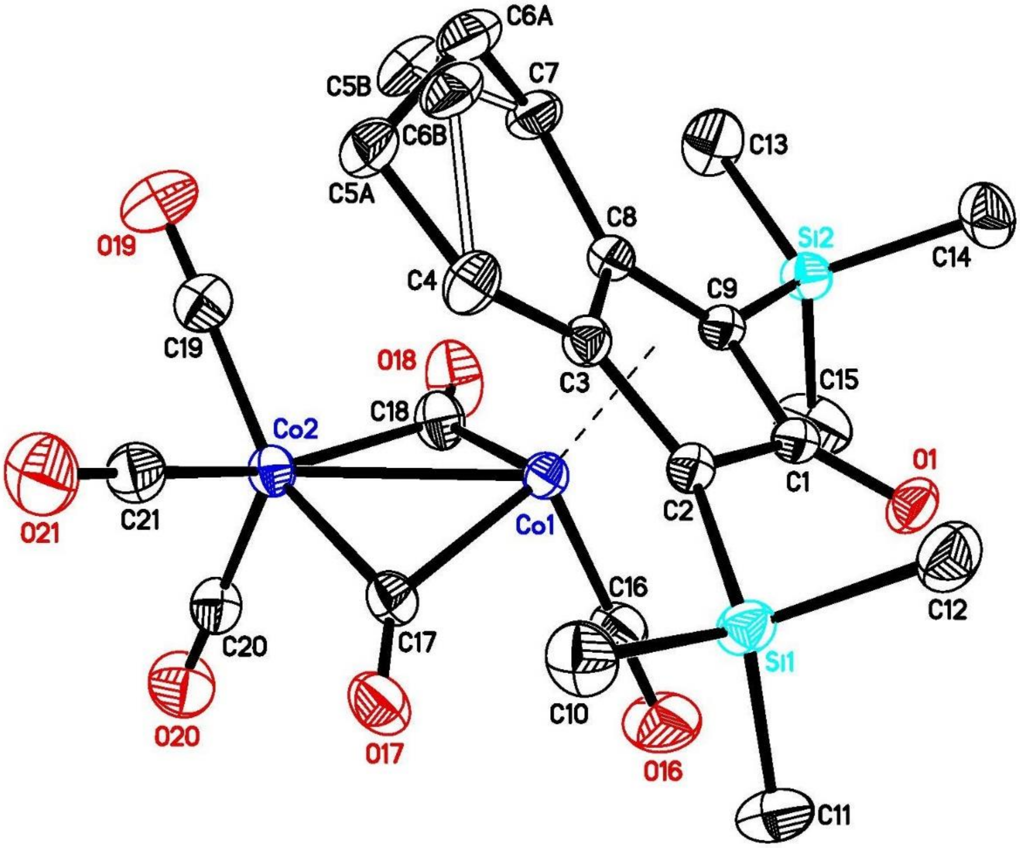

Figure 3.2 *ORTEP drawing of* ***8a*** *at the 50 % probability level. Selected bond lengths (Å) and angles (˚): Co-C(16) 1.8141(15), Co-C(1) 2.3515(13), O(1)-C(1) 1.2299(16), Co(1)-Co(2) 2.5470(3).*

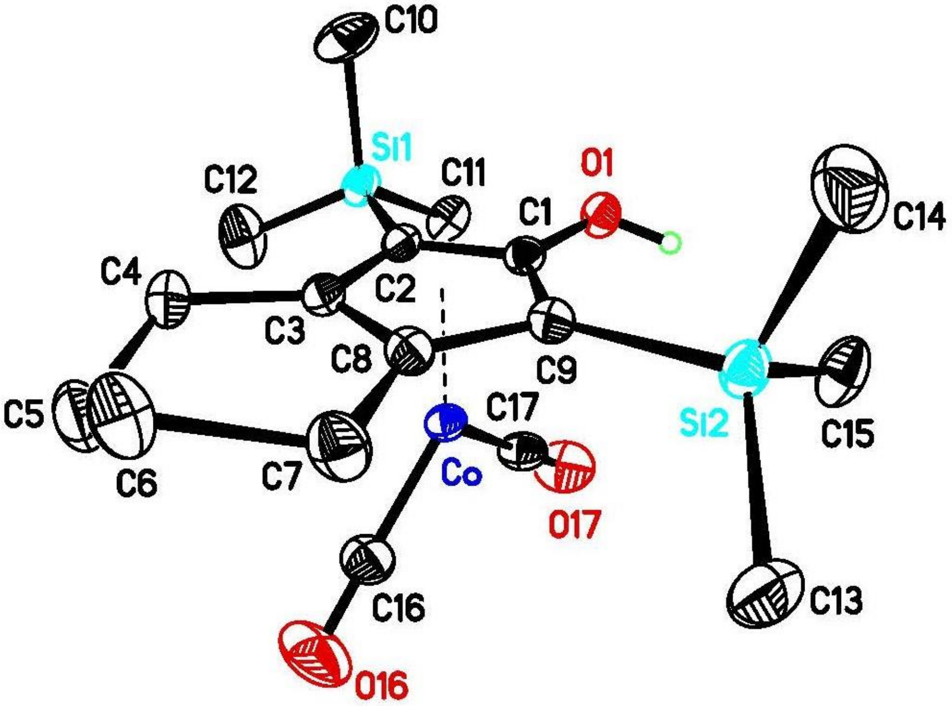

***Figure 3.3** ORTEP drawing of **6a** at the 50 % probability level. Selected bond lengths (Å) and angles (˚): Co-C(16) 1.7361(17), Co-C(1) 2.0809(14), O(1)-C(1) 1.3618(16).*

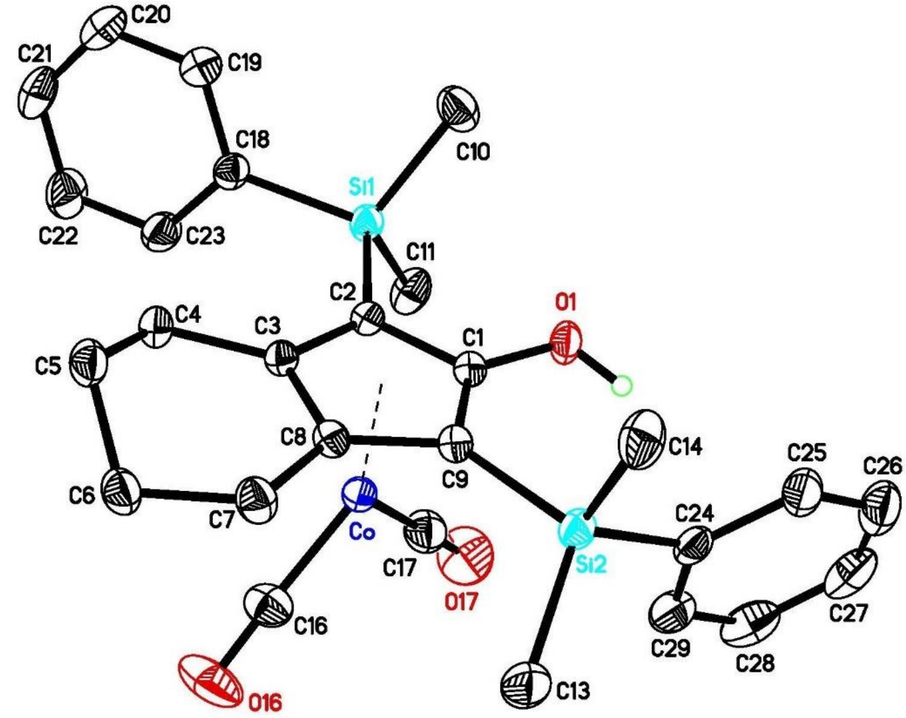

Figure 3.4 ORTEP drawing of **6b** at the 50 % probability level. Selected bond lengths (Å) and angles (˚): Co-C(22) 1.7360(19), Co-C(1) 2.0831(17), O(1)-C(1) 1.364(2).

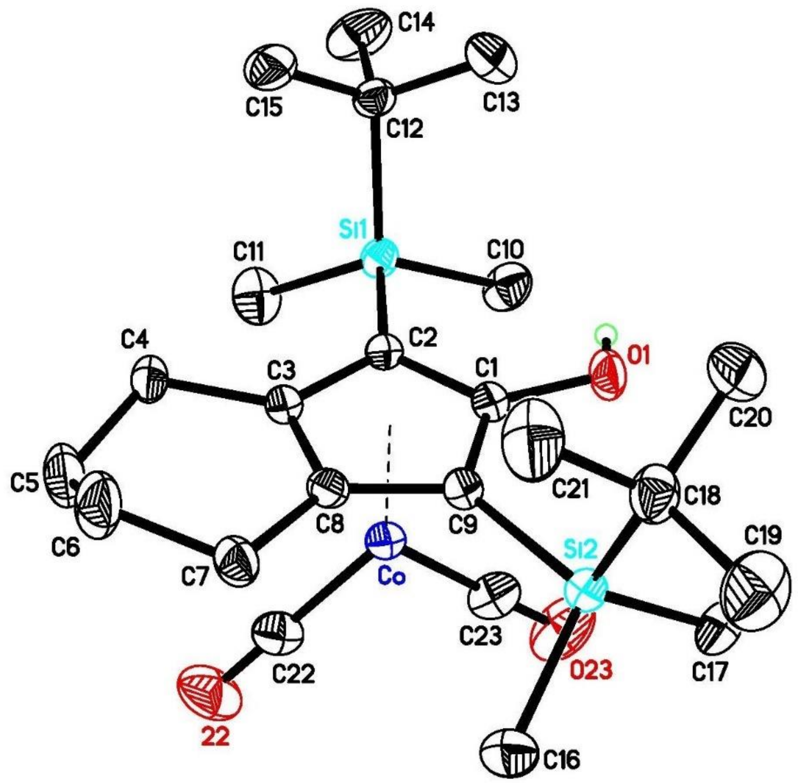

Figure 3.5 *ORTEP drawing of **6c** at the 50 % probability level. Selected bond lengths (Å) and angles (°): Co-C(16) 1.7344(18), Co-C(1) 2.0866(15), O(1)-C(1) 1.3602(18).*

Complexes **6a/b/c** were crystallographically similar to 1,2,3,4-tetraphenylcyclopentadienyl cobalt dicarbonyl complex discussed in Chapter 2 (or **3-OH** in Chart 3.1.) The Co-CO bond lengths and the Co-Cp bond lengths were similar. One noticeable difference between the crystal structures of **6a/b/c** and **3-OH** is the lengthening of the carbon monoxide CO bond in **6a/b/c**. This is explained by stronger back bonding to the CO ligands in these complexes**.** This is also supported by IR data (CO stretching frequencies) indicating that ligands **5a/b/c** are more electron donating than tetracyclone, as a negative charge on tetracyclone would be delocalized to its aromatic rings.

3.4 Reactivity of Hydroxycyclopentadienyl Cobalt Carbonyl Complexes

Given the hydride transfer reactivity of cobalt and manganese carbonyl complexes discussed in Chapter 2, we wanted to investigate cobalt complexes **6a/b/c** for their hydride transfer reactivities and assess any reactivity differences between the two classes of complexes. As with 1,2,3,4-hydroxycyclopentadienyl cobalt dicarbonyl complex (**3-OH**), cobalt-Knölker complexes **6a/b/c** could be oxidized to form stable, cationic, tris-acetonitrile cobalt cyclopentadienone complexes **9a/b/c** (Scheme 3.5 and Figure 3.6).

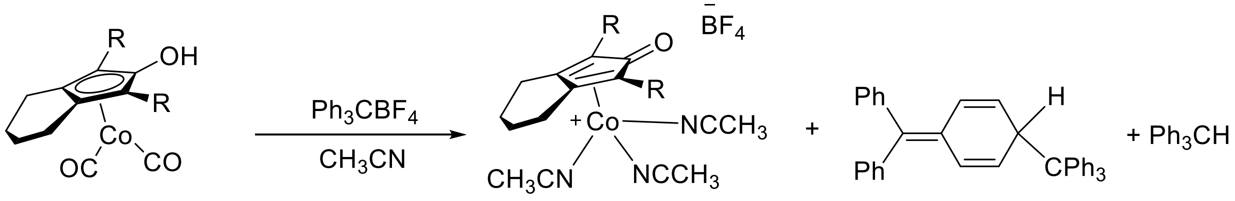

6a: R = Me_3Si
6b: R = $PhMe_2Si$
6c: R = $^tBuMe_2Si$

9a: R = Me_3Si
9b: R = $PhMe_2Si$
9c: R = $^tBuMe_2Si$

***Scheme 3.5** Reaction between Co-complexes **6a/b/c** and Ph_3CBF_4 in acetonitrile to yield cationic Co-complexes **9a/b/c** and organic products.*

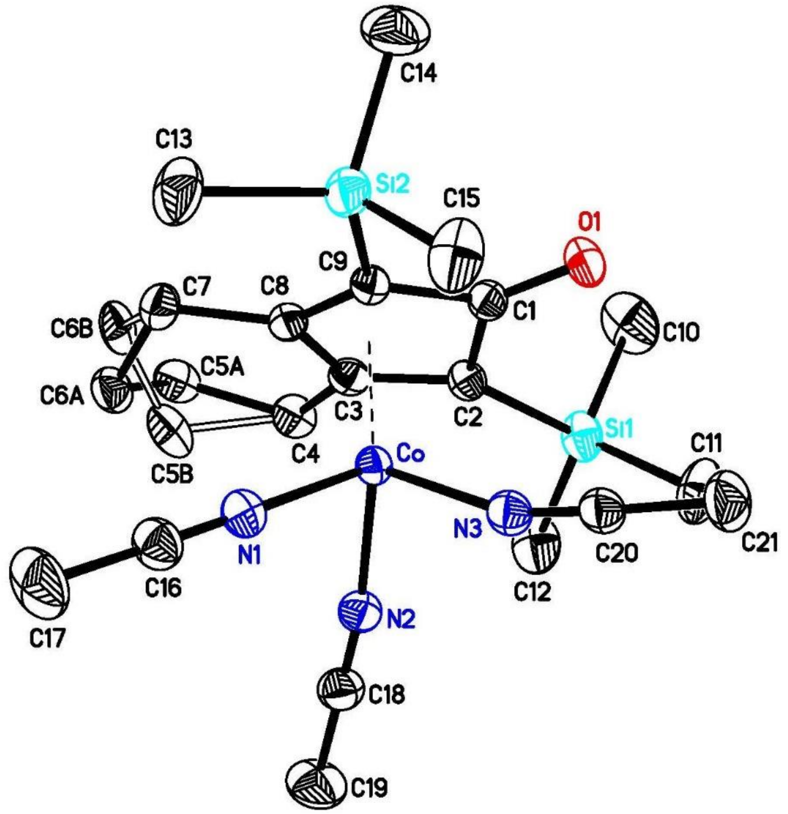

Figure 3.6 ORTEP drawing of ***9a*** *at the 50 % probability level. Selected bond lengths (Å) and angles (˚): Co-N(2)1.9426(17), Co-C(1) 2.3080(19), O(1)-C(1) 1.238(2), C(1)-C(2) 1.487(3), C(2)-C(3) 1.439(3).*

We observed that the change in the R-groups on the cyclopentadienone ligand had a subtle, yet identifiable impact on the outcome of the hydride transfer reactivity of the complexes **6a/b/c**. Using Ph_3CBF_4 as the hydride acceptor, cobalt complex **1** almost exclusively form the Gömberg dimer. In contrast, cobalt complexes **6a**/**b**/**c** reacted to form mostly Ph_3CH (Chart 3.1). Tetracyclone derived cobalt and manganese hydroxycyclopentadienyl complexes **3-OH** and **10**, resulted in intermediate mixtures of hydride transfer and single electron transfer products. There are several possible explanations for this difference in behavior. In the case of **1**, the low solubility of the complex in acetonitrile could result in an excess of Ph_3CBF_4 in solution relative to the complex. This excess might increase the chance of Gömberg dimer formation. This hypothesis is supported by the preference of **6b** for hydride transfer to Ph_3CBF_4, showing that a more soluble metal complex with a similar steric and electronic properties will favor hydride transfer. The mixture of Gömberg dimer and Ph_3CH observed in the reaction between **3-OH** or **10** and Ph_3CBF_4 could not be explained by low solubility and instead might be the result of the extended π-conjugation in the molecule, allowing electron transfer to take place from any surface along the molecule. This large reactive surface area may contrast with **6a/b/c** which may have a smaller reactive surface area. More experiments would need to be done to test this hypothesis.

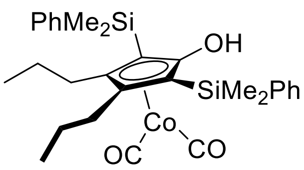

1

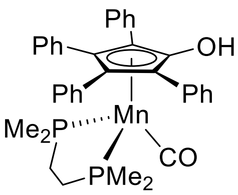

10

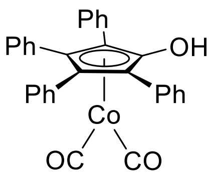

3-OH

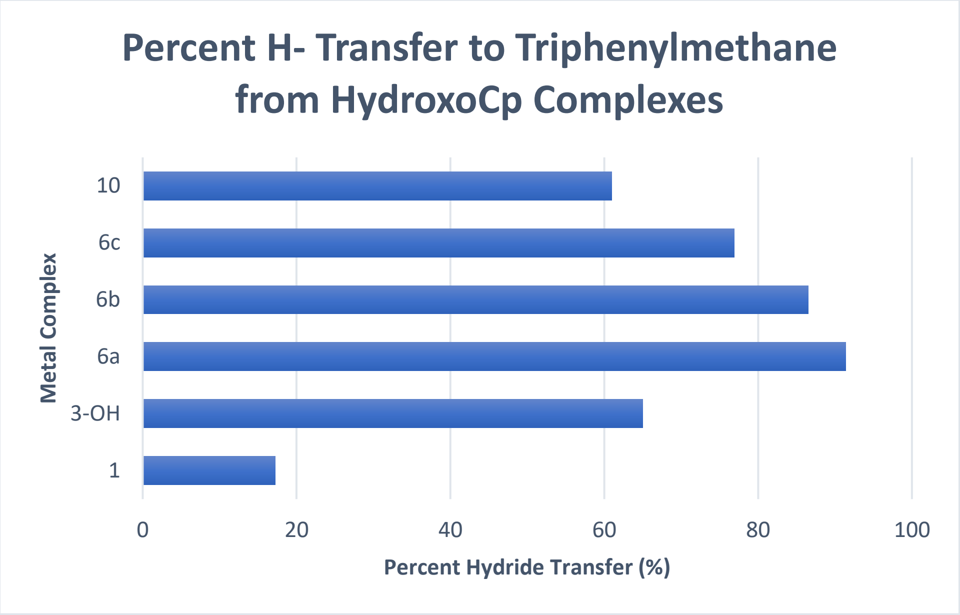

Table 3.1 *Favorability of H^- transfer from hydroxycyclopentadienyl metal complexes to Ph_3CBF_4 vs formation of Gömberg dimer.*

3.5 Conclusion

Three new cobalt carbonyl hydroxycyclopentadienyl complexes were synthesized and fully characterized, showing similar crystals structures and spectroscopic features to previously reported cobalt carbonyl hydroxycyclopentadienyl complexes. However, the slight changes in ligand environment found in complexes **6a/b/c** resulted in different hydride transfer efficiencies compared with Gomberg dimer formation. Brief investigations show that this may be due to solubility differences between complexes and lower surface area for single electron transfer for

6a/b/c compared with other complexes in the same class. Spectroscopic and hydrogen atom transfer studies show that the more electron rich cyclopentadienone ligands **5a/b/c** may promote the formation of cobalt(0) cyclopentadienone complexes, which are disfavored in the case of tetracyclone. This result is explained by the greater oxidizing potential of tetracyclone compared to these other ligands with electron donating R-groups.

3.6 Experimental

All compounds described in this chapter were prepared under an argon atmosphere using standard glovebox and Schlenk techniques unless otherwise stated. Benzene-d_6, acetonitrile-d_3 and methylene chloride-d_2 were purchased from Cambridge Isotope Laboratories, Inc. Benzene-d_6 was dried over sodium-benzophenone and distilled under an argon atmosphere. Acetonitrile-d_3 and acetonitrile were dried over CaH_2 and distilled under an argon atmosphere. Methylene chloride-d_2 was dried over 4 Å molecular sieves and degassed by three freeze-pump-thaw cycles. Acetic acid was dried over 4 Å molecular sieves and then deoxygenated by bubbling argon for 0.5 h. All other dry and oxygen-free solvents used for synthesis and workup (THF, diethyl ether, toluene, and pentane) were collected from an Innovative Technology solvent purification system. Benzaldehyde was freshly distilled prior to use. ^1H, $^{13}C\{^1H\}$, and $^{31}P\{^1H\}$ NMR spectra were recorded on a Bruker Avance 400 MHz NMR spectrometer. Chemical shift values in ^1H and $^{13}C\{^1H\}$ NMR spectra were referenced internally to the residual solvent resonances. $^{31}P\{^1H\}$ NMR spectra were referenced externally to 85% H_3PO_4 (0 ppm). Infrared spectra were recorded on a PerkinElmer Spectrum Two FT-IR spectrometer equipped with a smart orbit diamond attenuated total reflectance (ATR) accessory.

General Procedure for Demetalation of Knölker Type Complexes

Method A: In a dry Schlenk flask equipped with stir bar, Knölker's complex (0.5 g, 1.2 mmol) was dissolved in 20 mL of THF. This solution was cannula transferred into a concentrated solution of aqueous sodium hydroxide. The mixture was stirred in the dark for 3 h, then it was neutralized with H_3PO_4. The THF layer was separated and the aqueous layer was extracted with Et_2O (3 x 5 mL). The combined organic layers were dried over Na_2SO_4 and filtered to remove excess drying agents. $Na_2S_2O_3$ was added and the solution was exposed to air and stirred for 1 h over which time brown precipitate formed. The solution was filtered through celite and concentrated by rotary evaporation. The crude mixture was separated by column chromatography on silica using pentane (100%) to give the desired ligand.

Method B: In a dry Schlenk flask equipped with a stir bar, Knölker's complex (0.5 g, 1.2 mmol) was dissolved in 40 mL of dry acetonitrile. The mixture was irradiated with 365nm UV light source under argon for 1 h with a stream of argon bubbling through it. The solution turned dark purple. $Na_2S_2O_3$ was added and the solution was exposed to air and stirred for 1 h over which time brown precipitate formed. The solution was filtered through celite and concentrated by rotary evaporation. The crude mixture was separated by column chromatography on silica using pentane (100%) to give the desired ligand.

Method C: In a dry Schlenk flask, Knölker's complex (0.5 g, 1.2 mmol) and TMANO were dissolved in 30 mL of degassed acetone. The mixture was then refluxed under argon for 2 h. $Na_2S_2O_3$ was added and the solution was exposed to air and stirred for 1 h over which time brown precipitate formed. The solution was filtered through celite and concentrated by rotary evaporation. The crude mixture was separated by column chromatography on silica using pentane (100%) to give the desired ligand.

2,4-bis(dimethylphenylsilyl)bicyclo[3.3.0]nona-1,4-dien-3-one

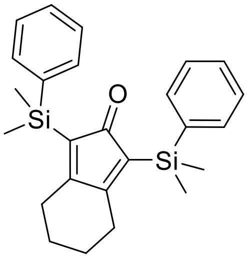

Yield: 33% (method C)

^{1}H NMR (400 MHz, CDCl$_3$) δ 7.53 – 7.43 (m, 4H), 7.33 – 7.22 (m, 6H), 2.30 (td, *J* = 4.4, 2.1 Hz, 4H), 1.39 (h, *J* = 2.8 Hz, 4H), 0.53 (s, 12H). ^{13}C{^{1}H} NMR (101 MHz, CDCl$_3$) δ 209.95, 170.55, 138.72, 134.05, 129.06, 127.91, 127.82, 125.18, 28.11, 22.72, -1.55. Selected ATR-IR data (solid, cm^{-1}): 2925 ($\nu_{C–H}$), 2854($\nu_{C–H}$), 1681 ($\nu_{C=O}$). HRMS (ESI) calcd (found) for [$C_{21}H_{39}OSi_2$]$^+$ 363.25344 (363.25343).

2,4-bis(dimethyl-*tert*-butylsilyl)bicyclo[3.3.0]nona-1,4-dien-3-one

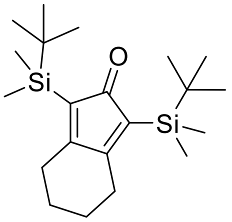

Yield: 40% (method C)

^{1}H NMR (400 MHz, CDCl$_3$) δ 2.68 (tt, *J* = 4.3, 2.2 Hz, 4H), 1.63 (tt, *J* = 4.3, 2.2 Hz, 4H), 0.84 (s, 18H), 0.18 (s, 12H). ^{13}C{^{1}H} NMR (101 MHz, CDCl$_3$) δ 210.30, 170.34, 125.54, 28.65, 26.96, 23.11, 18.18, -4.12. Selected ATR-IR data (solid, cm^{-1}): 3099($\nu_{CPh–H}$), 2928 ($\nu_{Csp3–H}$), 1680 ($\nu_{C=O}$). HRMS (ESI) calcd (found) for [$C_{25}H_{31}OSi_2$]$^+$ 403.19087 (403.1906).

(η5 -1-hydroxy-2,5-bis(trimethylsilyl)bicyclo[4.3.0]nona-1,4-dien)cobalt dicarbonyl (6a)

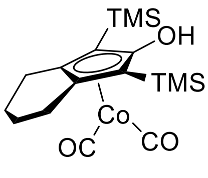

To an oven-dried Schlenk flask equipped with stir bar were placed $Co_2(CO)_8$ (0.129 g, 0.36 mmol) and the cyclopentadienone ligand (0.1g, 0.36 mmol). To this was added 20 mL of THF and 10 eq of isopropyl alcohol. The mixture was stirred at room temperature for 24 h under argon, over which time the solution changed from a dark brown to a clear red or orange. The solution was filtered through celite, and the solvent was evaporated. The dark red oily residue was dissolved in 10 mL of pentane and cooled to -20°C for 24 h. Spiny red crystals formed over this time and were removed by pipetting off the solvent. These crystals represent a mixture of **7a** and **8a.** The remaining pentane solution was concentrated by half and cooled again at -20 °C, resulting in the formation of blocky red crystals over several days. These crystals represented the product **6a** and were isolated in 35% yield. ^{1}H NMR (400 MHz, C_6D_6) δ 3.73 (s, 1H), 2.32 (dt, *J* = 16.3, 6.1 Hz, 2H), 2.06 (dt, *J* = 16.3, 6.1 Hz, 2H), 1.56 – 1.40 (m, 2H), 1.28 (m, 2H), 0.30 (s, 20H). $^{13}C\{^{1}H\}$ NMR (101 MHz, C_6D_6) δ 207.19, 140.58, 104.95, 78.05, 25.17, 23.27, 0.96. Selected ATR-IR data (solid, cm^{-1}): 3582 (ν_{O-H}), 2943 (ν_{C-H}), 1989 ($\nu_{C\equiv O}$), 1929 ($\nu_{C\equiv O}$).

(η5 -1-hydroxy-2,5-bis(dimethyl-phenylsilyl)bicyclo[4.3.0]nona-1,4-dien)cobalt dicarbonyl (6b)

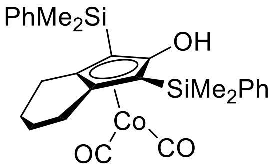

To an oven-dried Schlenk flask equipped with stir bar were placed $Co_2(CO)_8$ (0.1 g, 0.27 mmol) and the cyclopentadienone ligand (0.11 g, 0.27 mmol). To this was added 20 mL of THF and 10 eq of isopropyl alcohol. The mixture was stirred at room temperature for 24 h under argon, over which time the solution changed from a dark brown to a clear red or orange. The solution was filtered through celite, and the solvent was evaporated. The dark red oily residue was dissolved in 10 mL of pentane and cooled to -20 °C, resulting in the formation of blocky red crystals over several days. These crystals represented the product **6b** and were isolated in 38% yield. No **7b** or **8b** were observed. ^{1}H NMR (400 MHz, C_6D_6) δ 7.74 – 7.68

(m, 4H), 7.20 – 7.07 (m, 6H), 3.77 (s, 1H), 2.21 (dt, *J* = 16.6, 6.2 Hz, 2H), 1.99 (dt, *J* = 16.6, 6.2 Hz, 2H), 1.40 (m, 2H), 1.26 – 1.12 (m, 2H), 0.61 (s, 6H), 0.51 (s, 6H). $^{13}C\{^1H\}$ NMR (101 MHz, C_6D_6) δ 207.13, 141.30, 137.40, 134.75, 130.25, 128.74, 105.40, 76.51, 25.03, 23.16, 0.41, -0.95. Selected ATR-IR data (solid, cm^{-1}): 3457 ($\nu_{O\text{–}H}$), 3085($\nu_{CPh\text{–}H}$), 2941 ($\nu_{C\text{–}H}$), 1998 ($\nu_{C\equiv O}$), 1935 ($\nu_{C\equiv O}$).

(η5 -1-hydroxy-2,5-bis(dimethyl-tertbutylsilyl)bicyclo[4.3.0]nona-1,4-dien)cobalt dicarbonyl (6c)

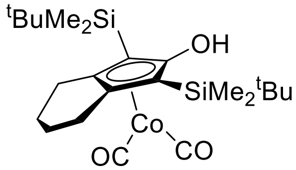

To an oven-dried Schlenk flask equipped with stir bar were placed $Co_2(CO)_8$ (0.198 g, 0.58 mmol) and the cyclopentadienone ligand (0.21 g, 0.58 mmol). To this was added 20 mL of THF and 10 eq of isopropyl alcohol. The mixture was stirred at room temperature for 24 h under argon, over which time the solution changed from a dark brown to a clear red or orange. The solution was filtered through celite, and the solvent was evaporated. The dark red oily residue was dissolved in 10 mL of pentane and cooled to -20 °C, resulting in the formation of blocky red crystals over several days. These crystals represented the product **6c** and were isolated in 41% yield. No **7c** or **8c** were observed. ^1H NMR (400 MHz, C_6D_6) δ 3.70 (s, 1H), 2.38 (m, 2H), 2.24 (m, 2H), 1.52 (m, 2H), 1.36 (m, 2H), 0.93 (s, 16H), 0.39 (s, 6H), 0.30 (s, 6H). ^{13}C NMR (101 MHz, C_6D_6) δ 207.11, 140.69, 105.60, 77.45, 26.94, 25.72, 23.39, 18.80, -3.03, -3.17. Selected ATR-IR data (solid, cm^{-1}): 3590 ($\nu_{O\text{–}H}$), 2925 ($\nu_{C\text{–}H}$), 2854($\nu_{C\text{–}H}$), 1998 ($\nu_{C\equiv O}$), 1933 ($\nu_{C\equiv O}$).

Chapter 4 – Iron-Nickel Bimetallic Cyclopentadienone Complexes

4.1 Introduction

Heterobimetallic complexes incorporating a cyclopentadienyl metal component are relatively well known in the literature.[52,80,81] These complexes have shown good stability and have revealed new and interesting bonding patterns. They have been employed in catalytic transformations in which the dual-metal system leads to unexpected selectivity for a specific transformation.[82] However, to date, there has been only one report of the related metal hydroxycyclopentadienyl fragment being incorporated into a well characterized heterobimetallic complex.[83]

Incorporating cyclopentadienone ligands into heterobimetallic complexes represents an interesting avenue to explore the tandem reactivity displayed by these complexes; however, it also adds a layer of complexity given the reactive nature of cyclopentadienone metal complexes. Previous work in the Guan group used the Knölker hydride complex (Scheme 4.1) in tandem with a copper NHC complex to catalyze the reduction of aldehydes and ketones through the reverse water-gas shift reaction.[83] In that research, new CuFe hydride complexes were isolated (Scheme 4.1) which raised interesting questions about the mechanistic pathway of the reactions the complex catalyzed and the reactivities of bridging hydrides.

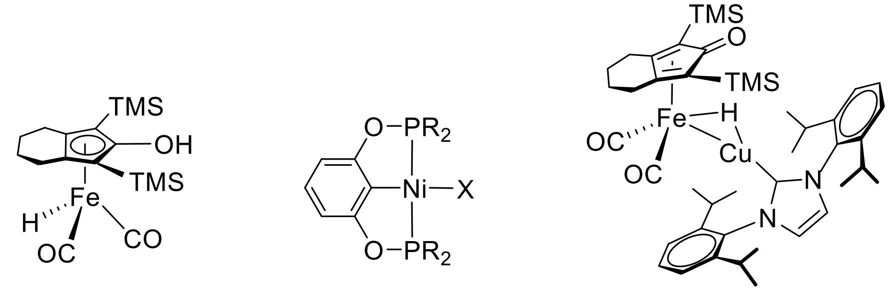

Knölker's Hydride

Ni-POCOP

[FeCu]-Bridged Hydride

Scheme 4.1 *Metal complexes investigated separately in the Guan group.*

There have been numerous examples of homobimetallic complexes made to incorporate pincer ligands;[84–87] however, cases of heterobimetallic complexes incorporating these ligands are less common.[88,89] Work in the Guan group has previously investigated the so-called 'Ni-POCOP' systems (Scheme 4.1). These are bis-phosphinite nickel pincer complexes with a L_2X-type ligand system derived from resorcinol. The ligand is highly rigid, and the anionic carbon atom is a strongly *trans*-directing group. This leads to stronger hydride donor ability of the Ni-POCOP hydride complexes compared to other nickel pincer complexes with weaker *trans*-directing ligands such as nitrogen-centered pincer systems. These Ni-POCOP complexes have been employed in CO_2[90] and aldehyde[91] reduction reactions and have shown good stability combined with relative ease of synthesis.

Given the interesting properties of the Knölker based FeCu bimetallic system, the known catalytic activity of the Ni-POCOP complexes and the interest around FeNi hydrides[51,92,93], we wanted to investigate a FeNi heterobimetallic complex, using Knölker's complex and a Ni-POCOP complex.

4.2 Synthesis of the Heterobimetallic Complexes

Synthesis of the CuFe hydride complex could be accomplished through several methods.[83] One route was to react the free NHC-CuH complex **2-H** with the Knölker hydride complex **1-H**. In this reaction, the OH group of complex **1-H** reacts with the hydride of **2-H** to generate dihydrogen and a Cu alkoxide, Fe hydroxycyclopentadienyl hydride bimetallic complex (Scheme 4.2). This complex then crystallizes to give the bridging hydride complex, which exists in small amounts in solution. The second route to this complex is reaction of the NHC-CuOH complex **2** with the Knölker tricarbonyl complex **1**. This reaction proceeds by the reverse water-gas shift reaction, in which one of the iron-bound CO ligands is attacked by the copper hydroxide, which generates CO_2 and the desired bimetallic complex. Guided by this previous work, these methods were investigated for their applicability to the synthesis of FeNi bimetallic hydride complexes.

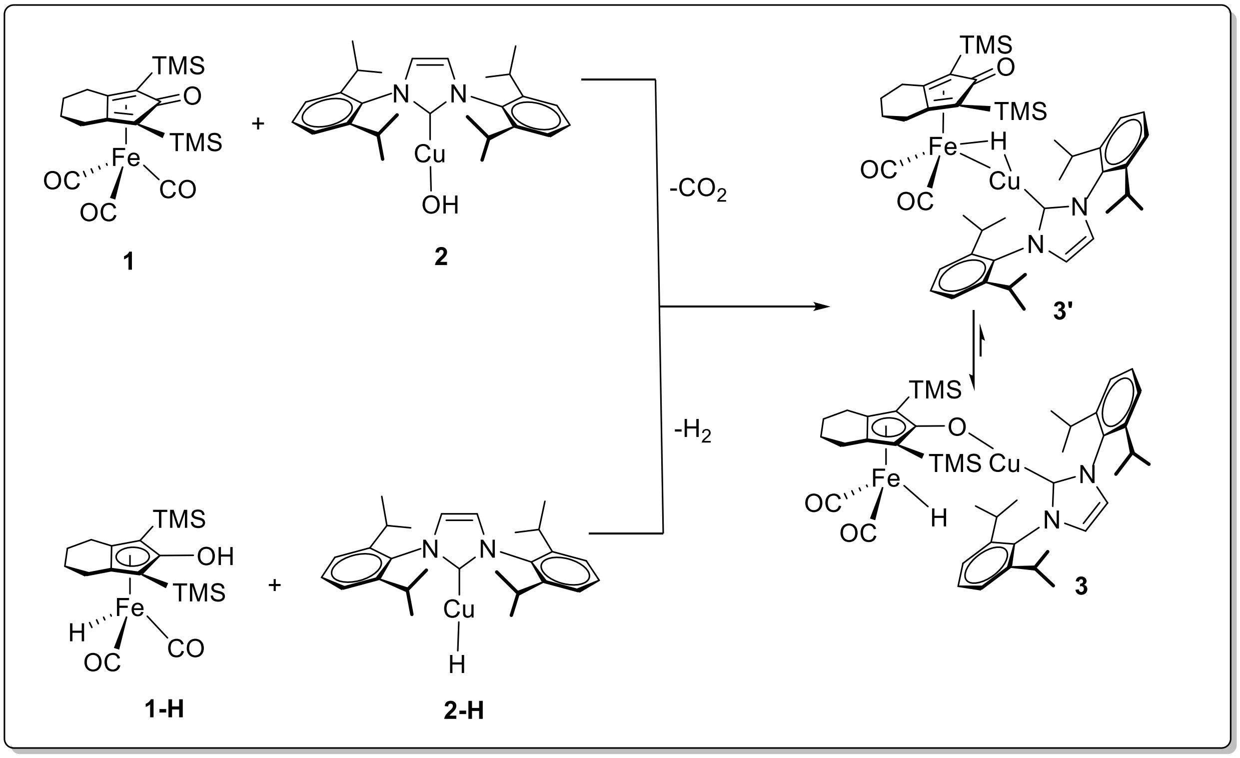

Scheme 4.2 *Synthetic pathways to the FeCu bimetallic hydride complex employed as a carbonyl reduction catalyst.*

To begin our investigation of the synthesis of FeNi bimetallic hydride complexes, we investigated the reactivity of ($^{tBu}P^{O}C^{O}P^{tBu}$)NiH (**4b**) with Knölker's FeH complex **1-H** with the hope that the nickel hydride would react with the acidic OH proton on the iron hydride (Scheme 4.3) to form a bimetallic complex, similarly to how the NHC-CuH had behaved. We were interested in this POCOP ligand because its bulky *tert*-butyl groups might drive the formation of a μ_2-H NiFe, as we hypothesized that bonding between the hydroxyl oxygen on Knölker's complex and nickel might be unfavorable. Unfortunately, the two components were unreactive with each other, and no bimetallic complex could be observed by NMR spectroscopy.

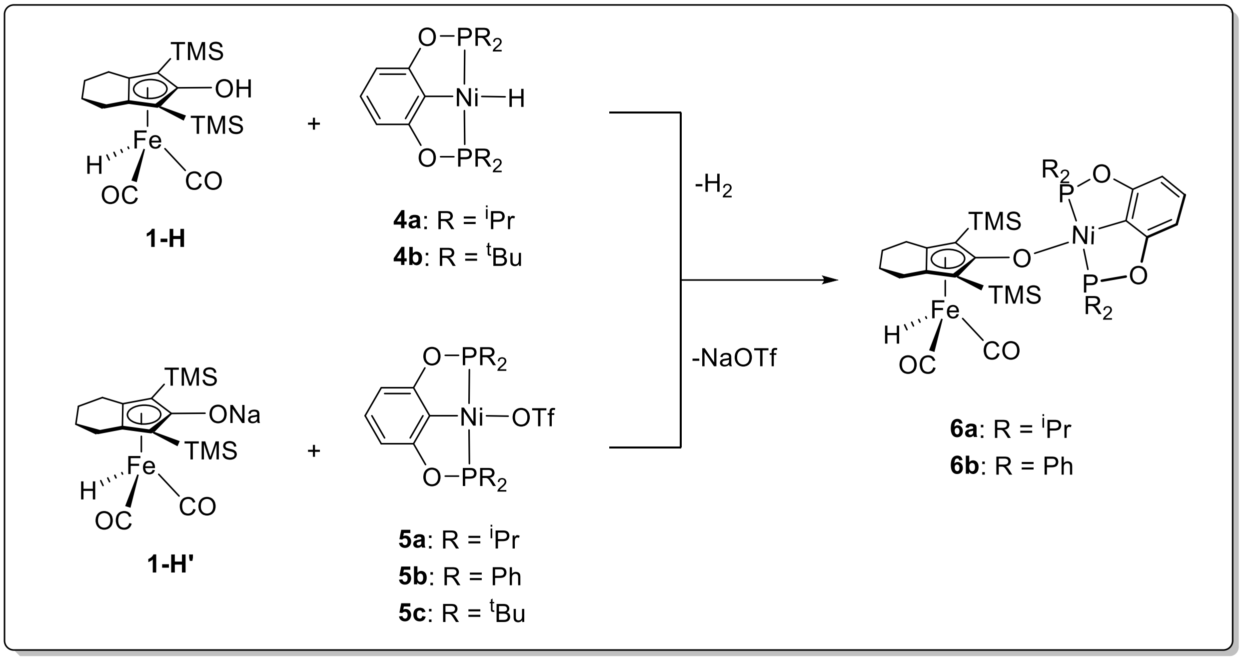

Scheme 4.3 Synthetic methods to the FeNi bimetallic hydride complexes.

Next, ($^{tBu}P^{O}C^{O}P^{tBu}$)NiOTf (**5c**) was synthesized in order to explore another possible avenue of synthesis. The OH group of Knölker's hydride could be deprotonated to form the Knölker alkoxide complex **1-H'**,[19] which could in turn react with **5c** by replacing the labile OTf ligand to form the bimetallic complex. Unfortunately, this method was not successful either. ($^{tBu}P^{O}C^{O}P^{tBu}$)NiOH that could be easily synthesized from **5c** and and NaOH was used to investigate the possibility of synthesizing the bimetallic through a reverse water-gas shift mechanism. Unfortunately, this method was unsuccessful, only resulting in a slight decomposition of the POCOP ligand.

We hypothesized that the ($^{tBu}P^{O}C^{O}P^{tBu}$)Ni fragment was too bulky around the nickel center to interact with the hydroxycyclopentadienyl ligand on the iron; therefore less sterically hindered ($^{iPr}P^{O}C^{O}P^{iPr}$)NiH should be investigated instead. In this case, the nickel hydride slowly reacted with the Knölker hydroxyl group to produce hydrogen and cleanly formed a bimetallic complex. However, because of the slow reactivity between the hydride and the acidic hydrogen, other methods were investigated to more efficiently form the complex for characterization. The two methods mentioned above were pursued. It was found that using ($^{iPr}P^{O}C^{O}P^{iPr}$)NiOTf (**5a**) and the deprotonated Knölker alkoxide complex, the desired bimetallic complex could be efficiently synthesized and isolated within an hour. However, the reaction was slightly less clean due to the difficulties in synthesizing moisture-free **5a** and Knölker alkoxide complex. While we were able to isolate the desired complex cleanly through this method, the reaction between the two hydrides was preferred.

We briefly investigated the possibility of using ($^{iPr}P^{O}C^{O}P^{iPr}$)NiOH in order to synthesize the desired complex through a reverse water-gas shift reaction with the Knölker tricaronyl complex; however, synthesis of the ($^{iPr}P^{O}C^{O}P^{iPr}$)NiOH complex proved challenging and the reaction with the Knölker complex did not yield the desired complex. In studying this reaction, ($^{iPr}P^{O}C^{O}P^{iPr}$)NiOH was characterized, and its reactivity was briefly investigated. Unfortunately, no crystal structure of pure ($^{iPr}P^{O}C^{O}P^{iPr}$)NiOH was obtained yet; instead, a dinuclear nickel structure was solved (Figure 4.1), featuring ($^{iPr}P^{O}C^{O}P^{iPr}$)NiOH and [($^{iPr}P^{O}C^{O}P^{iPr}$)Ni(OH_2)]OTf linked by hydrogen bonds. From our investigations, it seems that ($^{iPr}P^{O}C^{O}P^{iPr}$)NiOH is an exceptionally unstable complex due to its phosphinite arms and has a strong tendency to form clusters. NMR evidence showed that as the moisture levels in the starting materials increased, the NMR spectra broadened accordingly. Additionally, highly concentrated solutions and over longer periods of time tended to favor the decomposition reactions.

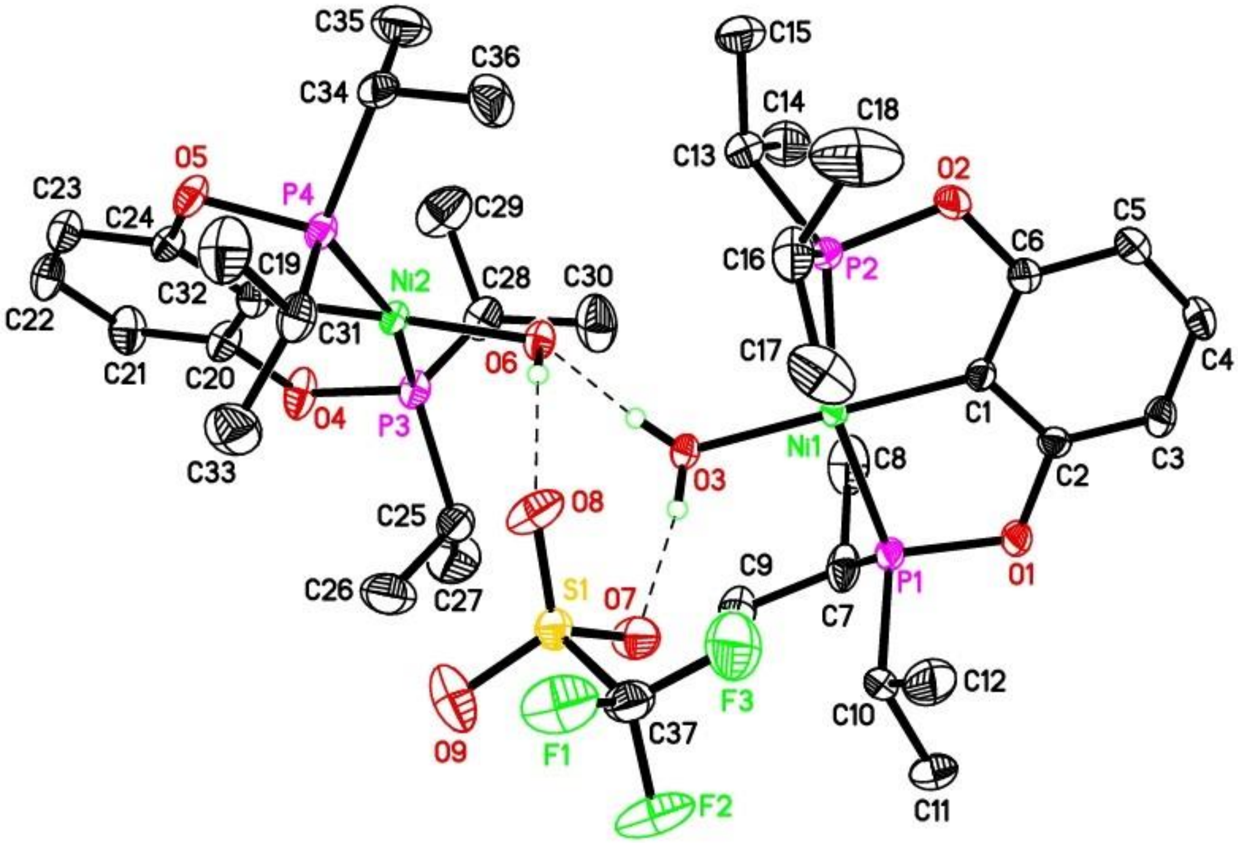

Figure 4.1 ORTEP drawing of nickel hydroxide/water cluster at the 50% probability level. Selected bond lengths (Å) and angles (°): Ni(1)-C(1) 1.881(3), Ni(1)-O(3) 1.913(2), Ni(2)-O(6) 1.917(2), Ni(2)-C(19) 1.887(3).

Finally, we wanted to investigate the synthesis of an FeNi-bimetallic complex containing the ($^{Ph}P^{O}C^{O}P^{Ph}$)Ni pincer moiety. This complex is unique because it is less sterically bulky than the ^{i}Pr or ^{t}Bu derivatives; however, its synthetic routes are more limited as the nickel hydride complex ($^{Ph}P^{O}C^{O}P^{Ph}$)NiH remains elusive. In order to synthesize this bimetallic compound, ($^{Ph}P^{O}C^{O}P^{Ph}$)NiOTf (**5b**) was synthesized first and then added to a solution of **1-H'**. These components reacted cleanly to yield the desired bimetallic complex.

4.3 Characterization of the Heterobimetallic Complexes

Proton NMR spectroscopy supported the formation of the bimetallic complexes, as evidenced by the disappearance of the Knölker iron hydride signal and the emergence of a new hydride which is shifted slightly to the upfield region. This new hydride resonance was sharp and appeared as a singlet, indicating that in solution it was primarily a terminally bound iron hydride. In proton-decoupled phosphorus NMR spectra, the bimetallic complexes appeared as an AB quartet, indicating that the two phosphorus atoms were chemically inequivalent and were coupling to each other through the nickel center. This indicates that the nickel-oxygen bond in the complex does not freely rotate on the NMR timescale.

Crystallographic evidence shows that the nickel does bind the Knölker complex through the alkoxide oxygen and no evidence for a μ_2-H species was observed (Figure 4.2).

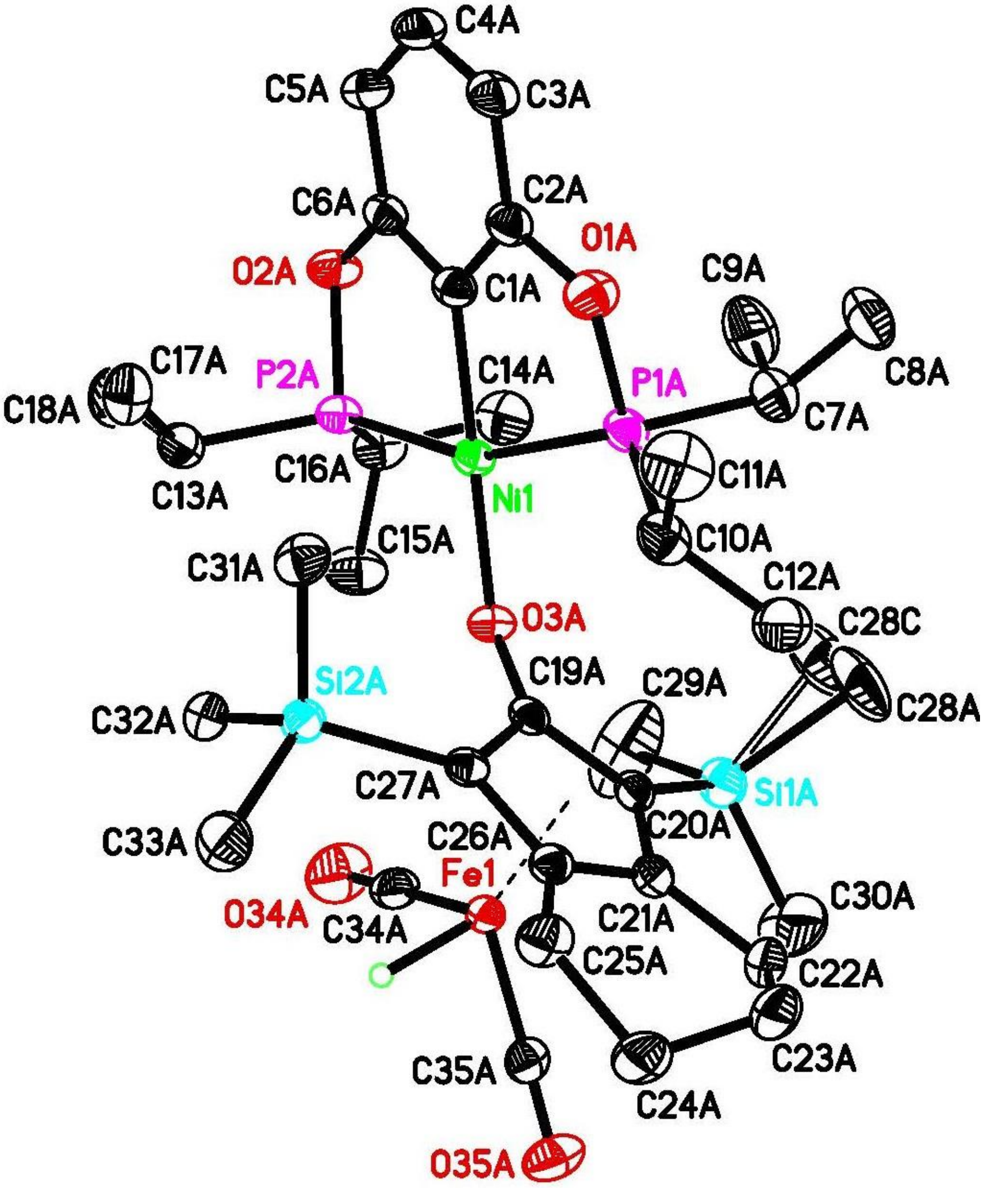

Figure 4.2 *ORTEP drawing of* ***6a*** *at the 50% probability level. One of two independent molecules in the crystal lattice is shown. Selected bond lengths (Å) and angles (°): Fe(1)-H(1) 1.42(3), Ni(1)-O(3A) 1.9120(18), Fe(1)-C(19A) 2.229(3), Ni(1)-C(1A) 1.898(3).*

IR spectra of the complexes showed that the carbonyl stretching frequencies of the CO ligands had decreased, indicating greater backdonation and indicating a largely ionic bond between the nickel and the oxygen. This was true for both ($^{Ph}P^{O}C^{O}P^{Ph}$)Ni and ($^{iPr}P^{O}C^{O}P^{iPr}$)Ni systems.

4.4 Reactivities of the Heterobimetallic Complexes

Given the unique crystal structure of the bimetallic complex **6a**, we wanted to investigate the reactivity of this complex as a frustrated Lewis pair (FLP). Nickel POCOP complexes have been investigated extensively by our group. While they are highly active catalysts in some reactions, these complexes have not been shown to be capable of activating dihydrogen for hydrogenation reactions.[94] However, we hypothesized that the sterically hindered nature of the oxygen-nickel bond might facilitate heterolytic cleavage of dihydrogen. Indeed, upon introducing one atmosphere of dihydrogen into a J-Young tube containing **6a** in C_6D_6 at room temperature, the bimetallic complex was converted back into **1-H** and **4a** within several minutes. This indicates to us that the sterically crowded environment around the nickel center allows for more efficient activation of dihydrogen compared to less bulky nickel alkoxide species.[95]

Given the FLP reactivity of complex **6a** observed with dihydrogen, we wanted to briefly investigate other reactivities at the nickel center. Some FLP systems have been shown to activate CO_2 towards various reduction pathways,[96] so we wanted to test the reactivity of CO_2 with this bimetallic complex. When 1 atm of CO_2 was added to a C_6D_6 solution of **6a,** a new hydride species (singlet at the upfield region) was observed. Given that it was not shifted greatly with respect to the original bimetallic hydride, we hypothesized that it might be a bimetallic carbonate forming from the insertion of CO_2 into the Ni-O bond. Unfortunately, we could not successfully drive this reaction to completion, so full characterization of this new hydride was not accomplished.

Complex **6a** showed high sensitivity towards moisture, and quickly decomposed in wet solvents, yielding **1-H** and a nickel hydroxide complex. Complex **6b** was still sensitive to moisture; however, it could not be used to activate dihydrogen. Reactions between these complexes and alkynes and alkenes did not result in any activation of those substrates.

Given the known photochemical reactivity of hydride complex **1-H**, we were interested in investigating the photochemical reactivity of the newly synthesized bimetallic complexes. A C_6D_6 solution of **6a** in a sealed J-Young tube exposed to the ambient light for 24 h, resulting in decomposition to reform the Ni-H complex **4a**. The fate of the iron complex in this reaction was not determined. This interesting process indicated to us that in the excited state, the iron hydride might become hydridic enough to transfer to the nickel center.

Irradiation of a solution of **4b** and **1** in a 1:1 molar ratio in C_6D_6 with 366 nm UV lamp under a flow of argon resulted in the formation of interesting upfield hydride signals between -19.5 to -20 ppm. Unfortunately, further irradiation did not result in increased yields of these hydrides and instead complete disappearance of the hydride signals was observed.

We investigated the reactivity of ^{R}POCOP^{R}-NiOCHO (R = ^{t}Bu, ^{i}Pr) complexes, formed from the reaction of **6a/b** and CO_2, and **1-H**. We wanted to see if the iron hydride could regenerate the ^{R}(POCOP)^{R}-NiH complexes, thereby enabling hydrogenation. Unfortunately, even with heating the two complexes were unreactive. UV irradiation (366 nm) resulted in complex rearrangements of the ligands, with formation of iron-pincer complexes and unknown nickel products.

The high moisture sensitivity of these complexes was disconcerting; however, we still wanted to investigate the complex to see if it had any reactivity at all for unique reduction reactions. Obviously, given the high reactivity of both complexes on their own, it did not make sense to investigate the complexes reactivities in process that either were competent in alone. Instead, we investigated the reactivities of these complexes for CO_2 hydrogenation and ester hydrogenation, something that neither complex alone was able to catalyze, although complex **1-H** has been shown to be somewhat active under harsh conditions to produce formic acid in the presence of a base[97] and can reduce electron poor esters under 70 bar of hydrogen pressure at 110 ^{o}C.[98]

Unfortunately, no ester hydrogenation activity was observed after 24h under 40 bars of hydrogen pressure and with heating at 100 ^{o}C in dimethoxyethane (DME). Heating complex **6a** at 80 ^{o}C in DME under 80 psig of hydrogen pressure resulted in the formation of nickel formate complex in addition to other decomposition products. Despite the difficulties in handling the complexes and the lack of catalytic applications, further study here is warranted as very interesting spectroscopic impurities indicate that combinations of these complexes may lead to undiscovered reactivities and metal complexes.

4.5 Experimental

All compounds described in this chapter were prepared under an argon atmosphere using standard glovebox and Schlenk techniques. Benzene-*d*$_6$, acetonitrile-*d*$_3$ and methylene chloride-*d*$_2$ were purchased from Cambridge Isotope Laboratories, Inc. Benzene-*d*$_6$ was dried over sodium-benzophenone and distilled under an argon atmosphere. Acetonitrile-*d*$_3$ and acetonitrile were dried over CaH_2 and distilled under an argon atmosphere. Methylene chloride-*d*$_2$ was dried over 4 Å molecular sieves and degassed by three freeze-pump-thaw cycles. Acetic acid was dried over 4 Å molecular sieves and then deoxygenated by bubbling argon for 0.5 h. All other dry and oxygen-free solvents used for synthesis and workup (THF, diethyl ether, toluene, and pentane) were collected from an Innovative Technology solvent purification system. Benzaldehyde was freshly distilled prior to use. ^{1}H, $^{13}C\{^{1}H\}$, and $^{31}P\{^{1}H\}$ NMR spectra were recorded on a Bruker Avance 400 MHz NMR spectrometer. Chemical shift values in ^{1}H and $^{13}C\{^{1}H\}$ NMR spectra were referenced internally to the residual solvent resonances. $^{31}P\{^{1}H\}$ NMR spectra were referenced externally to 85% H_3PO_4 (0 ppm). Infrared spectra were recorded on a PerkinElmer Spectrum Two FT-IR spectrometer equipped with a smart orbit diamond attenuated total reflectance (ATR) accessory.

Synthesis of Complex 6a

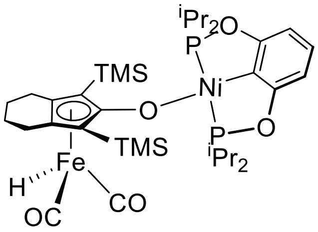

Method A: In an oven dried vial equipped with a small stir bar, **1-H**(0.21 g, 0.51 mmol) and **4a** (0.204 g, 0.51mmol) were combined and dissolved in 5 mL of toluene. The solution was capped with a soft-foam membrane cap which was punctured with a needle to allow hydrogen gas to escape the system. The solution was heated to 40 °C for 72 h, over which time the yellow solution became dark red. The remaining toluene was evaporated, and the residue was dissolved in pentane. This solution was cooled to -30 °C for 24 h, over which time thin, hairlike needles formed representing the crystallized bimetallic product in 45% yield.

Method B: In an oven dried vial equipped with a small stir bar, **1-H** (0.2 g, 0.51mmol) and NaH (0.06 g, 2.5 mmol) were combined with 10 mL of toluene. The cloudy solution was stirred for 1 h under argon in a vented vial. The solution was then filtered and **5a** (0.31 g, 0.51 mmol) was added in a toluene solution and the mixture was stirred for an addition 3 h. After this time, the solution had become dark red and cloudy. The solution was filtered through celite, and the toluene was evaporated. The residue was redissolved in pentane and placed in a freezer at -30 ^{o}C for 24 h, over which time needly orange crystals formed representing the crystallized bimetallic product **6a** in 62% yield.

^{1}H NMR (400 MHz, C_6D_6) δ 6.75 (t, J = 7.9 Hz, 1H), 6.39 (d, J = 8.4 Hz, 1H), 2.62 (m, 2H), 2.48 (m, 2H), 2.36 (m, 2H), 2.15 (m, 2H), 1.70 (m, 2H), 1.37 (m, 8H), 1.25 (m, 13H), 0.95 (m, J = 9.2 Hz, 5H), 0.71 (s, 18H), -12.16 (s, 1H). ^{13}C{^{1}H} NMR (101 MHz, C_6D_6) δ 218.78, 174.39 – 173.40 (m), 169.96 – 168.80 (m), 167.74 (dd, J = 10.6, 7.1 Hz), 128.06, 115.07 (dd, J = 25.2, 22.3 Hz), 105.99 (d, J = 10.1 Hz), 105.61 (d, J = 10.1 Hz), 29.03 (dd, J = 12.1, 6.1 Hz), 28.51 (dd, J = 12.6, 5.6 Hz), 26.70, 23.77, 19.39, 17.30, 16.95, 4.01. ^{31}P{^{1}H} NMR (162 MHz, C_6D_6) δ = 159.82 (AB, J_{AB} = 306.2 Hz), 158.02 (AB, J_{AB} = 306.2 Hz). Selected ATR-IR data (solid, cm^{-1}): 2962 (ν_{C-H}), 1962 ($\nu_{C\equiv O}$), 1919 ($\nu_{C\equiv O}$).

Synthesis of 6b

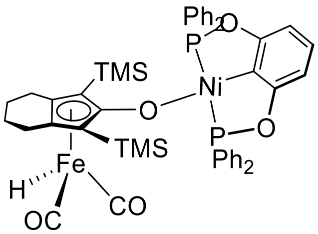

In an oven dried vial equipped with a small stir bar, **1-H** (0.1 g, 0.25 mmol) and KO^{t}Bu (0.022 g, 0.3 mmol) were combined with 10 mL of toluene. The cloudy solution was stirred for 1h under argon in a vented vial. The solution was then filtered and **5b** (0.17 g, 0.25 mmol) was added in a toluene solution and the mixture was stirred for an addition 3 h. After this time, the solution had become dark red and cloudy. The solution was filtered through celite, and the toluene was evaporated. The residue was redissolved in pentane and placed in a freezer at -30 ^{o}C for 24 h, over which time needly orange crystals formed representing the crystallized bimetallic product **6b** in 61% yield.

^{1}H NMR (400 MHz, C_6D_6) δ 7.93 (dt, *J* = 69.4, 8.4 Hz, 9H), 7.20 (s, 5H), 6.94 (s, 7H), 6.81 (t, *J* = 7.9 Hz, 1H), 6.58 (dd, *J* = 36.9, 7.9 Hz, 2H), 2.17 (d, *J* = 255.3 Hz, 5H), 1.51 (d, *J* = 111.1 Hz, 5H), 0.40 (s, 20H), -12.19 (s, 1H). ^{31}P{^{1}H} NMR (162 MHz, C_6D_6) δ = 125.17 (AB, J_{AB} = 359.6 Hz), 119.67(AB, J_{AB} = 359.6 Hz). ^{13}C{^{1}H} NMR (101 MHz, C_6D_6) δ 218.91, 170.81, 167.88 (dd, *J* = 15.1, 6.9 Hz), 164.94 (dd, *J* = 14.4, 5.8 Hz), 133.41 (d, *J* = 13.4 Hz), 133.05 (d, *J* = 6.5 Hz), 132.68 (d, *J* = 6.3 Hz), 131.97 – 131.65 (m), 130.10, 129.20 (d, *J* = 9.9 Hz), 128.44 (d, *J* = 9.9 Hz), 118.08 (d, *J* = 52.0 Hz), 107.41 (dd, *J* = 19.2, 13.0 Hz), 102.16, 70.61, 25.79, 23.35, 3.08. Selected ATR-IR data (solid, cm^{-1}): 3052(ν_{Ph-H}), 2942 (ν_{C-H}), 1969.4 ($\nu_{C\equiv O}$), 1903.17 ($\nu_{C\equiv O}$).

Synthesis of ($^{iPr}P^OC^OP^{Ph}$)NiOH**:**

In an oven dried vial equipped with dry stir bar, **5a** (0.046 g, 0.08 mmol) and NaOH (0.01 g, 0.25 mmol) were combined in 1 mL of benzene. The heterogeneous solution was stirred for 2 h over which time the color changed from a pale yellow to a darker yellow/orange. The solution was filtered through a glass syringe fitted with a 0.2 PES Nalgene membrane filter to give a solution of the product in benzene (Note: evaporation of the solvent resulted in decomposition of the product and as such no yield could be determined). ^{1}H NMR (400 MHz, C_6D_6) δ 6.85 (t, *J* = 7.9 Hz, 1H), 6.57 (d, *J* = 7.9 Hz, 2H), 2.09 (hept, *J* = 7.6 Hz, 5H), 1.42 – 1.31 (m, 8H), 1.25 (q, *J* = 7.0 Hz, 12H), -2.28 (s, 1H). ^{31}P{^{1}H} NMR (162 MHz, C_6D_6) δ 178.32. ^{13}C{^{1}H} NMR (101 MHz, C_6D_6) δ 169.43, 105.37, 27.77, 17.19, 16.80.

Synthesis of ($^{tBu}P^OC^OP^{Ph}$)NiOTf:

To a flame dried Schlenk flask was added [2,6-($tBu_2PO)_2C_6H_2$]NiCl (0.500 g, 0.91 mmol) and 25 mL of methylene chloride. Silver triflate (1.0 mmol) was then added to the solution and the suspension was stirred under dark conditions for 3 h. 30 mL of pentane was then added by syringe transfer to precipitate any dissolved silver salts. The mixture was then filtered via a glass tipped cannula and the collected solution was evaporated to dryness. The resulting yellow solid was used without further purification. 85% yield. ^{1}H NMR (400 MHz, C_6D_6) δ 6.75 (t, J = 7.9 Hz, 1H), 6.32 (d, J = 7.9 Hz, 2H), 1.52 – 1.26 (m, 36H). ^{31}P{^{1}H} NMR (162 MHz, C_6D_6) δ 190.64.

References

(1) Bullock, R. M.; Chen, J. G.; Gagliardi, L.; Chirik, P. J.; Farha, O. K.; Hendon, C. H.; Jones, C. W.; Keith, J. A.; Klosin, J.; Minteer, S. D.; Morris, R. H.; Radosevich, A. T.; Rauchfuss, T. B.; Strotman, N. A.; Vojvodic, A.; Ward, T. R.; Yang, J. Y.; Surendranath, Y. Using Nature's Blueprint to Expand Catalysis with Earth-Abundant Metals. *Science* **2020**, *369* (6505), eabc3183. https://doi.org/10.1126/science.abc3183.

(2) Franke, R.; Selent, D.; Börner, A. Applied Hydroformylation. *Chemical Reviews* **2012**, *112* (11), 5675–5732. https://doi.org/10.1021/cr3001803.

(3) Verendel, J. J.; Pàmies, O.; Diéguez, M.; Andersson, P. G. Asymmetric Hydrogenation of Olefins Using Chiral Crabtree-Type Catalysts: Scope and Limitations. *Chemical Reviews* **2013**, *114* (4), 2130–2169. https://doi.org/10.1021/cr400037u.

(4) Pal, R.; Mukherjee, S.; Chandrasekhar, S.; Guru Row, T. N. Exploring Cyclopentadienone Antiaromaticity: Charge Density Studies of Various Tetracyclones. *The Journal of Physical Chemistry A* **2014**, *118* (19), 3479–3489. https://doi.org/10.1021/jp5010924.

(5) Harmata, M.; Gomes, M. G. Intermolecular [4+2] Cycloadditions of a Reactive Cyclopentadienone. *European Journal of Organic Chemistry* **2006**, *2006* (10), 2273–2277. https://doi.org/10.1002/ejoc.200600173.

(6) Harmata, M.; Garimalla, A. Derivatives of Alkyl 2-Hydroxy-3-Oxocyclopent-1-Enecarboxylates and Intermolecular [4+2] Cycloadditions of Cyclopentadienones Prepared Therefrom. *Synthesis* **2018**, *50* (22), 4483–4489. https://doi.org/10.1055/s-0037-1610184.

(7) Ogliaruso, M. A.; Romanelli, M. G.; Becker, E. I. Chemistry of Cyclopentadienones. *Chemical Reviews* **1965**, *65* (3), 261–367. https://doi.org/10.1021/cr60235a001.

(8) Nisa, K.; Khatri, V.; Kumar, S.; Arora, S.; Ahmad, S.; Dandia, A.; Thirumal, M.; Kashyap, H. K.; Chauhan, S. M. S. Synthesis and Redox Properties of Superbenzene Porphyrin Conjugates. *Inorganic Chemistry* **2020**, *59* (22), 16168–16177. https://doi.org/10.1021/acs.inorgchem.0c01682.

(9) Potter, R. G.; Hughes, T. S. Predicting the UV−Vis Spectra of Tetraarylcyclopentadienones: Using DFT Molecular Orbital Energies to Model Electronic Transitions of Organic Materials. *The Journal of Organic Chemistry* **2008**, *73* (8), 2995–3004. https://doi.org/10.1021/jo701676x.

(10) McGlinchey, M. J. Diels-Alder Additions as Mechanistic Probes–Interception of Silyl-Isoindenes: Organometallic Derivatives of Polyphenylated Cycloheptatrienes and Related Seven-Membered Rings. *Molecules* **2020**, *25* (20), 4730. https://doi.org/10.3390/molecules25204730.

(11) Tang, Y.; Meador, R. I. L.; Malinchak, C. T.; Harrison, E. E.; McCaskey, K. A.; Hempel, M. C.; Funk, T. W. (Cyclopentadienone)Iron-Catalyzed Transfer Dehydrogenation of Symmetrical and Unsymmetrical Diols to Lactones. *The Journal of Organic Chemistry* **2019**, *85* (4), 1823–1834. https://doi.org/10.1021/acs.joc.9b01884.

(12) Rosas-Hernández, A.; Junge, H.; Beller, M.; Roemelt, M.; Francke, R. Cyclopentadienone Iron Complexes as Efficient and Selective Catalysts for the Electroreduction of CO2 to CO. *Catalysis Science & Technology* **2017**, *7* (2), 459–465. https://doi.org/10.1039/C6CY02352E.

(13) Ndiaye, D.; Coufourier, S.; Mbaye, M. D.; Gaillard, S.; Renaud, J.-L. Cyclopentadienone Iron Tricarbonyl Complexes-Catalyzed Hydrogen Transfer in Water. *Molecules* **2020**, *25* (2), 421. https://doi.org/10.3390/molecules25020421.

(14) Pignataro, L.; Gennari, C. Recent Catalytic Applications of (Cyclopentadienone)Iron Complexes. *European Journal of Organic Chemistry* **2020**, *2020* (22), 3192–3205. https://doi.org/10.1002/ejoc.201901925.

(15) Casey, C. P.; Guan, H. Cyclopentadienone Iron Alcohol Complexes: Synthesis, Reactivity, and Implications for the Mechanism of Iron Catalyzed Hydrogenation of Aldehydes. *Journal of the American Chemical Society* **2009**, *131* (7), 2499–2507. https://doi.org/10.1021/ja808683z.

(16) Elsby, M. R.; Baker, R. T. Strategies and Mechanisms of Metal–Ligand Cooperativity in First-Row Transition Metal Complex Catalysts. *Chemical Society Reviews* **2020**, *49* (24), 8933–8987. https://doi.org/10.1039/D0CS00509F.

(17) Casey, C. P.; Guan, H. An Efficient and Chemoselective Iron Catalyst for the Hydrogenation of Ketones. *Journal of the American Chemical Society* **2007**, *129* (18), 5816–5817. https://doi.org/10.1021/ja071159f.

(18) Lator, A.; Gaillard, S.; Poater, A.; Renaud, J.-L. Iron-Catalyzed Chemoselective Reduction of α,β-Unsaturated Ketones. *Chemistry - A European Journal* **2018**, *24* (22), 5770–5774. https://doi.org/10.1002/chem.201800995.

(19) Knölker, H.-J.; Baum, E.; Goesmann, H.; Klauss, R. Demetalation of Tricarbonyl(Cyclopentadienone)Iron Complexes Initiated by a Ligand Exchange Reaction with NaOH—X-Ray Analysis of a Complex with Nearly Square-Planar Coordinated Sodium. *Angewandte Chemie International Edition* **1999**, *38* (13–14), 2064–2066. https://doi.org/10.1002/(sici)1521-3773(19990712)38:13/14<2064::aid-anie2064>3.0.co;2-w.

(20) Polidano, K.; Williams, J. M. J.; Morrill, L. C. Iron-Catalyzed Borrowing Hydrogen β-C(Sp3)-Methylation of Alcohols. *ACS Catalysis* **2019**, *9* (9), 8575–8580. https://doi.org/10.1021/acscatal.9b02461.

(21) Rosas-Hernández, A.; Steinlechner, C.; Junge, H.; Beller, M. Earth-Abundant Photocatalytic Systems for the Visible-Light-Driven Reduction of CO2 to CO. *Green Chemistry* **2017**, *19* (10), 2356–2360. https://doi.org/10.1039/c6gc03527b.

(22) Conley, B. L.; Pennington-Boggio, M. K.; Boz, E.; Williams, T. J. Discovery, Applications, and Catalytic Mechanisms of Shvo's Catalyst. *Chemical Reviews* **2010**, *110* (4), 2294–2312. https://doi.org/10.1021/cr9003133.

(23) Gargir, M.; Ben-David, Y.; Leitus, G.; Diskin-Posner, Y.; Shimon, L. J. W.; Milstein, D. PNS-Type Ruthenium Pincer Complexes. *Organometallics* **2012**, *31* (17), 6207–6214. https://doi.org/10.1021/om300516j.

(24) Wu, W.; Seki, T.; Walker, K. L.; Waymouth, R. M. Transfer Hydrogenation of Aldehydes, Allylic Alcohols, Ketones, and Imines Using Molybdenum Cyclopentadienone Complexes. *Organometallics* **2018**, *37* (9), 1428–1431. https://doi.org/10.1021/acs.organomet.8b00086.

(25) Gupta, H. K.; Rampersad, N.; Stradiotto, M.; McGlinchey, M. J. Rhodium Acetylacetonate and Iron Tricarbonyl Complexes of Tetracyclone and 3-Ferrocenyl-2,4,5-Triphenylcyclopentadienone: An X-Ray Crystallographic and NMR Study. *Organometallics* **2000**, *19* (2), 184–191. https://doi.org/10.1021/om990559b.

(26) Higashi, T.; Kusumoto, S.; Nozaki, K. Umpolung of B−H Bonds by Metal–Ligand Cooperation with Cyclopentadienone Iridium Complexes. *Angewandte Chemie International Edition* **2020**, *60* (6), 2844–2848. https://doi.org/10.1002/anie.202011322.

(27) Wu, W.; Solis-Ibarra, D.; Walker, K. L.; Waymouth, R. M. Synthesis, Characterization, and Reactivity of Hydroxycyclopentadienyl Cobalt Complexes. *Organometallics* **2018**, *37* (19), 3298–3302. https://doi.org/10.1021/acs.organomet.8b00486.

(28) Weiss, E.; Hübel, W. Organometallic Complexes—V(1) π-Komplexe Aus Cyclischen Dienverbindungen Und Metallcarbonylen. *Journal of Inorganic and Nuclear Chemistry* **1959**, *11* (1), 42–55. https://doi.org/10.1016/0022-1902(59)80213-X.

(29) Hoffmann, F.; Wagler, J.; Roewer, G. Cyclopentadienone and Hydroxycyclopentadienyl Cobalt Complexes from the Reaction of an Alkynylphenylsilane with Co2(CO)8. *Organometallics* **2014**, *33* (20), 5622–5625. https://doi.org/10.1021/om500488w.

(30) Sheats, J. E.; Rausch, M. D. Synthesis and Properties of Cobalticinium Salts. I. Synthesis of Monosubstituted Cobalticinium Salts. *The Journal of Organic Chemistry* **1970**, *35* (10), 3245–3249. https://doi.org/10.1021/jo00835a014.

(31) Van Willigen, Hans.; Geiger, W. E.; Rausch, M. D. Paramagnetic Complexes Produced in the Electrochemical and Chemical Reduction of Cyclopentadienyl-Cobalt- and -Rhodium-Cyclopentadienone Complexes. *Inorganic Chemistry* **1977**, *16* (3), 581–584. https://doi.org/10.1021/ic50169a016.

(32) Plenio, H.; Warnecke, A. Simple Organometallic Alcohols: Synthesis of (C5H4OH)Mn(CO)3 (Hydroxycymantrene) and (C5H4OH)W(CO)3CH3. *Organometallics* **1996**, *15* (23), 5066–5068. https://doi.org/10.1021/om960611t.

(33) Ritter, F.; Mukherjee, D.; Spaniol, T. P.; Hoffmann, A.; Okuda, J. A Masked Cuprous Hydride as a Catalyst for Carbonyl Hydrosilylation in Aqueous Solutions. *Angewandte Chemie International Edition* **2019**, *58* (6), 1818–1822. https://doi.org/10.1002/anie.201811890.

(34) Fryzuk, M. D.; Mylvaganam, M.; Zaworotko, M. J.; MacGillivray, L. R. Reduction of Carbon Monoxide by Tandem Electron Transfer and Migratory Insertion of a Masked Zirconium(IV) Hydride. Formation of a Zirconium Formyl−Ylide Complex. *Organometallics* **1996**, *15* (4), 1134–1138. https://doi.org/10.1021/om950302n.

(35) Gavenonis, J.; Tilley, T. D. Reversible Intramolecular Hydride Transfer between Tantalum and an Aromatic Ring: An H5-Cyclohexadienyl Complex as a Masked Hydride. *Journal of the American Chemical Society* **2002**, *124* (29), 8536–8537. https://doi.org/10.1021/ja025684k.

(36) Tassano, E.; Hall, M. Enzymatic Self-Sufficient Hydride Transfer Processes. *Chemical Society Reviews* **2019**, *48* (23), 5596–5615. https://doi.org/10.1039/C8CS00903A.

(37) Connelly, N. G.; Geiger, W. E. Chemical Redox Agents for Organometallic Chemistry. *Chemical Reviews* **1996**, *96* (2), 877–910. https://doi.org/10.1021/cr940053x.

(38) Zhang, F.; Xu, X.; Zhao, Y.; Jia, J.; Tung, C.-H.; Wang, W. Solvent Effects on Hydride Transfer from Cp*(P-P)FeH to BNA+ Cation. *Organometallics* **2017**, *36* (7), 1238–1244. https://doi.org/10.1021/acs.organomet.6b00907.

(39) Guan, H.; Iimura, M.; Magee, M. P.; Norton, J. R.; Janak, K. E. Effect of Chelate Ring Size on the Rate of Hydride Transfer from CpRu(P−P)H (P−P = Chelating Diphosphine) to an Iminium Cation. *Organometallics* **2003**, *22* (20), 4084–4089. https://doi.org/10.1021/om0303404.

(40) Liu, T.; Guo, M.; Orthaber, A.; Lomoth, R.; Lundberg, M.; Ott, S.; Hammarström, L. Accelerating Proton-Coupled Electron Transfer of Metal Hydrides in Catalyst Model Reactions. *Nature Chemistry* **2018**, *10* (8), 881–887. https://doi.org/10.1038/s41557-018-0076-x.

(41) Badiei, Y. M.; Wang, W.-H.; Hull, J. F.; Szalda, D. J.; Muckerman, J. T.; Himeda, Y.; Fujita, E. Cp*Co(III) Catalysts with Proton-Responsive Ligands for Carbon Dioxide Hydrogenation in Aqueous Media. *Inorg. Chem.* **2013**, *52* (21), 12576–12586. https://doi.org/10.1021/ic401707u.

(42) Cook, A. W.; Emge, T. J.; Waldie, K. M. Insights into Formate Oxidation by a Series of Cobalt Piano-Stool Complexes Supported by Bis(Phosphino)Amine Ligands. *Inorg. Chem.* **2021**, *60* (10), 7372–7380. https://doi.org/10.1021/acs.inorgchem.1c00563.

(43) McLoughlin, E. A.; Giles, L. J.; Waymouth, R. M.; Sarangi, R. X-Ray Absorption Spectroscopy and Theoretical Investigation of the Reductive Protonation of Cyclopentadienyl Cobalt Compounds. *Inorg. Chem.* **2019**, *58* (2), 1167–1176. https://doi.org/10.1021/acs.inorgchem.8b02475.

(44) McLoughlin, E. A.; Waldie, K. M.; Ramakrishnan, S.; Waymouth, R. M. Protonation of a Cobalt Phenylazopyridine Complex at the Ligand Yields a Proton, Hydride, and Hydrogen Atom Transfer Reagent. *Journal of the American Chemical Society* **2018**, *140* (41), 13233–13241. https://doi.org/10.1021/jacs.8b06156.

(45) A molecular mediator for reductive concerted proton-electron transfers via electrocatalysis | Science https://science.sciencemag.org/content/369/6505/850 (accessed 2021 -06 -06).

(46) Robinson, T. P.; De Rosa, D. M.; Aldridge, S.; Goicoechea, J. M. E–H Bond Activation of Ammonia and Water by a Geometrically Constrained Phosphorus(III) Compound. *Angew Chem Int Ed Engl* **2015**, *54* (46), 13758–13763. https://doi.org/10.1002/anie.201506998.

(47) Tanushi, A.; Radosevich, A. T. Insertion of a Nontrigonal Phosphorus Ligand into a Transition Metal-Hydride: Direct Access to a Metallohydrophosphorane. *Journal of the American Chemical Society* **2018**, *140* (26), 8114–8118. https://doi.org/10.1021/jacs.8b05156.

(48) Quintana, L. M. A.; Johnson, S. I.; Corona, S. L.; Villatoro, W.; Goddard, W. A.; Takase, M. K.; VanderVelde, D. G.; Winkler, J. R.; Gray, H. B.; Blakemore, J. D. Proton–Hydride Tautomerism in Hydrogen Evolution Catalysis. *Proc Natl Acad Sci U S A* **2016**, *113* (23), 6409–6414. https://doi.org/10.1073/pnas.1606018113.

(49) Meredith, J. M.; Goldberg, K. I.; Kaminsky, W.; Heinekey, D. M. H6-Tetramethylfulvene and μ-H3:H3-Benzene Complexes of Iridium. *Organometallics* **2012**, *31* (23), 8459–8462. https://doi.org/10.1021/om3010492.

(50) Yoo, C.; Lee, Y. Carbon Dioxide Binding at a Ni/Fe Center: Synthesis and Characterization of Ni(H1-CO2-KC) and Ni-μ-CO2-KC:K2 O,O′-Fe †Electronic Supplementary Information (ESI) Available: Characterization Data for 3 and 5. CCDC 1492006 and 1492007. For ESI and Crystallographic Data in CIF or Other Electronic Format See DOI: 10.1039/C6sc03450k Click Here for Additional Data File. Click Here for Additional Data File. *Chem Sci* **2017**, *8* (1), 600–605. https://doi.org/10.1039/c6sc03450k.

(51) Manor, B. C.; Rauchfuss, T. B. Hydrogen Activation by Biomimetic [NiFe]-Hydrogenase Model Containing Protected Cyanide Cofactors. *J. Am. Chem. Soc.* **2013**, *135* (32), 11895–11900. https://doi.org/10.1021/ja404580r.

(52) Canaguier, S.; Fontecave, M.; Artero, V. Cp*–-Ruthenium–Nickel-Based H2-Evolving Electrocatalysts as Bio-Inspired Models of NiFe Hydrogenases. *European Journal of Inorganic Chemistry* **2011**, *2011* (7), 1094–1099. https://doi.org/10.1002/ejic.201000944.

(53) Cammarota, R. C.; Vollmer, M. V.; Xie, J.; Ye, J.; Linehan, J. C.; Burgess, S. A.; Appel, A. M.; Gagliardi, L.; Lu, C. C. A Bimetallic Nickel–Gallium Complex Catalyzes CO2 Hydrogenation via the Intermediacy of an Anionic D10 Nickel Hydride. *J. Am. Chem. Soc.* **2017**, *139* (40), 14244–14250. https://doi.org/10.1021/jacs.7b07911.

(54) Greenwood, B. P.; Rowe, G. T.; Chen, C.-H.; Foxman, B. M.; Thomas, C. M. Metal−Metal Multiple Bonds in Early/Late Heterobimetallics Support Unusual Trigonal Monopyramidal Geometries at Both Zr and Co. *J. Am. Chem. Soc.* **2010**, *132* (1), 44–45. https://doi.org/10.1021/ja909310t.

(55) Karunananda, M. K.; Parmelee, S. R.; Waldhart, G. W.; Mankad, N. P. Experimental and Computational Characterization of the Transition State for C–X Bimetallic Oxidative Addition at a Cu–Fe Reaction Center. *Organometallics* **2015**, *34* (15), 3857–3864. https://doi.org/10.1021/acs.organomet.5b00476.

(56) Funk, T. W.; Mahoney, A. R.; Sponenburg, R. A.; Zimmerman, K. P.; Kim, D. K.; Harrison, E. E. Synthesis and Catalytic Activity of (3,4-Diphenylcyclopentadienone)Iron Tricarbonyl Compounds in Transfer Hydrogenations and Dehydrogenations. *Organometallics* **2018**, *37* (7), 1133–1140. https://doi.org/10.1021/acs.organomet.8b00037.

(57) Murakami, S.; Sonehara, T.; Iwakami, K.; Tsuji, H.; Kawatsura, M. Synthesis of Trifluoromethyl-Group-Containing Cyclopentadienones by the Palladium-Catalyzed [2 + 2 + 1] Cycloaddition of Aryl- and Trifluoromethyl-Group Substituted Internal Alkynes and Carbon Monoxide. *Tetrahedron Letters* **2019**, *60* (8), 598–601. https://doi.org/10.1016/j.tetlet.2019.01.036.

(58) Peressin, N.; Adamski, M.; Schibli, E. M.; Ye, E.; Frisken, B. J.; Holdcroft, S. Structure–Property Relationships in Sterically Congested Proton-Conducting Poly(Phenylene)s: The Impact of Biphenyl Linearity. *Macromolecules* **2020**, *53* (8), 3119–3138. https://doi.org/10.1021/acs.macromol.0c00310.

(59) Batool, M.; Martin, T. A.; Algarra, A. G.; George, M. W.; Macgregor, S. A.; Mahon, M. F.; Whittlesey, M. K. Photochemistry of Cp′Mn(CO)2(NHC) (Cp′ = H5-C5H4Me) Species: Synthesis, Time-Resolved IR Spectroscopy, and DFT Calculations. *Organometallics* **2012**, *31* (14), 4971–4979. https://doi.org/10.1021/om300209a.

(60) Piper, T. S.; Cotton, F. A.; Wilkinson, G. Cyclopentadienyl-Carbon Monoxide and Related Compounds of Some Transitional Metals. *Journal of Inorganic and Nuclear Chemistry* **1955**, *1* (3), 165–174. https://doi.org/10.1016/0022-1902(55)80053-X.

(61) Avanzino, S. C.; Jolly, W. L. A Study of Bridging and Terminal Carbonyl Groups in Transition Metal Complexes by X-Ray Photoelectron Spectroscopy. *Journal of the American Chemical Society* **1976**, *98* (21), 6505–6507. https://doi.org/10.1021/ja00437a014.

(62) Frost, A. A. Oxidation Potential-Free Energy Diagrams. *Journal of the American Chemical Society* **1951**, *73* (6), 2680–2682. https://doi.org/10.1021/ja01150a074.

(63) Kütt, A.; Tshepelevitsh, S.; Saame, J.; Lõkov, M.; Kaljurand, I.; Selberg, S.; Leito, I. Strengths of Acids in Acetonitrile. *European Journal of Organic Chemistry* **2021**, *2021* (9), 1407–1419. https://doi.org/10.1002/ejoc.202001649.

(64) Moore, E. J.; Sullivan, J. M.; Norton, J. R. Kinetic and Thermodynamic Acidity of Hydrido Transition-Metal Complexes. 3. Thermodynamic Acidity of Common Mononuclear Carbonyl Hydrides. *J. Am. Chem. Soc.* **1986**, *108* (9), 2257–2263. https://doi.org/10.1021/ja00269a022.

(65) Herberhold, M.; Pfeifer, A.; Milius, W. Halfsandwich Carbonylmetal Complexes of Vanadium, Chromium, and Manganese Containing Tri(1-Cyclohepta-2, 4, 6-Trienyl)Phosphane, P(C7H7)3. *Zeitschrift für anorganische und allgemeine Chemie* **2002**, *628* (13), 2919–2929. https://doi.org/10.1002/1521-3749(200213)628:13<2919::AID-ZAAC2919>3.0.CO;2-7.

(66) Cheng, T.-Y.; Bullock, R. M. Hydride Transfer from (H5-C5Me5)(CO)2MH (M = Fe, Ru, Os) to Trityl Cation: Different Products from Different Metals and the Kinetics of Hydride Transfer. *Organometallics* **2002**, *21* (11), 2325–2331. https://doi.org/10.1021/om020012o.

(67) Pan, X.; Lacôte, E.; Lalevée, J.; Curran, D. P. Polarity Reversal Catalysis in Radical Reductions of Halides by N-Heterocyclic Carbene Boranes. *J. Am. Chem. Soc.* **2012**, *134* (12), 5669–5674. https://doi.org/10.1021/ja300416f.

(68) Colomer, E.; Corriu, R. J. P.; Vioux, A. Synthesis and Properties of Manganese Hydrides Having a Functional Silicon. *Inorg. Chem.* **1979**, *18* (3), 695–700. https://doi.org/10.1021/ic50193a033.

(69) Moselage, M.; Li, J.; Ackermann, L. Cobalt-Catalyzed C–H Activation. *ACS Catal.* **2016**, *6* (2), 498–525. https://doi.org/10.1021/acscatal.5b02344.

(70) Fleischer, S.; Zhou, S.; Junge, K.; Beller, M. General and Highly Efficient Iron-Catalyzed Hydrogenation of Aldehydes, Ketones, and α,β-Unsaturated Aldehydes. *Angewandte Chemie International Edition* **2013**, *52* (19), 5120–5124. https://doi.org/10.1002/anie.201301239.

(71) Casey, C. P.; Guan, H. An Efficient and Chemoselective Iron Catalyst for the Hydrogenation of Ketones. *Journal of the American Chemical Society* **2007**, *129* (18), 5816–5817. https://doi.org/10.1021/ja071159f.

(72) Rajesh, T.; Periasamy, M. Carbonylative Cyclization of Alkynes Using Cobalt Carbonyl Species Prepared via Reduction of CoBr2 with Zn under a Carbon Monoxide Atmosphere. *Organometallics* **1999**, *18* (26), 5709–5712. https://doi.org/10.1021/om990534c.

(73) Edgell, W. F.; Lyford, J. Studies of Some Aspects of Solution Character by Molecular Spectroscopy. V. Identification, Population, and Equilibrium of the Anion Sites for NaCo(CO)4 in Tetrahydrofuran. *J. Am. Chem. Soc.* **1971**, *93* (24), 6407–6414. https://doi.org/10.1021/ja00753a013.

(74) Moulin, S.; Dentel, H.; Pagnoux-Ozherelyeva, A.; Gaillard, S.; Poater, A.; Cavallo, L.; Lohier, J.-F.; Renaud, J.-L. Bifunctional (Cyclopentadienone)Iron–Tricarbonyl Complexes: Synthesis, Computational Studies and Application in Reductive Amination. *Chemistry – A European Journal* **2013**, *19* (52), 17881–17890. https://doi.org/10.1002/chem.201302432.

(75) Knölker, H.-J.; Goesmann, H.; Klauss, R. A Novel Method for the Demetalation of Tricarbonyliron-Diene Complexes by a Photolytically Induced Ligand Exchange Reaction with Acetonitrile. *Angew Chem Int Ed Engl* **1999**, *38* (5), 702–705. https://doi.org/10.1002/(SICI)1521-3773(19990301)38:5<702::AID-ANIE702>3.0.CO;2-W.

(76) Shvo, Y.; Hazum, E. A Simple Method for the Disengagement of Organic Ligands from Iron Complexes. *J. Chem. Soc., Chem. Commun.* **1974**, No. 9, 336–337. https://doi.org/10.1039/C39740000336.

(77) Yamaguchi, S.; Jin, R.-Z.; Tamao, K.; Sato, F. A Convenient One-Pot Synthesis of 1,4-Dihalobutadienes from Alkynes via Titanacyclopentadienes and Their Transformation to a Series of Silole Derivatives. *The Journal of Organic Chemistry* **1998**, *63* (26), 10060–10062. https://doi.org/10.1021/jo981533h.

(78) Negishi, E.; Cederbaum, F. E.; Takahashi, T. Reaction of Zirconocene Dichloride with Alkyllithiums or Alkyl Grignard Reagents as a Convenient Method for Generating a "Zirconocene" Equivalant and Its Use in Zirconium-Promoted Cyclization of Alkenes, Alkynes, Dienes, Enynes, and Diynes. *Tetrahedron Letters* **1986**, *27* (25), 2829–2832. https://doi.org/10.1016/S0040-4039(00)84653-5.

(79) Xi, Z.; Song, Q. Efficient Synthesis of Cyclopentadienone Derivatives by the Reaction of Carbon Dioxide with 1,4-Dilithio-1,3-Dienes. *The Journal of Organic Chemistry* **2000**, *65* (26), 9157–9159. https://doi.org/10.1021/jo005641r.

(80) Heck, J.; Brussard, H. C.; Dabek, S.; Meyer-Friedrichsen, T.; Wong, H. Bimetallic Sandwichlike Complexes as Novel NLO Chromophores. In *Nonlinear Optical Properties of Organic Materials X*; International Society for Optics and Photonics, 1997; Vol. 3147, pp 53–61. https://doi.org/10.1117/12.284254.

(81) Jayarathne, U.; Parmelee, S. R.; Mankad, N. P. Small Molecule Activation Chemistry of Cu–Fe Heterobimetallic Complexes Toward CS2 and N2O. *Inorg. Chem.* **2014**, *53* (14), 7730–7737. https://doi.org/10.1021/ic501054z.

(82) Leon, N. J.; Yu, H.-C.; Mazzacano, T. J.; Mankad, N. P. Pursuit of C–H Borylation Reactions with Non-Precious Heterobimetallic Catalysts: Hypothesis-Driven Variations on a Design Theme. *Synlett* **2020**, *31* (02), 125–132. https://doi.org/10.1055/s-0039-1691504.

(83) Chakraborty, A.; Kinney, R. G.; Krause, J. A.; Guan, H. Cooperative Iron–Oxygen–Copper Catalysis in the Reduction of Benzaldehyde under Water-Gas Shift Reaction Conditions. *ACS Catal.* **2016**, *6* (11), 7855–7864. https://doi.org/10.1021/acscatal.6b01994.

(84) Rozenel, S. S.; Arnold, J. Bimetallic Ruthenium PNP Pincer Complex As a Platform to Model Proposed Intermediates in Dinitrogen Reduction to Ammonia. *Inorg. Chem.* **2012**, *51* (18), 9730–9739. https://doi.org/10.1021/ic3010322.

(85) Goldberg, J. M.; Guard, L. M.; Wong, G. W.; Brayton, D. F.; Kaminsky, W.; Goldberg, K. I.; Heinekey, D. M. Preparation and Reactivity of Bimetallic (Pincer)Ir Complexes. *Organometallics* **2020**, *39* (18), 3323–3334. https://doi.org/10.1021/acs.organomet.0c00403.

(86) Tay, W. S.; Yang, X.-Y.; Li, Y.; Pullarkat, S. A.; Leung, P.-H. Efficient and Stereoselective Synthesis of Monomeric and Bimetallic Pincer Complexes Containing Pd-Bonded Stereogenic Carbons. *RSC Adv.* **2016**, *6* (79), 75951–75959. https://doi.org/10.1039/C6RA16721G.

(87) Wellala, N. P. N.; Dong, H. T.; Krause, J. A.; Guan, H. Janus POCOP Pincer Complexes of Nickel. *Organometallics* **2018**, *37* (21), 4031–4039. https://doi.org/10.1021/acs.organomet.8b00619.

(88) Wong, J. L.; Higgins, R. F.; Bhowmick, I.; Cao, D. X.; Szigethy, G.; Ziller, J. W.; Shores, M. P.; Heyduk, A. F. Bimetallic Iron–Iron and Iron–Zinc Complexes of the Redox-Active

ONO Pincer Ligand. *Chem. Sci.* **2016**, *7* (2), 1594–1599. https://doi.org/10.1039/C5SC03006D.

(89) Pichaandi, K. R.; Fanwick, P. E.; Abu-Omar, M. M. C–H Activation of Methyltrioxorhenium by Pincer Iridium Hydride To Give Agile Ir–Re Bimetallic Compounds. *Organometallics* **2014**, *33* (19), 5089–5092. https://doi.org/10.1021/om500807a.

(90) Chakraborty, S.; Zhang, J.; Krause, J. A.; Guan, H. An Efficient Nickel Catalyst for the Reduction of Carbon Dioxide with a Borane. *J. Am. Chem. Soc.* **2010**, *132* (26), 8872–8873. https://doi.org/10.1021/ja103982t.

(91) Chakraborty, S.; Krause, J. A.; Guan, H. Hydrosilylation of Aldehydes and Ketones Catalyzed by Nickel PCP-Pincer Hydride Complexes. *Organometallics* **2009**, *28* (2), 582–586. https://doi.org/10.1021/om800948f.

(92) Simmons, T. R.; Berggren, G.; Bacchi, M.; Fontecave, M.; Artero, V. Mimicking Hydrogenases: From Biomimetics to Artificial Enzymes. *Coordination Chemistry Reviews* **2014**, *270–271*, 127–150. https://doi.org/10.1016/j.ccr.2013.12.018.

(93) Tang, H.; Hall, M. B. Biomimetics of [NiFe]-Hydrogenase: Nickel- or Iron-Centered Proton Reduction Catalysis? *J. Am. Chem. Soc.* **2017**, *139* (49), 18065–18070. https://doi.org/10.1021/jacs.7b10425.

(94) Adhikary, A.; Schwartz, J. R.; Meadows, L. M.; Krause, J. A.; Guan, H. Interaction of Alkynes with Palladium POCOP-Pincer Hydride Complexes and Its Unexpected Relation to Palladium-Catalyzed Hydrogenation of Alkynes. *Inorg. Chem. Front.* **2014**, *1* (1), 71–82. https://doi.org/10.1039/C3QI00073G.

(95) Eberhardt, N. A.; Guan, H. Nickel Hydride Complexes. *Chem. Rev.* **2016**, *116* (15), 8373–8426. https://doi.org/10.1021/acs.chemrev.6b00259.

(96) von Wolff, N.; Lefèvre, G.; Berthet, J.-C.; Thuéry, P.; Cantat, T. Implications of CO2 Activation by Frustrated Lewis Pairs in the Catalytic Hydroboration of CO2: A View Using N/Si+ Frustrated Lewis Pairs. *ACS Catal.* **2016**, *6* (7), 4526–4535. https://doi.org/10.1021/acscatal.6b00421.

(97) Zhu, F.; Zhu-Ge, L.; Yang, G.; Zhou, S. Iron-Catalyzed Hydrogenation of Bicarbonates and Carbon Dioxide to Formates. *ChemSusChem* **2015**, *8* (4), 609–612. https://doi.org/10.1002/cssc.201403234.

(98) Gajewski, P.; Gonzalez-de-Castro, A.; Renom-Carrasco, M.; Piarulli, U.; Gennari, C.; de Vries, J. G.; Lefort, L.; Pignataro, L. Expanding the Catalytic Scope of (Cyclopentadienone)Iron Complexes to the Hydrogenation of Activated Esters to Alcohols. *ChemCatChem* **2016**, *8* (22), 3431–3435. https://doi.org/10.1002/cctc.201600972.